Exploring human T lymphocytes expressing a CAR directed to the tumor-neoantigen EGFRvIII for adoptive cellular therapy to non-small cell lung cancer

Dissertation

Zur Erlangung des Grades

Doktor der Naturwissenschaften

Am Fachbereich Biologie

Der Johannes Gutenberg-Universität Mainz

vorgelegt von

Anita Bhatti

geb. am 21.07.1983 in Mannheim

Mainz, 2018

Dekan:

1. Berichterstatter:

2. Berichterstatter:

Tag der mündlichen Prüfung:

Statement

_____

Ort, Datum   Unterschrift

Table of contents

Abstract

Adoptive cellular therapy (ACT) using genetically engineered T cells expressing a chimeric-antigen-receptor (CAR) to redirect their specificity holds great promise in tumor immunotherapy. However, in contrast to remarkable clinical responses observed with CD19-CAR T cells for B-cell leukemias, efficacy of ACT in solid tumors is often hampered by insufficient and non-durable immunity of T cells facing an immunosuppressive tumor microenvironment. Moreover, identifying tumor-specific neoantigens with low off-target activity is difficult. The epithelial growth factor variant III (EGFRvIII) is only found on neoplastic tissue and represents a promising candidate target for ACT in e.g. glioblastoma as already shown in clinical trials and has also been described for non-small cell lung cancer (NSCLC). EGFRvIII-CAR T cells have not yet been tested in NSCLC, we therefore aimed in this preclinical study to evaluate antitumor immunity of EGFRvIII-CAR T cells against NSLCL *in vitro* and *in vivo* using a xenograft mouse model. Human, preactivated T cells were retrovirally transduced, and CAR expression was analyzed by flow cytometry 7 days (d) post transduction. Stably transfecetd EGFRvIII+ cells of a HLA class I/II-deficient melanoma cell line (Ma-Mel-86) or the NSLCL cell line A549 were used as targets. EGFRvIII-CAR T cells were examined for IFN-γ/Granzyme B release and cytotoxicity using ELISpot-, ^{51}Cr-release- and 48h co-culture assays. To evaluate the therapeutic potential *in vivo*, intratumoral T-cell transfer into NSG mice displaying palpable subcutaneous tumor engraftment was performed. Upon retroviral transduction >85% T cells expressed the EGFRvIII-CAR as confirmed by flow cytometry. EGFRvIII-CAR T cells induced vigorous responses to both EGFRvIII+ tumor targets *in vitro* as measured by IFN-γ and Granzyme B release and elicited potent cytotoxicity (>60%) upon short-term 5h coculture (^{51}Cr-release) and >90% in co-culture assays after 2d. Moreover, we generated EGFRvIII-CAR redirected T cells derived from naïve, CD45RA+ precursors displaying a stem cell and central memory phenotype, which have been previously reported to elicit superior antitumor immunity as compared to more differentiated T cells. The less differentiated EGFRvIII-CAR redirected T cells showed comparable anti-EGFRvIII responses when compared to EGFRvIII-CAR T cells obtained from bulk cultures regarding stimulation activity and cytokine response. In this study we could prove effective reactivity of EGFRvIII-CAR T cells towards EGFRvIII-expressing melanoma and lung cancer cells *in vitro*. To evaluate the therapeutic potential of EGFRvIII-CAR T cells *in vivo*, further exploitation and optimization regarding the mouse model is required to overcome obstacles we encountered in preliminary studies. Although EGFRvIII appears not to be a dominant target among the different EGFR mutations found in NSCLC patients, EGFRvIII-CAR ACT might provide

valuable information as a proof of concept study for immunotherapy in lung cancer and might contribute to improve ACT for solid tumors.

Zusammenfassung

Die adoptive zelluläre Immuntherapie (ACT), die genetisch modifizierte T-Zellen verwendet, die einen chimärischer Antigen-Rezeptor (CAR) exprimieren, um die T-Zell Spezifität zu reprogrammieren, stellt eine vielversprechende Methode bei der Immuntherapie von Tumoren dar. CD19-CAR T-Zellen konnten bereits beträchtliche klinische Ergebnisse bei der Behandlung von B-Zell Leukämien erzielen. Bei der Behandlung von soliden Tumoren allerdings, wird das Potenzial der ACT durch eine unzureichende und kurzlebige Immunität der T-Zellen, die auf ein immun-suppressives Tumormilieu stoßen, unterdrückt. Des Weiteren ist es äußerst schwierig ein tumorspezifisches Neoantigen zu identifizieren, welches eine geringe off-target Aktivität besitzt. Das EGFRvIII ist ausschließlich auf malignen Geweben exprimiert und zeichnet sich daher als ein vielsprechendes Antigen für die ACT bei der Behandlung von beispielsweise Glioblastomen aus, für welche bereits klinische Studien anstehen. Da EGFRvIII-CAR T-Zellen bisher nicht für die Behandlung vom nichtkleinzelligen Bronchialkarzinom (NSCLC) untersucht wurden, war es unser Ziel, die anti-Tumor Immunität von EGFRvIII-CAR T- Zellen gegen NSCLC sowohl *in vitro* als auch *in vivo* mithilfe eines Xenograft Tumormodells zu evaluieren. Humane, zuvor aktivierte T-Zellen wurden retroviral transduziert, und die CAR Expression wurde mittels Durchflusszytometrie 7 Tage nach Transduktion analysiert. Stabil transfizierte EGFRvIII$^+$ Zellen einer HLA Klasse-I/II defizienten Melanom Zelllinie (Ma-mel86) und die Adenomakarzinoma Zelllinie A549 dienten als Targetzellen. EGFRvIII-CAR T-Zellen wurden mittels ELISpot-, ^{51}Cr-Freisetzungs-, und Ko-Kultur Assays auf ihre Funktionalität untersucht. Zur Evaluierung des therapeutischen Potenzials in vivo, wurde ein T-Zell Transfer in NSG Mäusen durchgeführt, die zuvor mit EGFRvIII$^+$ Tumorzellen engraftet wurden. EGFRvIII-CAR T-Zellen induzierten starke Reaktivitäten gegen EGFRvIII$^+$ Targetzellen *in vitro*, ermittelt anhand der Ergebnisse der ELISpot Assays und spiegelten eindeutige Zytotoxizität sowohl im ^{51}Cr-Freisetzungsassay (<60%) als auch im 48h Ko-Kultur Assay (<90%) wider. Zudem haben wir EGFRvIII-CAR T-Zellen generiert, die von naiven CD45RA$^+$ T-Zellen stammen, und einen *stem cell memory (T$_{SCM}$)* Phänotyp aufweisen. Diese sind beschrieben worden, eine verbessere anti-Tumor Aktivität im Vergleich zu weiter differenzierten T-Zellen auszuüben. Die T$_{SCM}$ EGFRvIII-CAR T-Zellen zeigten eine vergleichbar gute anti-Tumor Aktivität im Vergleich zu den weiter differenzierten unselektierten total EGFRvIII-CAR T-Zellen hinsichtlich der Stimulation und Zytokin Sekretion von IFN-γ und Granzym B gegen EGFRvIII$^+$ Targetzellen *in vitro*. Um das therapeutische Potenzial der EGFRvIII-CAR T-Zellen *in vivo* genauer zu examinieren, ist eine Optimierung und genauere Betrachtung des Xenograft Mausmodells notwendig, um

Problemstellungen zu lösen, auf die wir in den präklinischen Studien gestoßen sind. Auch wenn EGFRvIII nicht zu den dominant auftretenden Mutationen beim nicht-kleinzelligen Bronchialkarzinom zählt, könnte die EGFRvIII-CAR Therapie wertvolle Informationen als *Proof of Concept* Studie für die Immuntherapie von Lungenkrebst liefern und möglicherweise dazu beitragen, die ACT für solide Tumore zu verbessern.

1. Introduction

1.1 A glance at the immune system

Our body's defense mechanism protects us from pathogens and microbes we are permanently exposed to and can be divided into two major components: the innate/nonspecific and the adaptive/specific immune system. The innate immunity comprises physical barriers such as the skin, epithelial cilia and antimicrobial proteins secreted on surface of mucosal surface. If these barriers are overcome, other components of the innate response come into play, always present to combat invading pathogens or toxins, including phagocytic leukocytes (macrophages and neutrophils) and small molecules such as cytokines and chemokines released upon activation. Furthermore, the innate immune system is characterized by membrane bound receptors and cytoplasmic proteins binding molecular patterns expressed on the surface of microbes [1]. All these cellular components originate from hematopoietic stem cells in the bone marrow. Two major lineages arise from pluripotent hematopoietic cells: the common myeloid lineage, comprising erythrocytes (red blood cells), megakaryocytes, granulocytes and platelets, largely contributing to the innate immune system. The lymphoid lineage gives rise to B cells, T cells, Natural killer cell (NK cells), and NK-T cells. NK cells are large granular lymphocytes that lack antigen-specificity but can recognize and eliminate malignant cells and are therefore considered part of the innate immunity. Response mechanisms of adaptive immunity are mostly based on antigen-specific receptors, encoded by gene elements, somatically rearranged to assemble T cell receptors (TCR) and immunoglobulins (B cell antigen receptor; Ig), that are expressed on the surfaces of T- and B- lymphocytes, respectively. Since adaptive immunity comprises only a small number of cells with high specificity for any antigen pathogen, toxin or allergen, the response takes more time to develop as cells must undergo clonal expansion upon antigen encounter. During the immune response most of the antigen-specific T cells undergo cell death, however some form an immune memory, conferred by the production of long-lived cells persisting in a dormant state and able to gain effector functions upon re-encounter with the same antigen, even decades after initial sensitizing. Both arms of the immune system, the innate and adaptive, are required to synergize to mount a fully efficient immune response-with the innate immunity being the first line of host defense, triggering the adaptive immunity, that develops in a few days and likewise recruits components of the innate immunity to boost the immune response.

1.2 T cell biology

1.2.1 T cell development

T cell receptors are encoded by variable, diversity and joining gene elements, somatically rearranged to form mature VαJα chains and VβDβJβ chains, resulting in the formation of millions of different antigen receptors, with an estimated number of 10^{20} [2] possible TCRs with exclusive specificity. Since non-functional genes are also assembled during that process, a selection of T cells bearing functional TCRs takes place in the thymus. Here, T cells must pass three compartments and are further distinguished by their selective surface expression of CD4 and CD8. In the subcapsular zone, double-negative thymocytes ($CD4^-CD8^-$), derived from the bone marrow start to differentiate, proliferate and rearrange their ß chains before reaching the cortex, where the α chain gene element rearranges to form a potentially functional αß TCR, further leading to the formation of double positive thymocytes ($CD4^+CD8^+$). In a process of a positive selection, developing lymphocytes are then tested for a sufficient affinity towards self-MHC molecules, allowing them to recognize antigen-MHC complexes [3]. If cells fail to do so, they undergo apoptosis and are eliminated by thymic cortical macrophages. Double positive cells selected by MHC class I molecules then become single-positive $CD4^-CD8^+$ and those selected by MHC class II molecules become $CD4^+CD8^-$. In the thymic medulla, cells are screened for potential autoreactivity, that includes testing reactivity towards a broad array of proteins expressed by epithelial cells in the thymus. Cells showing reactivity towards self-peptides derived from these cells also undergo apoptosis, remaining cells, that survive the positive and negative selection, roughly less than 5% are permitted to enter circulation. Lymphocytes then pass further post-thymic maturation stages, which includes downregulation of the CD3-TCR and the upregulation of CD28 to finally reach the status of mature naïve T cells [4]. Approximately 90-95% of circulating cells comprise αβ TCR, the other 5-10% are characterized by TCRs formed by γδ chains, that are similarly assembled by somatic rearrangement. αβ TCRs have progressed primarily to target antigens presented in a complex with MHC molecules. Both, the α and β chain of the TCR are composed of a variable (v) and a constant (c) region, with the antigen-binding site being formed within the v region of both chains.

1.2.2 Antigen recognition by the TCR

T cells detect foreign antigens if displayed on the surface of the body´s own cells by the expression of the highly variable TCR, a membrane bound protein that senses specific antigen and is associated with an intracellular signaling complex for T cell activation. T cells can only react to infected or malignant cells, recognizing both, a self-component and a microbial

structure. This problem is solved by the presence of MHC molecules encoded in a large cluster of genes known as the major histocompatibility complex (MHC). MHC molecules, known as human leukocyte-associated (HLA) antigens in humans, are cell surface glycoproteins expressed on all nucleated cells. There are two major types of MHC molecules: MHC class I molecules, that are further subdivided in 3 major classes namely HLA-A, HLA-B and HLA-C, that bind peptide fragments derived from intracellular or nuclear proteins. In general, CD8$^+$ T cells sense antigens presented by MHC class I molecules. MHC class II molecules are expressed constitutively on antigen-presenting cells (APCs), such as dendritic cells, macrophages and B cells and bind peptide fragments derived from the extracellular fluid that have been internalized by endocytosis. Antigens presented by MHC class II molecules are generally recognized by CD4$^+$ T cells. There are three major classes of HLA-class II molecules, designated as HLA-DR, HLA-DQ and HLA-DP. While the TCR binds to the antigen and to the MHC molecule itself, the coreceptors CD8 or CD4 only interact with the MHC class I or class II molecule, respectively. The necessity of the TCR to recognize both, antigen and MHC molecule is known as MHC restriction [1]. The TCR is stabilized by further accessory chains forming the CD3 complex, consisting of the invariant dimers CD3γε, CD3δε, and a largely intracytoplasmic homodimer of two CD3ζ chains, serving to transduce signaling [5]. A simplified schematic of the formation of the TCR/MHC complex is illustrated in Fig.1A. However, interaction of the TCR/CD3 complex with the antigen peptide is not sufficient for cell activation. For a full activation, additional interaction of a co-stimulatory molecule such as CD28 on the T cell with CD80 (B7.1) or CD86 (B7.2) on the antigen-presenting cell is required [6]. Inhibitory molecules such as CTLA-4 are also present on the T cell surface and competitively bind costimulatory ligands to release an inhibitory signal, which can result in T cell anergy or apoptosis. A third signal, conferring to optimal activation of CD8$^+$ T cells, are cytokines, such as IL-12 and IFN-γ that are secreted by APCs and are important for effector functions and proliferation of activated T cells (Fig.1B). The cytoplasmic portions of the CD3 chains contain sequence motifs designated immunoreceptor tyrosine-based activation motifs (ITAM), that are phosphorylated at key tyrosines. Binding of the coreceptors CD4/CD8 to the MHC triggers the phosphorylation of ITAMs by the lymphocyte-specific protein tyrosine kinase (Lck) [7], which initiates an activation cascade involving many downstream proteins, finally resulting in activation of genes that regulate lymphocyte proliferation and differentiation.
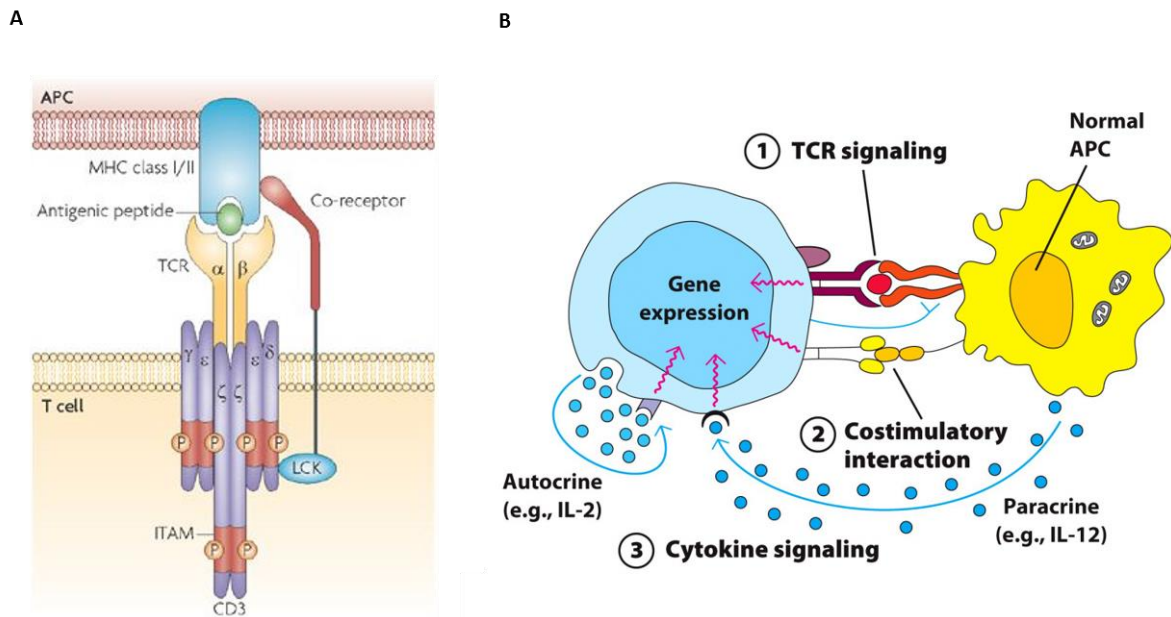
Figure 1:Activation of T cell receptor (TCR) upon antigen binding. (A) TCR complex associated with CD3 binds to antigen peptide presented by MHC class I or II molecule by an antigen presenting cell (APC). (B) 3-Signal Model for T cell activation, comprising formation of TCR-MHC-antigen complex, co-stimulatory interaction of CD28 with its ligand and cytokine signaling. (Adapted and modified from Gascoigne, 2009 and Freeman and Company, 2013).

1.2.3 T cell effector mechanism

When T cells are activated upon antigen encounter, they proliferate and differentiate into three types of effector T cells with distinct functions, including, killing, activation and regulation. Cytotoxic T cells kill cells, that are recognized as abnormal (infected with virus or other intracellular pathogens), helper T cells function by exerting signaling to recruit other immune cells and effect their behavior, and regulatory T cells are responsible for suppression of immune cells to control immune response. CD8$^+$ T cells are essential for elimination of infected or tumorigenic cells, by inducing apoptosis in the target cell. When cytotoxic CD8$^+$ cells recognize antigen on target cells, apoptosis is triggered by the calcium-dependent release of specialized lytic granules. These granules are secretory lysosomes containing the preformed highly cytotoxic effector molecules perforin and granzyme [8], which however are non-functional, until after their release. Perforin punches holes in the target cell membrane, enabling the serine proteases granzyme to enter target cell. Within the target cell Granzyme A causes single-strand breaks in the DNA and Granzyme B induces activation of caspase signaling, resulting in apoptotic cell death. Effector molecules are released by exocytosis in a narrowly focused manner, towards a defined contact point opposite the target cell (immune synapse), thus ensuring killing of single infected or malignant cells only, sparing healthy neighboring cells. Another mechanism to destroy target cells, similarly requires cell-cell contact between effector and target cells and involves binding of the Fas ligand, which is expressed on the surface of the CTLs to Fas receptor (Fas, CD95) on the target cell, inducing apoptosis by the classical caspase

cascade [9]. CTLs also secrete cytokines, such as IFN-γ and tumor necrosis factor α (TNFα) to boost their cytotoxic potential by increasing antigen presentation by MHC class I molecules and by enhanced expression of Fas on target cells [10].

1.2.4 T cell differentiation

T lymphocytes are designated naïve T cells until after encountering their specific antigen. Upon antigen encounter, T cells proliferate, differentiate and undergo clonal expansion. During immune response most of the cells that acquired effector functions undergo apoptosis. A small population persists as long-lived memory cells, able to exert a more rapid and efficient response if repeatedly exposed to the antigen. Memory T cells are further subdivided into central memory (T_{CM}), effector memory (T_{EM}) and the recently described stem cell memory (T_{SCM}) T cells, with the latter being the most less differentiated T cell subset, arising from antigenic stimulation. T_{SCM} cells share functional and phenotypic characteristics, reflecting properties of hematopoietic stem cells and can differentiate into all further T cell subsets [11]. The differentiation stages following antigen stimulation can be distinguished by the expression of various cell surface markers. For example, T_{CM} and T_{SCM} express high levels of the homing receptor L-selectin CD62-L and the chemokine receptor CCR7, enabling them to migrate to lymphoid tissues, whereas effector memory and terminally differentiated effector T cells (T_{EF}) display a low expression of these surface markers. An important marker to distinguish T_{CM} cells from T_{SCM} cells is CD45RA, an isoform of CD45, which is highly expressed on T_{SCM} but not on T_{CM}. For a precise description and definition of the different subsets several surface markers are used, as illustrated in Fig.2. The differentiation stages of T cells arising from the original naïve T cell have been reported to correlate with proliferative capacity and anti-tumor efficacy in the context of ACT, both decrease with progressing differentiations stages [12].

Figure 2: Memory subsets arising from naïve T cells upon priming. Different memory subsets are distinguished by surface marker expression patterns and their differentiation state correlates with proliferative capacity and anti-tumor efficacy (Irving et al., 2017).

1.3 Epidermal growth factor receptor

The epidermal growth factor receptor, a protein of a size of 170 kDa, is a member of the ErbB family of receptor tyrosine kinases (RTK) consisting of four receptors: ErbB-1 (EGFR), ErbB-2 (HER2 or Neu), ErbB-3, and ErbB-4 [13, 14], all sharing a similar structure. The EGFR gene is located at 7p11.2, which is the short (p) arm of chromosome 7 at position 11.2. The EGFR is composed of an extracellular ligand-binding and dimerization arm (exon1-16), a hydrophobic transmembrane domain (exon 17), and the cytoplasmic tyrosine kinase and C-terminal tail domains (exon 18-28) [15]. EGFR plays a pivotal role in regulating normal cellular growth, differentiation and survival in tissues of epithelial origin. Binding of its activating ligands leads to receptor homo-or heterodimerization with other members of the receptor family, which is essential for the activation and phosphorylation of the intracellular tyrosine kinase. Subsequent autophosphorylation triggers binding of specific signaling molecules containing Src homology 2 (SH_2) domains such as growth factor receptor-bound protein 2 (GRB2), phosphoinositide 3-kinase (PI3K) and signal transducer and activator of transcription (STAT) proteins [16, 17]. Association of these signaling proteins further initiates signaling pathways including

Ras/MAPK, Pi(3)K/Akt and others [18, 19]. Fig.3 gives a simplified overview of pathways activated by EGFR or its mutant variant EGFRvIII. Several ligands are known to bind to and activate EGFR, including epidermal growth factor (EGF), transforming growth factor α (TGF-α), amphiregulin, betacellulin, betacellulin, epigen, epiregulin, heparin-binding EGF etc. [20, 21]. Aberrant signaling, caused by receptor overexpression, mutation or ligand independent activation, however, is associated with development of various epithelial malignancies [22]. The EGFR was the first receptor that was linked with cancer progression [23]. Hence, EGFR has become a potential target for cancer therapy. Several EGFR gene mutations, either occurring in the intracellular tyrosine kinase domain or the extracellular ligand binding domain, have been described and linked with different cancers. The tumor specific EGFRvIII (also known as de2-7EGFR or deltaEGFR), which results from an in-frame deletion of 801 bp spanning exons 2-7, is the most common mutation of the extracellular domain. The truncated extracellular domain comprises a novel glycine residue at the junction site, that is absent from the wild type receptor [24].

The EGFRvIII is unable of binding any ligand but exerts a constitutive tyrosine activity, which is believed to be only 10% of the strength of ligand-induced wildtype (wt) EGFR signaling activity. However, as a result of impaired endocytosis due to inefficient ubiquitination and rapid recycling EGFRvIII signaling displays a prolonged signaling ability [25]. Constitutive activation of downstream signaling is thought to enhance tumorigenicity, as sustained activity of the Akt pathway ultimately results in proliferation, upregulation of the anti-apoptotic Bcl-X and transcription of genes promoting angiogenesis and invasion [26] . EGFRvIII activates signaling either through formation of transient homodimers or through heterodimers with EGFR or ErbB2 [27]. It has also been reported that EGFRvIII positive tumor cells secrete microvesicles expressing EGFRvIII into neighboring cells, which results in EGFRvIII mediated aberrant signaling in EGFRvIII negative cells [28] and thereby further enhances tumorigenicity. The tumor specific EGFRvIII mutation is associated and described for various malignancies such as head and neck squamous carcinoma, breast cancer, ovarian cancer, prostate cancer and lung cancer, in the case of Non-small cell lung cancer [29–31]. Most research has been performed on Glioblastoma Multiforme (GBM), a high-grade and most lethal neoplasm in adults, where the EGFRvIII is the most common mutation alongside with EGFR overexpression and occurs in 67-75% in cases of EGFR overexpression [32–34]. Various immunotherapies for GBM targeting EGFRvIII are being investigated in form of monoclonal antibodies, peptide vaccines and genetically modified T cells.
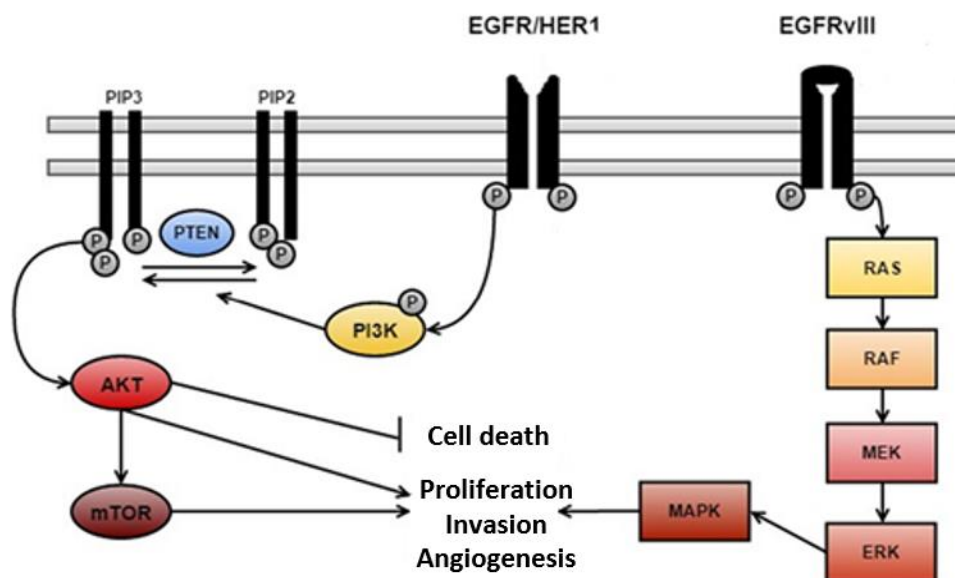
Figure 3: EGFR and EGFRvIII signaling pathways. Constitutive or aberrant activation of Pi3K/Akt or RAS/MAPK pathways confer to enhanced proliferation, invasion and angiogenesis (Mod. from Padfield et al. 2015).

1.4 Lung cancer

Lung cancer is the leading cause of cancer associated deaths with approximately 1.5 million incidences per year and a poor prognosis, with the 5-year survival rate being less than 18% [35]. Lung cancer is typically divided in small-cell lung cancer and non-small cell lung cancer, comprising 15% and 85%, respectively. NSCLC is further subdivided into adenocarcinoma, which is the most common form of lung cancer, squamous cell carcinoma, accounting for 25% and large cell carcinoma, accounting for about 10% of all lung cancers. Besides genetic risk factors and environmental exposures, cigarette smoking has been defined as the leading cause of lung cancers. The different stages of lung cancer are determined by whether the tumor is local or spread from lungs to nearby lymph nodes or metastasized to other organs. According to the staging different treatment options are available including surgery, radiation, chemotherapy, targeted therapy and immunotherapy, either alone or in combination. Due to a better understanding of the tumor biology and discovery of druggable oncogenic driver mutations treatment of lung cancer shifted towards personalized medicine to improve survival in selected patients [36]. This progress required genetic screening of cancer patients to match therapy according to molecular alterations. The mutation profile of lung cancer reveals a high heterogeneity with several mutations been described for NSCLC and KRAS being the most common (40%), followed by EGFR. Interestingly, frequencies of EGFR mutations vary greatly depending on region and ethnicity [37]. Most of the mutations affecting EGFR are described for the tyrosine kinase (TK) domain, whereas EGFRvIII mutation is described in <10% of

NSCLC and is associated with poor prognosis in NSCLC, breast and glioblastoma patients [38, 39].

1.4.1 Treatment of NSCLC

Surgery. If the tumor is found to be resectable and the patient is healthy enough, surgery is applied for stage I, II and some selected cases of stage IIIA patients, which is the most effective therapy in these stages. Hereby many surgeons utilize a video-assisted thorascopic surgery (VATS) to remove the lobe or section of the lung, containing the tumor. A thin tube with a light and a camera is inserted through a small incision on the chest, avoiding making larger incisions [40]. In order to prolong survival surgery is combined with chemotherapy and/or radiotherapy before (neoadjuvant) or after surgery (adjuvant) to eliminate remaining cancer cells [41].

Chemotherapy and Radiotherapy. For stage III NSCLC patients with unresectable tumor usually chemotherapy in combination with thoracic radiation is used. Radiotherapy aims to eliminate tumor cells at specific sites by damaging cells using high-energy beams. In cases of early-stage NSCLC with a single small nodule in the lung that didn't spread to nearby lymph nodes, the stereotactic body radiation therapy (SBRT) is used to enable delivery of concentrated and precisely located radiation treatment. This special technique is used for patients who are not suitable for surgery [35]. For late stage NSCLC patients radiotherapy is applied in a palliative manner to relieve symptoms. Since NSCLC doesn't cause prominent symptoms in early stages, the tumor is mostly diagnosed when already spread. About 40% of newly diagnosed NSCLC patients are stage IV and not eligible for surgery. In this case, first-line treatment is a combined cytotoxic chemotherapy, a Platinum-based doublet therapy in combination with another cytotoxic therapy. Treatment comprises mostly Cisplatin or carboplatin combined with docetaxel (Taxotere), gemcitabine (Gemzar), paclitaxel (Taxol and others), vinorelbine (Navelbine and others) or pemetrexed (Alimta) [42]. In case tumor growth control can be achieved upon initial chemotherapy (after four to six cycles) treatment, a maintenance therapy can be offered [43] . Decision of specific treatment combinations are influenced by additional factors such as, histology, age versus comorbidity and performance status and are made on individual basis [44]. However, advanced stage NSCLS have a poor prognosis with a median survival of 8-10 months [45].

Targeted Therapies. The discovery of mutated EGFR in NSCLC and the resulting sensitivity to EGFR TKIs led to development of molecular drugs targeting the EGFR pathway by inhibiting the tyrosine kinase domain of the receptor. Another option to inhibit EGFR activation is the implementation of monoclonal antibodies (mAbs) targeting the extracellular

domain. They inhibit EGFR signaling either by competitive inhibition of ligands binding to the receptor or by forming antibody-receptor complexes resulting in endocytosis and degradation. Based on published results of the Iressa Pan-Asia study, demonstrating significant improvement regarding progression-free survival (PFS) and overall response rate when comparing first-line Gefitinib versus Carboplatin/Cisplatin, Gefitinib was given regulatory approval by the FDA [46]. Initial response rates of clinical trials seemed to be inefficient regarding tumor control but showed significant response for a specific patient group: Asian ethnicity and never smokers [47, 48]. In the last decades immense progress has been made developing different EGFR TKIs and establishing this treatment as an option for first line treatment in advanced NSCLC patients. So far, Gefitinib, Erlotinib and Afatinib have been approved by the FDA [49]. The most common mutation causing sensitivity to EGFR TKIs comprises deletions in exon 19 and a missense mutation on exon 20 (L858R). First-generation TKIs target only EGFR and are reversible competitive ATP inhibitors, whereas second-generation TKIs (afatinib, dacomitinib) additionally target HER2 and HER4 and are irreversible inhibitors. Another mutation on exon 20, with a threonine-to-methionine substitution on codon 790 (T790M) is one cause of acquired resistance to first-generation TKIs, dampening the initial efficacy either by steric hindrance or increased affinity of the tyrosine kinase domain for ATP [50, 51]. The acquired resistance is reported to be developed after a median of one year of treatment [52]. Third-generation TKIs were developed to target the original sensitizing and the T790M mutation. Osimertinib, a third-generation TKI was applied for patients affected by a T790M mutation following progression after first-generation TKI [53] and exhibited better effects in terms of overall response rate and progression-free survival when compared to platinum base cytotoxic therapy [54]. Osimertinib was further evaluated in a randomized trial in comparison to gefitinib or erlotinib in previously untreated patients. Treatment with Osimertinib significantly improved progression-free survival and was thus established as a first-line treatment option [54, 55]. Further efforts were made to unravel additional gene alteration, including ALK rearrangements, ROS1 fusions and BRAF mutations, also leading to development of effective targeted therapies. However, overcoming acquired resistance, which in many cases is caused by rise of further mutations, and also occurs for ALK and ROS1 inhibitor treatment, remains one of the big challenges of TKI treatment.

Immunotherapy. To date, there are three main types of immunotherapy currently investigated for NSCLC patients: immune checkpoint inhibitors, therapeutic cancer vaccines and adoptive T cell transfer. Clinical trials investigating effects of adoptive T cell therapy and cancer vaccines are being conducted among lung cancer patients. The only immunotherapy drugs that

received approval by the FDA belong to the group of checkpoint inhibitors. Immune checkpoint blockers (ICB) target immune checkpoint pathways to prevent the immune system from limiting itself and to enhance the original tumor response. Monoclonal antibodies are used to target the inhibitory receptors cytotoxic T-Lymphocyte-associated antigen 4 (CTLA-4), which plays a key role in downregulation of T cell activation, proliferation and effector functions [56].Other targets include the programmed cell death-1 (PD-1) and its ligand (PD-L1). PD-1 signaling, mostly mediated by adaptive expression of PD-L1 within the tumor, results in inactivation of T cells hindering them from recognizing tumor-specific antigens, allowing the tumor to thrive [57, 58]. Thus, by blocking the PD-1 and PD-L1 axis, T cell mediated tumor response can be restored [59–61]. In 2015, the FDA approved the ICB nivolumab (Opdivo) for management of patients following disease progress during or after platinum-based therapy. Treatment with Nivolumab showed a significantly improved median overall survival in comparison to docetaxel among patients affected by tumor progression during or after platinum-based cytotoxic therapy [62, 63]. Currently there are three other FDA-approved ICBs for treatment of NSCLC: pembrolizumab (Keytruda) and atezolizumab (Tecentriq), which are used for late stage NSCLC and durvalumab (Imfinzi), which is used for patients at an earlier stage. Of note, as a first-line option, pembrolizumab was introduced as a standard of care for patients with advanced or metastatic NSCLC meeting the criteria of a minimum PD-L1 expression level of 50% in the tumor, which is true for approximately 30% of newly diagnosed patients. Combined treatment of pembrolizumab and carboplatin and pemetrexed showed improved overall response rate and progression-free survival among advanced NSCLC patients when compared to sole application of cytotoxic therapy [64]. According to studies that have been reported to date, approximately 20% of patients treated with ICBs responded to the treatment, including patients who were tested positive or negative for PD-1 and PD-L1 expression. Nevertheless, despite observing initial beneficial responses, most tumors acquire resistance to currently applied immunotherapies. Here also the challenge remains to find rational treatment combinations and pushing ICB treatment to earlier stages aiming to prolong survival. For this, it is necessary to find better predictors for response to immunotherapy and improve our understanding of acquired resistance mechanisms.

1.5 Cancer and the immune system

The role of the immune system in tumor development has been discussed by several influential immunologists of the last 100 years. In 1909, Paul Ehrlich considered a role of the host defense in preventing nascent transformed cells to develop tumors by stating that: "in the enormously complicated course of fetal and post-fetal development, aberrant cells become unusually

common. Fortunately, in the majority of people, they remain completely latent thanks to the organism's positive mechanisms." [65] The idea of the immune system as a defense mechanism against cancer was further formulated in the 1950s in the "immune surveillance hypothesis" by Burnet and Thomas, implying that cells of the immune system were able to recognize and destroy tumor cells. Still, despite immune surveillance, tumors do develop in patients with a functioning immune system. This is due to the complex nature of the relationship between immune system and cancer and so the hypothesis has been modified and described as the concept of "cancer immunoediting" by Dunn and Schreiber, which is divided into three phases: elimination, equilibrium and escape [66]. In the elimination phase, a more modern view of the immunosurveillance hypothesis, the innate (NK cells) and adaptive immune system (CD4$^+$ and CD8$^+$ T cells) detect and destroy tumor cells. In case that not all tumor cells are cleared, the theory describes the equilibrium phase, a temporary state where tumor cells are held functionally dormant by the immune system and some tumor cells acquire new changes, such as DNA mutations or changes in gene expression [67]. The adaptive immune system further exerts selective pressure keeping hold on tumor growth, but as it fails to completely remove transformed cells, tumor clones arise, that are able to resist or avoid antitumor response. Thus, leading to the escape phase, in which less immunogenic tumor cells progressively grow and become clinically detectable. Tumor cells are able to evade immune recognition due to loss of tumor antigen or MHC class I or co-stimulatory molecules, upregulation of pro-survival genes and by developing a immunosuppressive tumor microenvironment [66]. The escape from immune surveillance is now recognized as one of the "Hallmarks of Cancer" [68].

1.5.1 Immunotherapy for cancer

In recent years we could witness huge progress in the field of immunotherapy as for some cancers, such as melanoma and lymphoma unprecedented results have been shown, making it possible to establish immunotherapy as the fourth pillar of cancer treatment next to surgery, chemotherapy and radiation. Immunotherapy, also known as biological therapy, harnesses the body's own ability to fight cancer aiming to boost its immune response and to prevent the cancer from escaping the immune system. This can be achieved by either using the body's own cells or components manufactured in a laboratory to stop or slow down cancer growth. There are several approaches used for treatment, including monoclonal antibodies, cancer vaccines, oncolytic viruses or transfer of engineered T cells. The treatment also differs in terms of their targets, dosage and combination with other treatment options.

Oncolytic virus therapy is an emerging option in cancer treatment, that utilizes genetically modified viruses to destroy cancer cells, lacking many of anti-viral defenses at cost of their

growth potential. Virus is injected into the tumor resulting in cell lysis and release of antigens, which in return stimulates the immune system to target and eliminate malignant cells expressing the same antigen [69]. In 2015 the US FDA approved the oncolytic virus, T-VEC, for treatment of patients with advanced melanoma. T-VEC is modified to express GM-CSF to further stimulate proliferation of immune cells and is injected into areas of irresectable melanomas. There are several clinical trials ongoing exploring potential of oncolytic viruses for different tumor entities.

Cancer vaccines comprise two approaches: prevention vaccines and therapeutic vaccines. Prevention vaccines are administered to healthy people to prevent certain cancers from growing. Two commonly known and approved vaccines are the Human papillomavirus (HPV) vaccine approved to prevent cervical, vaginal and vulvar cancer and the Hepatitis B vaccine, as a long-lasting infection can result in liver cancer. Treatment vaccines are given to cancer patients with disease progression after treatment. The vaccines are either made of the patients own immune cells or employ destroyed cancer cells or specific cancer antigens. However, the only vaccine approved so far is the Sipuleucel-T, a dendritic cell vaccine used for treatment of metastatic prostate cancer, achieving an improved median survival of 4 months [70]. Currently many other vaccines are examined in clinical trials.

Monoclonal antibodies are drugs manufactured in the laboratory, some designed to target and destroy cancer cells expressing specific proteins. To mention a few, these include: Alemtuzumab, targeting CD52 often overexpressed on malignant lymphocytes, granulocytes macrophages and natural killer cells, is approved for lymphocytic leukemia patients with a disease progression after treatment with alkylating agents [71, 72]. Cetuximab is a chimeric (human/mouse) monoclonal antibody used for treatment with aberrant EGFR expression, such as colon cancer and head and neck cancer [73, 74]. Cetuximab targets the extracellular ligand binding domain of the EGFR resulting in its inactivation. Another type of mAbs, so called immune checkpoint inhibitors are used to release the brakes off the immune system, which are pushed at certain times to suppress immune response. Most inhibitors approved for cancer treatment target negative regulators of T cell activity, the cytotoxic T-lymphocyte antigen-4 (CTLA-4), programmed death-1 and its ligand PD-L1 [75, 76].

Adoptive cellular therapy represents one powerful modality for immunotherapy that involves isolation of the patients T cells, a makeover and expansion of T cells in the laboratory to polish their fighting potential against cancer cells. After sufficient expansion of T cells, they are

reinfused and seek out to target and destroy malignant cells. This approach will be further discussed in the following chapter.

1.6 Adoptive Cellular Therapy

Adoptive T cell therapy implies administration of tumor-specific cytotoxic T cells to cancer patients, aiming to recognize and eradicate malignant cells. Allogeneic hematopoietic stem cell transplantation is probably the first example of a cellular therapy demonstrating anti-cancer response of T cells; it not only turned out to be a simple replacement of leukemic bone marrow with healthy transplant, but also led to the recognition of graft versus leukemia effect [77]. There are different approaches practiced for ACT: tumor specific T cells, so called tumor-infiltrating lymphocytes (TILs) are either directly obtained from the tumor, or T cells are harvested from peripheral blood lymphocytes (PBLs), in which tumor specificity has to be induced through antigen-specific expansion. Another option is to redirect T cell specificity by genetic engineering using either conventional T-cell-receptors or chimeric antigen receptors (CARs), which are kind of artificial TCR. Tumor specific T cells are stimulated to grow, expanded in large numbers (up to 10^{11}) and are re-infused into the patient. The description of T cell growth factor IL-2 in 1976 as an adjuvant allowing to grow T cells ex vivo without loss of effector functions facilitated the development of ACT [78].

The first successful demonstration of ACT using autologous tumor infiltrating lymphocytes was conducted in 1988 leading to regression of cancer in patients with metastatic melanoma [79]. The short duration of responses however raised concerns, as rarely any transferred T cells were detected in the circulation just a few days after administration. A breakthrough was achieved in 2002 with studies showing that addition of lymphodepletion prior to ACT led to enhanced tumor response and prolonged persistence of transferred T cells [80]. Following lymphodepletion using a nonmyeloablative chemotherapy regimen, transferred T cells found in some patients comprised up to 80% of CD8$^+$ T cells in the circulation few months after T cell transfer. Despite impressive results achieved for treatment of some melanoma patients, same responses couldn't be repeated for other tumor entities, in which TILs where not detected or in which their culture seemed to be challenging. These obstacles led to studies of genetic engineering of T cells in order to broaden ACT approach for multiple tumor types. The first administration of TCR gene modified T cells was conducted in 2006. In this study T cells were redirected to express a TCR recognizing the MART-1 melanoma-melanocyte via retroviral gene transfer and their administration resulted in tumor regression [81]. The advantage of TCR gene modified T cells is that they can target both, intracellular and cell surface tumor associated antigens. Furthermore, TCR mediated antigen response engages with antigen-presenting cells

resulting in recruitment, activation and co-stimulation of further T cells, thus deploying the entire signaling network [82]. TCR redirected T cells can be engineered for many antigens, but due to HLA restriction of TCRs, new specificities have to be described for each tumor antigen and need to be matched with the patient's haplotype. Another key concern of TCR gene modified T cells is the possibility of TCR mispairing, as endogenous αß chains can pair with transgenic αß chains resulting in new specificities. Unlike TCRs, CARs provide an HLA independent recognition of the target antigen, enabling them to overcome one of the tumor escape mechanisms employed by tumor cells to hide from attacking T cells, which includes downregulation of HLA molecules or proteasomal antigen processing [83, 84]. CARs can target various antigens expressed on the surface of the tumor cell, including proteins, carbohydrates, and gangliosides [85, 86], regardless of HLA restriction, thus being universally applicable to a broader range of patients. In 2010 the administration of T cells genetically redirected to express the CAR against B cell antigen CD19 (CD19-CAR) exhibited regression in patients with advanced B cell lymphoma. These encouraging results paved the way for extensive development of genetically engineered T cells for cancer treatment. Since this project involves adoptive transfer of CAR modified T cells the following chapter will focus on CAR redirected T cells.

1.6.1 Chimeric antigen receptors

Chimeric antigen receptors are a kind of artificial TCRs that are composed of an extracellular, antibody derived single-chain variable fragment (scFv) that specifically targets a certain antigen, a hinge/spacer and a transmembrane domain linked to various combinations of intracellular signaling domains for T cell activation. Over time optimized CARs were developed to enhance T cell proliferation and persistence. First generation CARs comprise the endodomain of CD3ζ only, providing signal 1 of T cell activation. Second and third generation CARs include additional one or two costimulatory endodomains (mostly 41BB or CD28), respectively for signal 2 of T cell activation. Recently "armored CAR T cells" are being explored, known as the 4th Generation of CARs, developed to improve persistence in tumor microenvironment by coupling an additional gene to the vector for cytokine secretion (Fig.4). So far implication of CAR therapy for the treatment of blood-borne tumors has proven to be successful, emphasizing the unprecedented results yielded by CD19-CAR T cells treating relapsed B-cell acute lymphoblastic leukemia (B-ALL), chronic lymphocytic leukemia and B - cell non-Hodgkin lymphoma with complete remission ranging from 74% to 94% in different trials [87]. Several groups have demonstrated effective treatment targeting CD19 in patients with different hematological malignancies such as large-cell lymphomas, chronic lymphocytic

leukemia and follicular leukemia [88–90]. Since CD19 is expressed on healthy and malignant cells, patients are often affected by B cell aplasia, which however is mostly manageable by immunoglobulin treatment and attentive infection monitoring. Another side effect occurring due to T cell therapy includes cytokine release syndrome, its severity varies among the patients and is mostly treatable by administration of steroids or antibodies neutralizing IL-6 [91].
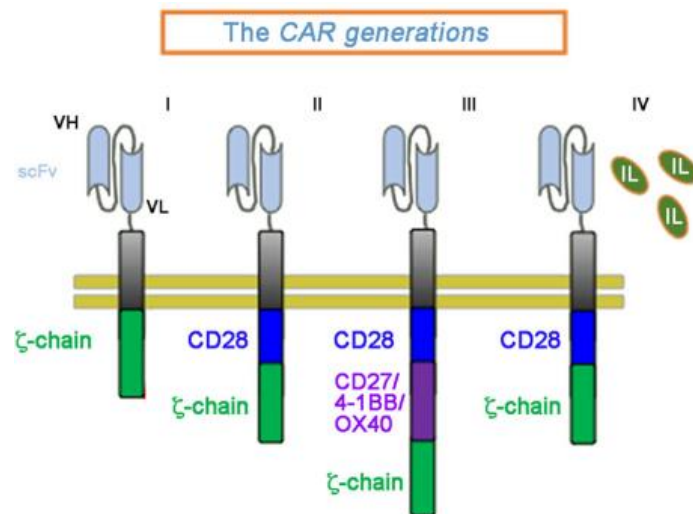
Figure 4: Development of different chimeric antigen receptor (CAR) generations. Development of different chimeric antigen receptor (CAR) generations. CARS are comprised of an antigen specific single chain variable fragment (scFV), a hinge/spacer, a transmembrane domain and intracellular signaling domains for T cell activation. First generation of CARS contain the stimulatory domain of CD3ζ only, second and third generation CARS were further equipped with one or two co-stimulatory domains (CD28/4-1BB), respectively. Fourth generation of CARS is further are so called armored CARS, additionally engineered for cytokine secretion (D`Aloia et al., 2018).

1.6.2 CAR-T cells for solid tumors

Solid tumors account for 90% of all cancer fatalities, yet convincing results couldn't be obtained following CAR therapy. The first brick for a promising ACT using CARs is finding an appropriate tumor associated antigen (TAA), which in the ideal case is selectively expressed, or at least only lowly expressed on the surface of malignant cells and not on essential normal tissues. Whilst CD19, only expressed on leukemic B cells and "dispensable B cells was found to be a promising target for some hematological malignancies, identification of such a promising target leading to similar success stories in solid tumor, remains challenging. There are approximately 30 antigens for solid tumors being examines in clinical trials, including mesothelin, carcinoembryonic antigen (CEA), the GD2 interleukin 13 receptor α (IL13Ra), human epidermal growth factor 2(HER-2) and fibroblast activation protein (FAP), just to mention a few [92, 93]. Most of the initial studies used first generation CARs and unfortunately clinical results have been disappointing, probably due to poor persistence and activation of T cells and other multifactorial reasons yet unknown. Besides, severe on/-target/off-target toxicity has been reported in some cases, such as the HER-2 CAR, resulting in a patient's death likely

due to reactivity with cognate antigen expressed in low level on lung epithelium [94, 95]. One countermeasure to prevent such incidence is using a scFv with a lower affinity, only able to be activated by high cell surface expression, occurring on the tumor cells only. Another option is to target antigens exclusively expressed on tumor, unfortunately there are only very few described, one example is the EGFRvIII. As a matter of fact, CAR T cells have to encounter additional issues fighting solid cancers, they do not have to face when targeting "liquid tumors". The challenge for a successful CAR therapy involves three major hurdles: finding a suitable TAA, dealing with the tumor microenvironment and selecting the ideal T-cell subpopulation.

Finding a suitable **tumor associated antigen** that is ideally only expressed on malignant cells is not an easy task to solve. One such attractive neoantigen is EGFRvIII, which is the most common oncogenic mutation of the EGF receptor, resulting from an in-frame deletion of 801 base pairs spanning exons 2 – 7 [96, 97]. Since EGFRvIII is expressed on cell surface and is known to promote tumor growth, migration, and therapeutic resistance and also correlates with a poor long-term survival [98] it appears to be an ideal target for CAR therapy. The EGFRvIII mutation occurs on ~40% of high-grade glioblastomas and attempts to target this molecule using CARs are in progress [99]. EGFRvIII CARs have already shown curative potential in treating animal models of glioblastomas [100, 99] and clinical trials testing their potential in patients with glioblastoma are in progress. There have been several reports claiming EGFRvIII expression on various cancers, such as pancreatic cancer, breast carcinoma, head and neck squamous cell carcinoma and as well lung carcinoma.

Another obstacle CAR-T cells have to face in solid tumors is a very unhostile **tumor microenvironment**. CAR T cells have to successfully traffic to and infiltrate to tumor sites, which might already be challenging due to chemokine/receptor mismatches. Most cancers are characterized by a stromal compartment, which not only promotes tumor growth but is also capable of inducing anergy in T cells. Even if able to infiltrate, T cell have to fight oxidative stress, acidic pH, hypoxia, low nutrients and the presence of myeloid derived suppressor cells, all together rendering T cells incapable of effective tumor response [101]. Attempts are made to target inhibitory pathways (PD-1/PDL1 And CTLA4) dampening T cell response [102, 103]. So called checkpoint inhibitors, monoclonal antibodies blocking these inhibitory pathways showed positive clinical results in various malignancies [104, 105]. So called "armored" CAR T cells, engineered to express cytokines such as IL-12 to increase T cell persistence, showed to reduce T cell suppression caused by the tumor microenvironment [106] . Combining Car T cell therapy with administration of checkpoint inhibitors or engineering "armored" CAR T cells

with features combating the unhostile TME could be one approach to boost results in anti-tumor response.
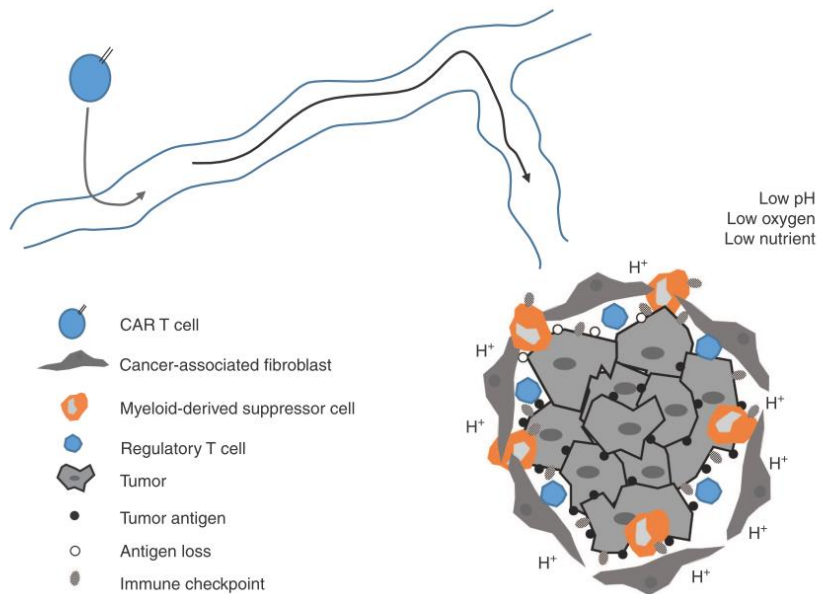
Figure 5: Immunosuppressive tumor microenvironment. Several negative factors, occurring in the tumor microenvironment of solid tumor contribute to ineffectiveness of CAR therapy (Newick et al., 2016).

Another issue that needs to be addressed is selecting **the ultimate T cell population** for therapy. Over time some effector cells undergo apoptosis while others differentiate into memory cells. It is also recognized that $CD8^+$ effector cells are hypo functional in the tumor microenvironment. As mentioned above they also struggle for an appropriate homing to tumor sites. There is growing interest in T memory stem cells for therapy. T_{SCM} are a rare T cell subpopulation that has proven enhanced capacity of self-renewal, engraftment and superior anti-tumor responses targeting B-cell malignancies [11, 107]. In a recent paper Gattinoni and colleagues published data on the generation of clinical grade CD19- CAR modified T_{SCM} for the treatment of human B-cell malignancies [108].

1.6.3 Generating early memory T cells (T_{SCM}/T_{CM}) for T cell therapy

Less differentiated T cells are valuable subsets for application in T cell therapy, as they are described to have a long-life-span, self-renewal capacity and enhanced proliferative potential. Therefore, several approaches have been examined to restrain T cell differentiation to generate less differentiated T lymphocytes reflecting T_{SCM} and T_{CM} properties. For example, Gattinoni et al. showed, that it was possible to arrest differentiation by mimicking canonical Wnt-signaling using the GSK3 inhibitor TWS119, while generating TCR redirected T cells. Of note, the outcome was accompanied by a firm inhibition of proliferation. It was further demonstrated, that specific cytokines, such as IL-7 and IL-15 support formation of early memory T cell subsets

[109]. The The PI3K-Akt-mTOR pathway plays an important role in regulation of CD8^{+} T cell metabolism, survival, migration and differentiation [110] . The PI3K-Akt pathway is activated by signaling caused by formation of the TCR-MHC complex, costimulatory molecules and cytokines, which further results in activation of downstream mammalian target of rapamycin (mTOR) complex-1 and cytoplasmic sequestration of Forkhead box protein O1 (Foxo1). (van der wart paper). High levels of Akt activation resulted in downregulation of adhesion molecules CD62L and CCR7 in studies conducted by Macintyre et al. Sustained exposure of IL-2 to CD8^{+} T cells was associated with higher Akt activity, driving CD8^{+} T cells towards terminal differentiation. Sustained activity of Akt and mTOR impacts the transcriptional program in a way, resulting in terminal differentiation of CD8+ T cells, accompanied by loss of FOXO activity and down-regulation of the Wnt/b-catenin pathway [111]. Thus, Van der Waart et al. aimed to arrest CD8^{+}T cell differentiation by pharmacological inhibition of the Akt pathway. In their study, they were able to generate early memory T cells reflecting a CCR7^{+}CD62L^{+} phenotype by inhibition of Akt-signaling pathway using Akt inhibitor VIII, displaying enhanced proliferative capacity and superior antitumor efficacy in melanoma bearing mice [112].

1.7 Motivation and aim of the study

There is growing interest in reprograming T-cells with a tumor-specific chimeric antigen receptor (CAR) targeting tumor associated antigens for treatment of cancer. CARs recognize their antigen in an HLA independent manner, enabling cells to override flaws in antigen presentation that might occur due to immunoediting. Recalling the success stories of CD19-CAR modified T cells for treatment of B-cell malignancies, CAR therapy holds great promise for adoptive T cell therapy. However, their potential still needs to be explored for treatment of solid tumors. One major limitation for achieving success with CAR modified T cells is finding a suitable tumor associated antigen (TAA) that is not expressed on healthy cells in order to avoid off target effects. The neoantigen EGFRvIII, which is the most common oncogenic mutation of the EGF receptor, resulting from an in-frame deletion of 801 base pairs spanning exons 2 – 7 appears to be an ideal target, as it is exclusively expressed on malignant cells, is accessible on the cell surface and is associated with tumor growth, migration, and therapeutic resistance and is further associated with a poor long-term survival. EGFRvIII CARs have already shown curative potential in treating animal models of glioblastomas and clinical trials testing their potential in patience with glioblastoma are in progress. There have been several reports claiming EGFRvIII expression on various cancers, such as pancreatic cancer, breast carcinoma, head and neck squamous cell carcinoma and as well lung carcinoma, in case of

NSCLC. Despite improving therapy options, NSCLC remains the most leading cause of cancer related deaths and overall survival rates are poor. Thus, exploring alternative therapy options to improve therapy outcome are indeed worth studying. EGFRvIII-CAR T cells have yet not been examined for treatment of NSCLS, or any other cancer besides glioblastoma. Hence, the aim of our studies was to investigate the efficiency of a third-generation EGFRvIII-CAR (kindly supplied by the Rosenberg laboratory, NCI) targeting EGFRvIII$^+$ cell lines. The EGFRvIII-CAR is comprised of a single chain variable fragment (scFv) targeting the neoantigen EGFRvIII, the transmembrane domain CD8, and two co-stimulatory domains CD28 and 4-1BB (CD137) along with the intracellular signaling domain CD3ζ [113]. For this purpose, EGFRvIII-CAR redirected T cells had to be generated by transduction of T cells with retroviral particles using the retroviral pMX-EGFRvIII-CAR vector, that allows a positive selection of EGFRvIII-CAR$^+$ T cells. Then, EGFRvIII$^+$ cell lines, including an adenocarcinoma (A549) cell line, had to be established, serving as target cells, to evaluate functional properties of generated EGFRvIII-CAR T cells, in regards of antigen-specific T cell response. Analyses of functional properties, involved, stimulation activity, cytokine secretion, lysis activity and redirected T cells were further examined for phenotypic characteristics in terms of cell surface markers, reflecting the subset composition and differentiation stage.

Since tumor responses of T cell therapy targeting solid tumors are often hampered by insufficient proliferation, persistence and exhaustion of T cells, attention has grown towards a less differentiated T cell population, preferentially T_{SCM} (stem cell memory T cells), that have been described to exert improved survival and anti-tumor reactivity targeting B-cell malignancies. Thus, we aimed to generate less differentiated T cells (naive EGFRvIII-CAR T cells) redirected to express EGFRvIII-CAR to evaluate their functional properties in comparison to unselected EGFRvIII-CAR T cells (total EGFRvIII-CAR T cells).

2 Materials and Methods

2.1 Materials and Consumables
2.1.1 Laboratory Equipment

Table 1: Laboratory equipment

equipment	Manufactured/distributed by
Co$_2$ Incubator (Heracell 150i)	Thermo Scientific (Waltham, USA)
Counting chamber (Blaubrand, Neubauer)	Sigma-Aldrich (Steinheim, Germany)
Cryo freezing container	Nunc (Wiesbaden, Germany)
Electrophoresis Chamber Mini Horizontal	neoLab (Heidelberg, Germany)
Electrophoresis Power Supply Ev231	Consort (Turnhout, Belgium)
Flow Cytometer (BD FACSCanto II)	BD GmbH (Heidelberg, Germany)
Freezer (Herafreez -80°C)	Heraeus (Hanau, Germany)
Gamma-counter (Wizard 2)	Perkin-Elmer, Rodgau
Heating block (Thermomixer 5436)	Eppendorf (Hamburg, Germany)
Heraeus Megafuge 16R	Thermo Scientific (Waltham, USA)
Ice machine (UBE 50/35)	Ziegra (Isernhagen, Germany)
Immunospot® Analyzer	CTL Europe GmbH (Bonn, Germany)
Incubator (Hera cell 240)	Incubator (Hera cell 240)
Irradiator ^{137}Cs cells (Gammacell-2000)	Moolsgard Medical (Gansloe, Denmark)
MACS Multistand	Miltenyi Biotec (Bergisch-Gladbach, Germany)
MACS Separator (Mini/Midi)	Miltenyi Biotec (Bergisch-Gladbach, Germany)
Magentic stirrer	Thermo Scientific (Waltham, USA)
Microscope (Axiovert 25)	Carl Zeiss AG (Jena, Germany)
Microwave	Bosch (Stuttgart, Germany)
MRX TC Revelation Microplate Reader	Dynex Technologies GmbH (Denkendorf, Germany)
Multi-channel pipette (200 µL)	Eppendorf (Hamburg, Germany)
Nitrogen cyro bank (Espace 331 Gaz)	Air liquid DMC (Marne-la-Vallée, France)
PCR Cycler T Personal	Biometra GmbH (Göttingen, Germany)
Pipettor (Pipetboy acut)	Integra Biosciences (Fernwald, Germany)
Pipettor (pipetus)	Hirschmann Laborgeräte (Eberstadt, Germany)
Precision scale (EW150-3M)	Kern (Balingen-Frommern, Germany)
Refrigator-Freezer Combo (+4 °C/-20 °C)	Liebherr (Ochsenhausen, Germany)
Single-channel pipettes (10 µL, 200 µL, 100 µL, 1000 µL)	Brand (Wertheim, Germany)
Single-channel pipettes (10 µL, 200 µL, 1000 µL)	Gilson (Middleton,USA)
Sorvall™ R66 Plus Centrifuge	Thermo Scientific (Waltham, USA)
Spectrophotometer (NanoDrop-1000)	Thermo Scientific (Waltham, USA)
Sterilework bench (Herasafe HS18)	Heraeus (Hanau, Germany)
UV-Transilluminator	Biostep (Burkhardtsdorf, Germany)
Vortex mixer	VWR (Darmstadt, Germany)
Water bath	Memmert (Schwabach, Germany)
Water deionization machine	Elga LabWater (Celle, Germany)

2.1.2 consumables

Table 2: Consumables

item	Manufactured/distributed by
Cell culture dish (60/145 mm)	Greiner (Frickenhausen, Germany)
Cell culture flask (T25/T75/T175)	Greiner (Frickenhausen, Germany)
Cell culture plate (6/12/24/48/96 well)	Greiner (Frickenhausen, Germany)
Cryo tubes	Greiner (Frickenhausen, Germany)
Disposable Scalpel	Feather Safety Razor Co. (Osaka, Japan)
MACS columns (LS/MS)	Miltenyi Biotec (Bergisch Gladbach, Germany)
Multiscreen HST IP 96-well filtration plate	Merck Millipore (Darmstadt, Germany)
Pipette tips (TipOne (10/100/1000 µL)	Starlab (Ahrensburg, Germany)
Polypropylene centrifuge tubes (15/50 mL)	Greiner (Frickenhausen, Germany)
QIAshredder spin columns	Qiagen (Hilden, Germany)
Reaction tubes (0.2/1.5/2 mL)	Eppendorf (Hamburg, Germany)
Serological pipettes (Cellstar 2/5/10/25 mL)	Greiner (Frickenhausen, Germany)
Syringe (5/10 mL)	BD (Heidelberg, Germany)
Syringe-filter (0.45 µm)	VWR (Darmstadt, Germany)
Transwellplates	Corning Costar (Amsterdam, NL)

2.1.3 chemicals, reagents and supplements

Table 3: Chemicals, reagents and supplements

item	Manufactured/distributed by
3-amino-9-ehtylcarvazole (AEC) tablets	Sigma-Aldrich (Steinheim, Germany)
Acrylamide	Merck (Darmstadt, Germany)
Agarose (StarPure)	Starlab (Ahrensburg, Germany)
Ammonium chloride (NH_4CL)	AppliChem (Darmstadt, Germany)
Ampicillin (100 mg mL^{-1})	Sigma-Aldrich (Steinheim, Germany)
Biocoll Separating Solution	Biochrom GmbH (Berlin, Germany)
Bovine Serum Albumin (BSA)	Sigma-Aldrich (Steinheim, Germany)
Bromphenolblue	AppliChem (Darmstadt, Germany)
^{51} Chromium ($Na_2{}^{51}CrO$, sodium chromate)	Amersham Bioscience
Dimethyle Sulfoxide (DMSO)	Carl Roth (Karlsruhe, Germany)
DNA Ladder (Gene Ruler 1kb Plus)	Thermo Scientific (Waltham, USA)
DNA Ladder (Gene Ruler 1kb)	Thermo Scientific (Waltham, USA)
DNaseI	Roche (Mannheim, Germany)
Ethanol (EtOH, > 99%)	Carl Roth (Karlsruhe, Germany)
Ethylenediaminetetraacetic Acid (EDTA)	Sigma-Aldrich (Steinheim, Germany)
FuGENE HD	Promega (Mannheim, Germany)
Gel Loading Dye Blue (6x)	NEB GmbH (Frankfurt, Germany)
GelRed Nucleic Acid Stain	Biotium (Hayward, USA)
NEBuilder® Hifi DNA Assembly Master Mix	NEB GmbH (Frankfurt, Germany)
Glacial Acetic Acid	AppliChem (Darmstadt, Germany)
Glycerol	Sigma-Aldrich (Steinheim, Germany)
Glycine	Sigma-Aldrich (Steinheim, Germany)

Hexadimethrine bromide (Polybrene)	Sigma-Aldrich (Steinheim, Germany)
Hydrogen peroxide (30%, H_2O_2)	Sigma-Aldrich (Steinheim, Germany)
Isopropanol	Carl Roth (Karlsruhe, Germany)
Kanamycin (50 mg mL^{-1})	Sigma-Aldrich (Steinheim, Germany)
LB-agar	Sigma-Aldrich (Steinheim, Germany)
LB-medium	Sigma-Aldrich (Steinheim, Germany)
Methanol	Carl Roth (Karlsruhe, Germany)
Nuclease-Free Water	Qiagen (Hilden, Germany)
Paraformaldehyde (PFA)	Sigma-Aldrich (Steinheim, Germany)
Phosphate buffered saline (PBS)	Gibco BRL (Karlsruhe, Germany)
Phytohaemagglutinin (PHA)	Murex Biotech (Kent, UK)
Potassium acetate (KoAc)	AppliChem (Darmstadt, Germany)
Potassium bicarbonate (KHCO 3)	Sigma-Aldrich (Steinheim, Germany)
Puromycin (10 mg mL^{-1})	Sigma-Aldrich (Steinheim, Germany)
RetroNectin®	Takara Bio Europe/ SAS (Saint-Germain-en-Laye, France)
RNase A	Thermo Scientific (Waltham, USA)
Sodium acetate (CH 3 COONa)	Sigma-Aldrich (Steinheim, Germany)
Sodium azide (NaN 3)	Merck (Darmstadt, Germany)
Sodium Chloride (NaCl)	Carl Roth (Karlsruhe, Germany)
Sodium hydroxide	Carl Roth (Karlsruhe, Germany)
Sodium pyruvate (100 mM)	Gibco BRL, Karlsruhe, Germany
Sodiumdodecylsulfat (SDS)	Carl Roth (Karlsruhe, Germany)
TransIT-LT1	Mirus (Madison, USA)
Tris Base	Carl Roth (Karlsruhe, Germany)
Tris(hydroxymethyl)-aminomethan (Tris)	AppliChem (Darmstadt, Germany)
TritonX 100	AppliChem (Darmstadt, Germany)
Trypan Blue (0.4%)	Merck (Darmstadt, Germany)
Trypsin-EDTA (1x)	Pan-Biotech GmbH (Aidenbach, Germany)
Tween20	Bio-Rad (München, Germany)
β-Mercaptoethanol	AppliChem (Darmstadt, Germany)

2.1.4 Media and additives for cell culture

Table 4: Media and additives for cell culture

item	Manufactured/distributed by
AIM-V medium	Gibco BRL (Karlsruhe, Germany)
Akt-Inhibitor VIII	Cayman Chemical (USA)
DNaseI	Roche (Mannheim, Germany)
Dulbecco's Modified Eagle's Medium	Gibco BRL (Karlsruhe, Germany)
Geneticin	Gibco BRL (Karlsruhe, Germany)
Heparin	Ratiopharm (Ulm, Germany)
Human albumin	CSL Behring, Marburg
Opti-MEM® reduced serum medium	Gibco BRL, Karlsruhe, Germany
Penicillin (10,000 IU mL^{-1})/ Streptomycin (10 mg mL^{-1})	Sigma-Aldrich (Steinheim, Germany)
Puromycin (10 mg mL^{-1})	Sigma-Aldrich (Steinheim, Germany)
RPMI Medium 1640 (1x) + GlutaMAX^{TM}-I	Gibco BRL, Karlsruhe, Germany
TWS119 Biozol	Biozol (Eching, Germany)
X-Vivo 15 medium	Lonza (Cologne, Germany)

2.1.5 Media, Buffers and Solutions

Table 5: Media, Buffers and Solutions

Cell Culture	
General freezing medium	
RPMI Medium 1640 (1x) + GlutaMAX^{TM}-I	
Heparin	10 IU mL^{-1}
Human albumin	8% (v/v)
DMSO (added prior to use)	10% (v/v)
Freezing medium for T cells	
Human serum	90% (v/v)
DMSO (added prior to use)	10% (v/v)
Erythrocyte-Lysis buffer	
Ammonium chloride (NH$_4$Cl)	8.29 g
Potassium bicarbonate (KHCO$_3$)	1.00 g
EDTA	0.037 g
Molecular biology	
TE-Buffer	
Tris (pH8)	10 mM
EDTA	1 mM
TAE-Buffer (50x)	
Tris base	242 g
Glacial acetic acid	57.1 mL
EDTA 0.5 M (pH 8.3)	
→Filled up to 1 L with dH$_2$O	
Buffers for DNA miniprep	
Resuspension Buffer	
Tris (pH 7.4)	50 mM
EDTA	10 mM
RNAse A	100 µg mL^{-1}
Lysis Buffer	
NaOH	200 mM
SDS	1%
Neutralization Buffer	
KoAC	3 M (pH 5.5)
Fluorescence activated cell sorting (FACS)	
Wash buffer	
PBS	
BSA	0,5% (v/v)
Sodium azide	1.0% (v/v)
Cell fixation buffer	
PBS	
Paraformaldehyde	0.4% (v/v)
Wash buffer for Protein L staining	
PBS	
BSA	4% (v/v)
Sodium azide	1.0% (v/v)
MACS-buffer	
RPMI Medium 1640 (1x) + GlutaMAX^{TM}-I	

DNase I	0.1% (v/v)

Enzyme-Linked Immunosorbent Spot (ELISpot) assay	
Acetate buffer	
Sodium acetate	2.88 g
Acetic acid	1.5% (v/v)
→ *Filled up to 1 L with dH₂O*	
AEC solution	
AEC tablets	10 tablets
N,N-dimethylformamid (DMF)	25 mL
Acetate buffer	500 mL
→ Tablets were dissolved in DMF, acetate buffer was added and the solution was sterile-filtered and stored at 4 °C in the dark. Prior to use, 0.5 µL mL^{-1} 30% H_2O_2 was added.	
ELISpot wash buffer	
PBS	
Tween 20	0.05% (v/v)
Avidin/HRP-complex solution (ABC-Complex)	
PBS	10 mL
Tween 20	0.01% (v/v)
Vectastain Elite Kit Reagent A	1 drop
Vectastain Elite Kit Reagent B	1 drop
→The solution was incubated 30 minutes at room temperature in the dark.	

^{51}Cr release assay	
Lysis Buffer	
PBS	10 mL
Triton 100	0.01% (v/v)

Colony Forming assay (CFA)	
Staining solution	
PBS	
Neisser solution	1% (v/v)
Fixation buffer	
PBS	
Paraformaldehyde	0.4% (v/v)

2.1.6 Enzymes, reagents and kits

Table 6: Enzymes, reagents and kits

Item	**Manufactured/Distributed by**
Elite Pu 1600 Standard Vectastain ABC Kit	Machery-Nagel (Düren, Germany)
Human IFN-γ ELISpot^{BASIC}	Mabtech AB (Nacka Strand, Sweden)
Human Granzyme B ELISpot^{BASIC}	Mabtech AB (Nacka Strand, Sweden)
GeneRuler 1 kb Plus DNA Ladder	Life Technologies, Darmstadt
NuecleoBond Xtra plasmid Midiprep	Sigma-Aldrich (Steinheim, Germany)
Gibbson Assembly	
Q5 Polymerase 2x Mastermix	New England Biolabs
Restrictionendonucleases (various)	New England Biolabs
Vectastain Elite ABC Kit	Vector Laboratories, Peterborough, UK
Q5 Polymerase 2x Matermix	New England Biolabs
Restrictionendonucleases (various)	New England Biolabs

2.1.7 Cytokines

Table 7: Cytokines

Item	Manufacturer
IL-2	Novartis (Nürnberg, Germany)
IL-7	R&D Systems (Wiesbaden, Germany)
IL-12	R&D Systems (Wiesbaden, Germany)
IL-15	R&D Systems (Wiesbaden, Germany)
IL-21	R&D Systems (Wiesbaden, Germany)

2.1.8 Antibodies

Table 8: Antibodies

Item	Manufacturer
T cell culture	
CD3 microbeads, human	Miltenyi Biotec GmbH (Bergisch-Gladbach)
CD8 microbeads, human	Miltenyi Biotec GmbH (Bergisch-Gladbach)
CD28 mAb (Clone: YTH913.12)	AbD Serotec (Puchheim, Germany)
CD45RA microbeads, human	Miltenyi Biotec GmbH (Bergisch-Gladbach)
Dynabeads® Human T-Activator for T cell Expansion and Activation	Thermo Scientific (Waltham, USA)
InVivomAB anti h CD3 (clone: OKT3)	BioXCell (West Lebanon, USA)
Flow Cytometry	
CD3 (APC)	BioLegend® (San Diego, USA)
CD3 (PE)	BioLegend® (San Diego, USA)
CD3 (FITC)	BD Biosciences (Heidelberg, Germany)
CD4 (PE)	BioLegend® (San Diego, USA)
CD4 (APC)	BD Biosciences (Heidelberg, Germany)
CD8 (APC)	BD Biosciences (Heidelberg, Germany
CD8 (FITC)	BioLegend® (San Diego, USA)
CD45 RO (APC)	Beckmann Coulter (Krefeld, Germany)
CD45 RA (APC)	BD Biosciences (Heidelberg, Germany)
CCR7 FITC	BioLegend® (San Diego, USA)
CD62L (PE)	Beckmann Coulter (Krefeld, Germany)
SA-PE	BioLegend® (San Diego, USA)
Goat anti-mouse IgG (PE)	BD Biosciences (Heidelberg, Germany)
Protein L	BioLegend® (San Diego, USA)
Anti EGFRvIII mAB L8A4	Absolut Antibody (Oxford, England)
HLA-ABC (FITC)	BD Biosciences (Heidelberg, Germany)
HLA-DR (APC)	BD Biosciences (Heidelberg, Germany)

2.1.9 Primers

All applied oligonucleotides were obtained by Sigma-Aldrich.

Table 9: Primers

Name	Sequence 5' → 3'	Description
P2A_fwd	CTAGTGCCACCAACTTCTCC	5' sequencing primer binding in P2A
P2A_rev	CATATCGATGGGCCCAGGGTT	3' sequencing primer binding in P2A
pMX_IRES_Puro_fwd	TTACACAGTCCTGCTGACCACC	5' sequencing primer binding upstream to MCS in pMXs vectors
pMX_IRES_Puro_rev	AAGCGGCTTCGGCCAGTAAC	3' sequencing primer binding in IRES
pMX_EGFRvIII-CAR-fwd	gatctagctagttaattaagGCCATGGTTCTGCTGGTCAC	5' primer for cloning of EGFRvIII-CAR into pMX_IRES-Puro
pMX_EGFRvIII-CAR-rev	cggccctcgaggcctgcaggTTAGCGAGGGGGCAGGGC	3' primer for cloning of EGFRvIII-CAR into pMX_IRES-Puro

2.1.10 Plasmids

All plasmids applied for the generation of retroviral supernatant, including transfer vectors and vectors for packaging and virus envelope are listed below.

Table 10: Plasmids

Name	Properties	Resistance
pMXs-IRES-Puro	Retroviral transfer vector, Mo-MulV-LTRs, psi packaging signal, IRES, puromycin-resistance	Ampicillin
pHIT60*	Retroviral packaging plasmid providing the gene products gag and pol	Ampicillin
pCOLT-GalV**	GalV envelope coding plasmid	Ampicillin
pMX-Mock	GFP control, tranfervector, puromycin-resistance	Ampicilin
pMSGV-EGFRvIII-CAR***	Retroviral transfer vector, encoding EGFRvIII-CAR sequence: h139scFv-hCD8-CD3ζ-CD28-4-1BB	Ampicilin
pMX-EGFRvIII*	Retroviral transfer vector encoding receptor sequence of EGFRvIII, puromycin resistance	Ampicilin
pMX-EGFRvIII-CAR	Retroviral transfer vector, encoding EGFRvIII-CAR sequence: h139scFv-hCD8-CD3ζ-CD28-4-1BB puromycin selection	Ampicilin

* kindly provided by Dr. Catherine Wölfel (University Medical Center, Mainz, Germany).
** kindly provided by Dr. Hakim Echchannaoui (University Medical Center, Mainz, Germany).
*** kindly provided by the Rosenberg laboratory (National Cancer Institute, Maryland, USA).

2.1.11 Cells

Phoenix-Ampho

Phoenix cells are a second-generation retrovirus producer cell line, stably expressing amphotropic envelope (pColtGalV) and the packaging plasmid pHit60. The cell line is a derivate of the HEK 293T cell line, which is a human embryonic kidney line transformed with adenovirus and carrying a sensitive T antigen. Phoenix-Ampho cells were cultured in Dulbecco's modified Eagle Medium (DMEM with 10% FCS, 1% Pen/Strep).

Ma-mel86b ko [CIITA]

The Ma-mel86b were originally established from the subcutaneous metastasis of a 57-year old female patient with metastatic melanoma. Due to a mutation occurring after few years of culture the cells show a deletion of the ß2-microglobin gene resulting in deficient HLA-class I surface expression. Furthermore, a knockout of HLA-class II was performed using TALEN technology (conducted and kindly provided by Dr. C. Wölfel, group of Prof. T. Wölfel) to generate the Ma-mel86b ko [CIITA] cell line, which are referred to as Ma-mel wt cells. Cells were cultured in RPMI 1640 GlutaMax (with 10% FCS 1% Pen/Strep).

Ma-mel EGFRvIII[+]

The Ma-mel86b ko [CIITA] cell line was additionally transduced with EGFRvIII via retroviral gene transfer using the retroviral vector pmX-EGFRvIII-IRES-Neo (conducted by and kindly provided by Dr. C.Wölfel) and are referred to as Ma-mel EGFRvIII[+]. For positive selection of transduced cells geneticin was added to the culture medium (1 mg/ml).

A549

The NSCLC (non-small cell lung cancer) cell line was derived from cancerous lung tissue of a 58-year old male and cells produced were adenocarcinomic alveolar basal epithelial cells. The cells are squamous in nature and grow adherently as a monolayer in vitro. The cell line was kindly provided by Prof Kaina (Institute of Toxicology, University Medical Center Mainz). A549 cells were cultured in Dulbecco's modified Eagle Medium (DMEM with 10% FCS, 1% Pen/Strep).

A549 EGFRvIII[+]

A549 cells were further modified to express EGFRvIII through retroviral gene transfer using the retroviral pmX-EGFRvIII vector with a puromycin resistance. For positive selection of transduced cells puromycin was added to the culture medium (1.75 µg/ml).

Renca EGFRvIII$^+$

This cell line was derived from a renal cortical adenocarcinoma in a male BALB/cCr mice (Murphy and Hrushesky, 1973). Cells were stably transduced with hEGFRvIII (Hills et al.,1995) and were kindly provided by Prof Wels (GSH, Frankfurt). Renca EGFRvIII$^+$ cells were cultured in Dulbecco's modified Eagle Medium (DMEM with 10% FCS, 1% Pen/Strep, 480 µg/ml Geneticin, 250 µg/ml Zeocin).

2.2 Cell culture
2.2.1 Culturing, Freezing and thawing of cells

All procedures of cell culture were performed under sterile conditions. Cell lines and primary cells were cultivated at 37°C and 5% CO_2 in an incubator with 95% humidity and were split as they reached a confluency of 70-80 %. Adherent cells were treated with Trypsin/EDTA for approximately 2-3 mins and cultivation medium containing 10% FCS or HS was added to stop the dissociation reaction. Cells were then resuspended, collected and centrifuged to remove Trypsin/EDTA solution and further cultivated as needed. For cryo-preservation, cell lines, PBMCs or T cell subsets were harvested, counted and frozen in 1 ml of their appropriate freezing medium containing 10% DMSO in different portions ($> 3x10^6$). Cryo tubes were first transferred in cryo boxes for gradual freezing in a -80° freezer. Next day, cryo tubes were placed in the cryo bank with liquid nitrogen. For thawing, cryo tubes were quickly thawed in the water bath at 37°C, washed with PBS to remove residual DMSO and were then further cultivated in the appropriate cultivation medium. For counting of cells trypan blue solution was applied to the cell suspension for a dead-live staining.

2.2.2 Isolation of PBMCs from human peripheral blood

Buffy coats from healthy donors were ordered in advance from the blood transfusion center of the University Medical Center, Mainz. Peripheral blood mononuclear cells (PBMCs) were isolated by density gradient centrifugation using Ficoll-Paque. 15 ml of Ficoll-Plaque solution was loaded in a 50 ml falcon tube and 35 ml of diluted blood (in a 1:1 ratio with PBS) were carefully layered on the top and centrifuged at 836g per 20 min in a swinging-bucket rotor with the brakes off. Then, the upper plasma layer was carefully aspirated, leaving the interphase containing lymphocytes, monocytes and platelets, undisturbed. The mononuclear layer was collected and transferred to a new 50 ml falcon tube collecting a maximum of 30 ml in one tube. Then, 20 ml of cold PBS was added, and samples were centrifuged at 1700 rpm for 10 mins. The supernatant was completely removed, and cells were washed twice with ice cold PBS

in subsequent centrifugation steps at 470 g for 5 minutes. PBMCs were then counted and either cryopreserved or used for further application.

2.2.3 Magnetic cell sorting (MACS) for isolation of T cell subsets

The isolation of various cell subsets with specific surface markers is based on magnetic microbeads that are coupled to mAbs. Cells are magnetically labelled by direct incubation with microbeads or first with biotin-coupled mAbs and a subsequent incubation with anti-biotin microbeads. Thus, cells can then be isolated on a MACS column in a magnetic field as unlabeled cell pass through and magnetically labelled cells are retained in the column and can be eluted when removed from the magnetic field. $CD3^+$ or $CD8^+$ T cells were isolated from freshly isolated PBMCs or from frozen aliquots using appropriate MACS beads and according to manufacturer's instructions. Volumes of reagents and buffers are given for up to 10^7 cells and were scaled up accordingly. In brief, PBMCs were counted, centrifuged and resuspended in 80 µl of MACS buffer per 10^7 cells. Then, cells were magnetically labeled by adding 20 µl of anti-CD3 or anti-CD8 Microbeads. After incubation at 4°C for 15 minutes cells were washed with 1-2 ml cold buffer per 10^7 cells by centrifugation at 300g for 10 minutes. The supernatant was completely removed and up to 10^8 cells were resuspended in 500 µl of buffer and depending on the cell number, applied on a MS or LS column. Cells were then separated, conducting three washing steps. The $CD3^+$ or $CD8^+$ T cells bound in the column are eluted, counted and cultivated in T cell medium for further application. Purity of isolated cells is analyzed via flow cytometry.

2.2.4 Culturing and activation of T-cells

PBMCs or isolated T cell subsets were cultured in AIM-V medium with 10% HS. For T cell activation, the culture medium is supplemented with immobilized OKT3 (0,5 µg/ml), anti CD28 (0,5 µg/ml) and IL-2 (100 U/ml). T cells are restimulated weekly by adding OKT3 and IL-2 to the medium.

2.2.5 Generation and culturing of naive/CD45RA$^+$ T cells.

In order to generate T cells with stem cell memory (T_{SCM}) and central memory (T_{CM}) like properties, we first isolated CD45RA$^+$ cells from PBMCs. First, a MACS isolation was performed using human CD45RA MicroBeads according to the manufacturer's instructions. Besides monocytes and NK cells, these cells mainly contain naïve T cells. The CD45RA$^+$ isolated cells were cultured in T cell medium and stimulated with OKT3 (0.5 µg/ml) and anti-CD28 mAb (0.5 µg/ml). Additionally, the cytokines IL-7 (5 ng/ml), IL-15 (5 ng/ml) and IL-21 (10 ng/ml) and Akt-Inhibitor VIII (4 µM) or TWS119 (5 µM) were added to the medium,

supporting the naïve like phenotype. On day 7 after CD45RA isolation, CD3$^+$ or CD8$^+$ cells were isolated by MACS technology and cells were restimulated with OKT3 (0.5 µg/ml), IL-7 (5 ng/ml), IL-12 (1 ng/ml), IL-15 (5 ng/ml) and IL-21 (10 ng/ml). However, after two weeks of culture IL-12 was replaced by IL-2 (50 U/ml). The differentiation stage of T cells was analyzed by flow cytometry after staining of surface markers specific for T$_{SCM}$ (CD45RA$^+$CD62L$^+$CCR7$^+$) or T$_{CM}$ (CD45RO$^+$CD62L$^+$CCR7$^+$).

2.2.6 Generation of retroviral supernatant

For the generation of retrovirus, a second-generation retrovirus producer cell line (Phoenix-Ampho) was utilized that stably expresses gag-pol and the envelope vector pColtGalv. The day before transfection 2 x10^6 Phoenix cells were plated in a 100 mm cell culture dish with 6 ml culture medium. For transfection, vectors for packaging and virus envelope (pHit60 and pColtGalv) and the retroviral transfer vector were added to 1.5ml Opti-MEM and mixed by pipetting up and down. Then, the transfection reagent Transit LT1 was added and the mixture was incubated for 20 minutes at RT and applied on Phoenix cells dropwise. Retroviral supernatant was harvested 48 hours after transfection and sterile filtered using a 0.45 µm pore sized filter.

	100 mm cell culture dish
Opti-MEM	1500µl
Transit LT1 transfection reagent	45µ
pHit60 (packaging vector)	5µg
pCOLTGALV (envelope vector)	5µg
Transfervector: pMX-EGFRvIII-CAR pMX-EGFRvIII pMX-Mock	10µg

2.2.7 Transduction of T-cells

T cells were reprogrammed to express either GFP (Mock) or the EGFRvIII-specific CAR, both containing a puromycin resistance, allowing for a positive selection of transduced cells. Two days prior to transduction T cells were polyclonally stimulated as described in (2.2.4) and retroviral supernatant was generated as described in 2.2.7. For transduction, T cells were harvested, counted and centrifuged. Cell pellet of 2 x 10^6 cells was resuspended in 500 µl of retroviral supernatant and transferred to a 24- well plate. In order to enhance virus cell contact polybrene was added to a final concentration of 5 µg/ml. The plate was centrifuged at 1500 rmp for 90 min at 37°C. After 18 hours, viral supernatant is removed from T cells and replaced by fresh T cell medium containing OKT3 (0.5 µg/ml) and IL-2 (100 U/ml). 2 days after

transduction, puromycin is added to the medium to select for transduced cells. Expression of GFP or EGFRvIII-CAR was analyzed via flow cytometry.

2.2.8 Transduction of the target cell line A549

The NSCLC cell line A549 (kindly provided by Prof. B. Kaina, Mainz) was used as a target cell line for transduced T cells. The wildtype A549 are negative for EGFRvIII expression. Thus, the cell line was modified via retroviral gene transfer to express human EGFRvIII with a retroviral vector bearing the human EGFRvIII gene sequence and a puromycin resistance. 2×10^5 cells were seeded in a 6-well plate one day prior to transduction. Then, 500 µl retroviral supernatant was directly applied to the cell medium for a total volume of 1 ml. Polybrene was added to a final concentration of 8 µg/ml. Cells were then centrifuged for 1 h at 1500 rpm at 37°C. 18 hours after transduction, the medium was discarded and replaced by fresh culture medium. 2 days after transduction, puromycin was added for a positive selection of transduced cells. Expression of EGFRvIII was analyzed by flow cytometry after cell surface staining using the EGFRvIII L8A4 antibody.

2.3 Flow cytometry

Flow cytometry is a laser-based technology allowing phenotype analysis using antibodies, labeled with fluorophores directed against surface markers or intracellular targets. In a flow cytometer single cells flow through a capillary and pass light beams with different wave lengths and intensity of emitted light is measured. Thus, a simultaneous measurement of relative size, granularity and fluorescence can be achieved.

Staining of tumor cells and T cells

For direct staining of surface markers approximately 2×10^5 cells were collected in a FACS tube and washed with 1 ml of FACS-buffer. Optimal amount of fluorochrome conjugated monoclonal antibody was added to 200 µl FACS-buffer and incubated for 15 minutes at 4°C in the dark. Cells were then washed with 1 ml of FACS buffer to remove unbound antibody before they were resuspended in 200 µl FACS-fix for fixation. Stained cells were analyzed using the flow cytometer BD FACS Canto II and the BD FACS DIVA software. Viable cells were gated using the FSC/SSC-channel and a total of 10^4 viable cells was measured.

EGFRvIII staining

To confirm expression of EGFRvIII in tumor target cells, cells were indirectly stained with the unconjugated monoclonal antibody L8A4 (mouse IgG). 1 µl of the antibody was added to 2×10^5 cells and incubated for 20 minutes at 4°C. Afterwards, cells were washed with 1 ml FACS-

buffer and cells were stained with the secondary PE labeled goat-anti-mouse IgG antibody for further 15 minutes at 4°C. Cells were washed again and subsequently fixed with FACS-Fix.

Protein L staining

For detection of EGFRvIII-CAR expression of modified T cells, biotinylated Protein L was utilized. Protein L binds to a portion of the scvF of the EGFRvIII-CAR. Approximately 2×10^5 cells were collected in a FACS tube, washed with FACS-buffer containing 4% BSA, before 1 µl of Protein L was added and incubated for 45 minutes at 4°C. Cells were washed three times with Wash-buffer and stained with SA-PE antibody for 15 mins at 4°C in 200 µl of FACS-buffer. Next, cells were washed again and fixed in FACS-fix.

2.4 Functional assays
2.4.1 Crystal violet staining

Adherent cells detach from cell culture plates during cell death, either caused by cytotoxic compounds or lysis by effector cells. A simple and fast method for an indirect quantification of cell death is staining of attached cells with crystal violet solution, which binds to proteins and DNA. The more cells lose adherence due to cell death the less the amount of crystal violet staining. This method was applied to quantify lysis of EGFRvIII expressing target cells by T cells induced in a 48 hours co-culture assay. 2×10^5 tumor cells/well were plated in a 24-well plate and allowed to grow adherent before 4×10^5 T cells were added the following day. After 48 hours, T cells growing in suspension were removed, and culture wells were washed with PBS. Remaining attached target cells were fixated with Fix-buffer for 10 min at 4°C and then stained with crystal violet solution (1% in PBS). The amount of crystal violet solution can be quantified by measuring the OD in a 96-well plate reader. For this, the crystal violet solution was dissolved using PBS with 1% SDS and transferred to a 96-well reader plate. Additionally, images were taken after the staining procedure.

2.4.2 Chromium Release Assay

The chromium release assay is a golden standard for precise quantification of cytotoxicity by stimulated T cells. Main steps of the procedure are: labeling of cells with radioactively labeled chromate, release of chromium upon T cell recognition, and detection of released chromium. For detection and quantification, a gamma counter was used.

Up to 1×10^6 target cells were labeled with 100 µCi Na_2 $^{51}CrO_4$ in FCS for 90 minutes at 37°C. After repeating washing with cell culture medium three times, cells were seeded in a V-bottom 96-well plate in duplicates (1.500 target cells/well in 80 µl cell culture medium). T cells were added to target cells at effector to target ratios ranging from 60:1 to 1:1 to a total volume of 160

µl/well. The culture plate was then incubated for 5 hours at 37°C. Additionally, controls were set up for spontaneous and maximum chromium release. Labeled target cells cultured with medium only served as negative controls (spontaneous release), whereas labeled target cells treated with PBS and 1% TritonX served as positive controls (maximum ^{51}Cr release). After incubation the plate was centrifuged at 262g with the brakes off and 80 µl of the supernatant of each well was transferred to a polystyrene tube for subsequent setup in the gamma counter. The lysis efficiency was quantified by following formula: [(experimental release – spontaneous release) / (maximum release - spontaneous release)] x 100.

2.4.3 IFN-γ and Granzyme B ELISpot Assay

The Enzyme-Linked Immunosorbent Spot Assay (ELISpot Assay) was applied to evaluate T cell response upon stimulation by target cells and is available for several cytokines. A capture antibody binds to the membrane of a 96-well EliSpot plate. T cells and target cells are seeded on antibody coated wells and are co- cultured for 18 hours. Secreted cytokines locally bind to the antibody and the amount can be measured in a color reaction using a biotinylated secondary antibody and an Avidin-peroxidase complex. The enzyme converts its substrate (AEC) in a color reaction, resulting in visible red spots. The number of spots correlates with the reaction intensity of T cells. IFN-γ and Granzyme B secretion of EGFRvIII-CAR and Mock T cells was assessed by ELISpot Assay. First, the membrane of the ELISpot Assay plate (Merck Millipore) was equilibrated with 20 µl of 35% ethanol and immediately washed with PBS. Next, plates were coated with either Granzyme B or IFN-γ capture antibody (15 µg/ml in 5% BSA in PBS or 10 µg/ml in 5% FCS in PBS, respectively) and incubated at 4°C over night. Unbound antibody was washed out with PBS and membranes were blocked with AIM-V medium containing 10% HS for 1 hour at 37°C. T cells and target cells were seeded in a 2:1 ratio as duplicates to a total volume of 100 µl. After 18 hours of incubation at 37°C, plates were washed 5 times with PBS and biotinylated antibody was loaded on the plate for 2 hours at 37°C. After washing, the avidin / HRP-complex solution, which is prepared 30 mins in advance, was added and plates were incubated for 1 hour at room temperature. Plates were washed with wash buffer, followed by a washing step with PBS, before 100 µl of AEC solution was added. The color reaction was stopped after 10 mins by washing plates with tap water. Membranes were left to dry and spots were quantified using the Immunospot Analyzer software (CTL Europe GmbH).

2.5 Molecular biology methods

2.5.1 cloning of the pMX-EGFRvIII-CAR

Cloning of the transfervector pMX-EGFRvIII-CAR was conducted using the NEBuilder Hifi DNA Assembly Master Mix, which is a fast and efficient method for DNA assembly of 2 or multiple fragments in one isothermal reaction. We used the NEBuilder HiFi Assembly Master Mix for cloning of the EGFRvIII-CAR insert into the retroviral vector backbone pMX-IRES-Puro, that was digested with BamHI and EcoRI. First, specific primers had to be designed, using the NEBuilder Assembly Tool. Two components must be covered for primer design: first, there needs to be an overlap sequence, required for the assembly of adjacent fragments, secondly a gene-specific sequence is required for template priming during PCR. A PCR was performed using the original pMSGV-EGFRvIII-CAR vector as a template to generate the EGFRvIII-CAR insert with flanking overlapping regions, complementary to the destination vector. The reaction mixture was prepared as followed.

Reaction Setup:

Components	amount
Q5 High-Fidelity 2X Master Mix	12.5 µl
10µM Forward Primer	1µl
10µM Reverse Primer	1µl
Template DNA (pMSGV-EGFRvIII-CAR)	1µl
Nucelase-Free Water	to 25µl

The PCR tube was transferred to a thermocycler with the following PCR protocol.

Step	Temperature	Time	Cycles
Initital Denaturation	98°C	30 seconds	1
Denaturation	98°C	10 seconds	25
Annealing	70°C	20 seconds	
Elongation	70°C	30 seconds	
Final Extension	72°C	2 minutes	
Hold	4°C		

The PCR product (EGFRvIII-CAR Insert) and the destination vector pMX-IRES-Puro (digested with BamHI and EcoRI) were assembled using the NEBuilder Hifi DNA Assembly Master Mix in one isothermal reaction. The reaction includes three different enzymes working together in the same buffer. The exonuclease creates single stranded 3´ overhangs and thus facilitates annealing of the overlap region. The DNA polymerase fills in gaps within each annealed fragment and the DNA ligase seals nicks in the assembled DNA.

The reaction mix was set up according to manufacturer's instructions.

component	amount
DNA ratio (vector:insert, 3:1)	X µl
Assembly Master Mix (2x)	10 µl
Deionized water	10- X µl
Total volume	20 µl

The reaction tube was incubated in a thermo cycler at 50°C for 50 minutes and subsequently used for transformation (2 µl of assembled product).

2.5.2 Transformation

Transformation of bacteria was performed to replicate plasmid DNA using competent One Shot Stable 3 bacteria (NEB). First, bacteria aliquots (50 µl) were thawed on ice and 50-100 ng of plasmid DNA were added and gently mixed by pipetting up and down. The transformation tube was placed on ice for 30 mins, heat shocked at 42°C for 45 seconds and was chilled on ice for another 2 minutes. Then, 950 µl of LB medium (without antibiotic) were added to the mixture, and the tube was placed in a shaking incubator at 37°C for 1 hour. In the meanwhile, selection plates treated with the appropriate antibiotics were prewarmed at 37°C. Afterward 100 µl of the bacteria was spread on the plate and incubated upside down overnight at 37°C. The following day, single bacteria colonies were picked to inoculate an overnight liquid bacterial culture with LB medium. Plasmid DNA was then isolated using the NucleoBond Xtra plasmid Midiprep Kit (Machery-Nagel) according to the manufacturer´s instruction.

2.6 Therapeutic potential of EGFRVIII-CAR modified T cells *in vivo*

NSG mice (from the NOD.Cg-Prkdcscid Il2rgtm1Wjl/SzJ strain) were used to evaluate the therapeutic potential of EGFRvIII-CAR modified T cells *in vivo*. Mice were housed under specific pathogen free condition in the Animal Facility of the University Medical Center Mainz and treated as given by instruction. All experimental procedures were conducted according to guidelines of the European Union and Germany and were performed under the supervision of S. Khan within the group od PD Dr. U. Hartwig.

2.6.1 Engraftment of EGFRvIII expressing tumor cells in NSG mice

To assess kinetics of tumor engraftment different doses of EGFRvIII$^+$ tumor cells were tested in cohorts consisting of five mice. Three different tumor cell doses were tested for the Ma-mel EGFRvIII$^+$ cells ($1x10^6$, $2.5x10^6$ or $5x10^{6)}$) and two for the A549 EGFRvIII$^+$ cells ($1x10^6$, $2x10^6$). Every mouse received the appropriate tumor cell dose in 200 µl PBS supplemented with 0.5% FCS by subcutaneous injection into the right flank. Tumor growth was monitored

for 16 days by calipering and tumor volume was measured as soon as palpable every second day.

2.6.2 Adoptive T cell transfer in EGFRvIII⁺ tumor engrafted mice

Tumor bearing mice, that were engrafted with 2×10^6 A549 EGFRvIII⁺ tumor cells, received adoptive T cell transfer, when tumor volume reached about 100 mm^3 (7 days post tumor cell engraftment). Mice were randomized into three different cohorts, receiving either Mock T cells, EGFRvIII-CAR T cells or no T cells at all. The adoptive transfer of T cells was performed 5 days after restimulation of T cells to provide optimal condition for growth and reactivity. 4×10^6 T cells were administered in 200 µl PBS supplemented with 0.5% FCS by intratumoral injection. Each cohort consisted of 4 mice. The day before T cell transfer, T cells were phenotypically analyzed by flow cytometry and a colony forming assay or ELISpot Assay was conducted to confirm T cell reactivity in vitro. After T cell transfer, tumor growth was monitored every second day by measuring the tumor volume with the caliper until mice were sacrificed for endpoint analyses.

2.6.3 Endpoint analysis after adoptive T cell transfer in tumor engrafted NSG mice

The final tumor volumes were measured 7 days after adoptive transfer of T cells. Then, mice were sacrificed by cervical dislocation for endpoint analyses, that included analyzing the tumor mass for EGFRvIII expression, T cell presence and presence of myeloid derived suppressor cells (MDSC). Furthermore, spleen, bone marrow and peripheral blood were analyzed for the presence of T cells. Thus, tumor mass was excised, gently disrupted in small pieces and placed in a falcon tube with RPMI 1640 medium supplemented with Collagenase (0.5 mg/ml) for 30 mins at 37°C. Afterwards tumor cell suspension was pressed through a 100 µm cell strainer, centrifuged and washed with FACS buffer for subsequent staining of T cell surface markers. And EGFRvIII expression. Additionally, tumor cells were stained for markers of myeloid derived suppressor cells. Spleens were also taken out and shredded through a 100 µm cell strainer and washed out with 2 ml of prep medium. Furthermore, the femur was excised and cut at both ends to flush out bone marrow with prep medium using a syringe. Then, bone marrow and spleen suspension were centrifuged and incubated in lysis buffer for 3 min. Samples were washed again with prep medium followed by a washing step in FACS buffer for further staining of T cell surface markers.

3 Results

3.1 Experimental work flow

A simplified scheme giving an overview of the work flow for this project is illustrated in Fig.6. The EGFRvIII chimeric antigen receptor (EGFRvIII-CAR), a third generation CAR comprising two co-stimulatory domains (CD28 and 4-1BB) along with CD3ζ as the intracellular signaling domain, was originally derived from the pMSGV-EGFRvIII-CAR vector, provided by the Rosenberg laboratory (NCI, Maryland). First, we cloned the EGFRvIII-CAR sequence into the retroviral vector pMX-IRES-Puro to enable a positive selection of transduced cells by puromycin treatment. The cloning procedure is explained in paragraph 3.2. T cells were isolated from a buffy coat and stimulated polyclonally 2-3 days prior to transduction. Retroviral particles were generated by transfecting Phoenix-Ampho cells and harvested 48 hours after transfection to be used for transduction of T cells. Puromycin was added 48 hours after transduction and T cells were analyzed for phenotypic characteristics and EGFRvIII-CAR expression by FACS analyses. Several functional assays were conducted to assess cytokine response and lysis potential of EGFRvIII-CAR T cells upon antigen encounter *in vitro*. For this purpose, target cell lines were generated to express EGFRvIII by retroviral transduction. Mock T cells, transduced with pMX-Mock vector, containing GFP only, were used as control cells in all assays. Next, lysis potential of EGFRvIII-CAR redirected T cells was examined in a xenograft NSG mouse model.Therefore, engraftment kinetics of EGFRvIII transfected cell lines (Ma-mel EGFRvIII$^+$, A549 EGFRvIII$^+$) were first assessed in NSG mice by subcutaneous injection of tumor cells to determine appropriate tumor cell doses and time point to start T cell therapy. Tumor bearing NSG mice were then treated with Mock or EGFRvIII-CAR redirected T cells or left untreated and sacrificed for endpoint analyses 8 days after T cell administration.

Furthermore, for *in vitro* studies, EGFRvIII-CAR redirected T cells with a less differentiated state, reflecting a stem cell memory and central memory phenotype (T_{SCM}/T_{CM}), were generated according to a protocol established in preliminary studies for CD19-CAR T_{SCM}/T_{CM} cells. Naïve T cells were preselected from PBMCs by MACS isolation using CD45RA microbeads and were cultured with Akt Inhibitor VIII and a special cytokine mix, promoting T_{SCM}/T_{CM} phenotype. Several functional assays were performed to characterize functional properties of EGFRvIII-CAR redirected naïve T cells.
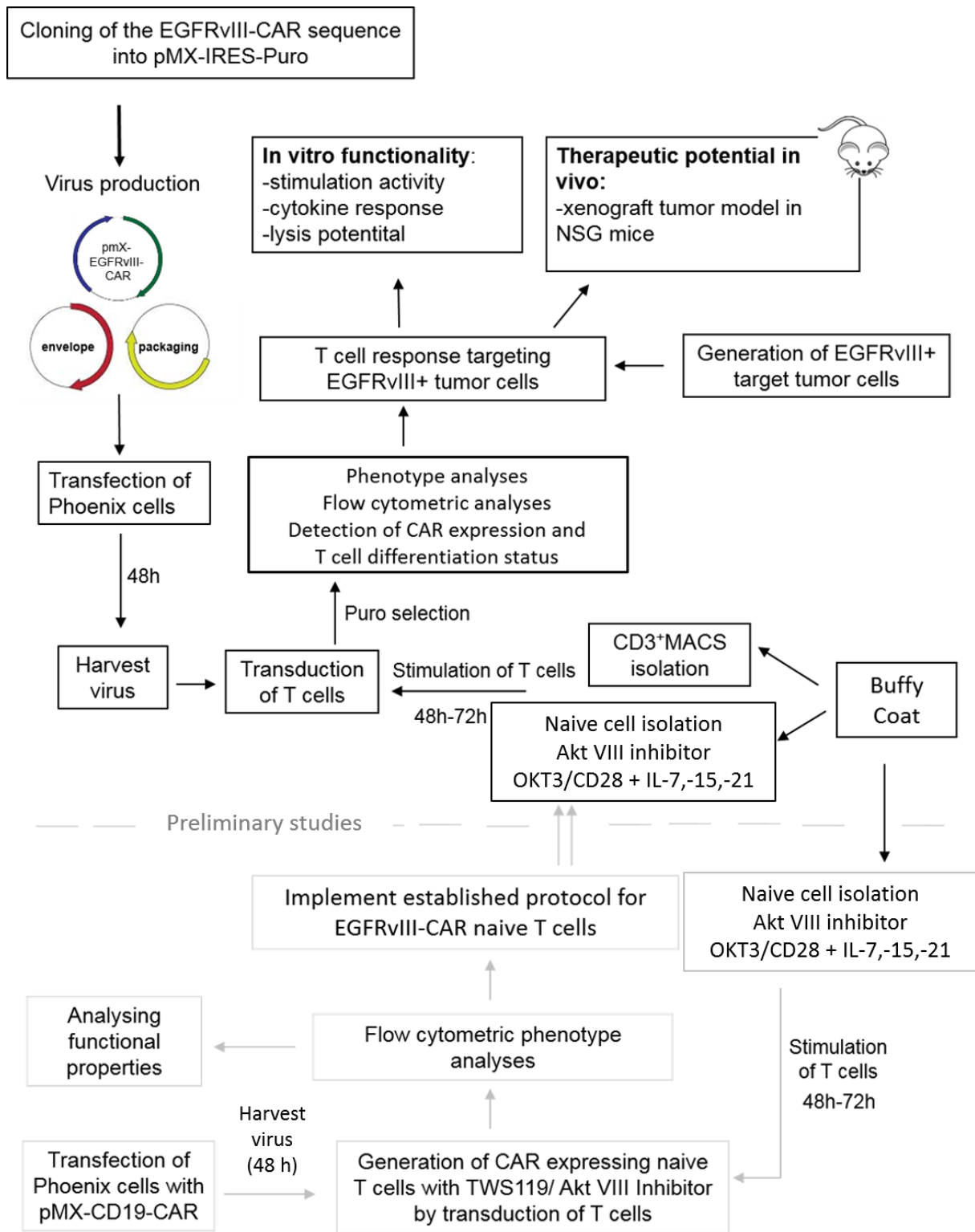
Figure 6: Simplified work flow.

3.2 Cloning of the EGFRvIII-CAR sequence into pMX-IRES-Puro

In this study, retroviral vectors served as important tools to modify T cells genetically by redirecting their specificity towards EGFRvIII. For this purpose, a third generation CAR, comprising two co-stimulatory domains (CD28, 4-1BB) along with CD3ζ was used. The EGFRvIII-CAR encoding sequence was first cloned into the retroviral pMX-vector containing a puromycin resistance gene to enable a positive selection of transduced cells. The cloning procedure is illustrated in Fig. 7A. Specific primers were designed to amplify the EGFRvIII-CAR sequence with appropriate overlapping ends for cloning into the linearized pMX-IRES-puro vector. The primers contained an overlap sequence at the 5´end homologous to the 5´end of the destination vector and a gene-specific sequence added after the overlap sequence for template priming. The pMSGV-EGFRvIII-CAR plasmid, kindly provided by the Rosenberg laboratory, served as a template. The expected size of the EGFRvIII-CAR insert is 1647 bp, which was confirmed by gel electrophoresis (Fig. 7B). The linearized destination vector pMX-IRES-Puro and the EGFRvIII-CAR insert were added to the NEB HiFi Assembly reaction mix to introduce the EGFRvIII-CAR insert into the pMX-IRES-Puro vector. Assembled DNA was used for transformation and single bacterial clones were picked to grow liquid bacterial cultures. Plasmid DNA was isolated and sent for sequencing using a forward and reverse primer, both binding to the vector backbone at flanking ends of the EGFRvIII-CAR sequence. For verification, sequencing results were aligned with the original CAR sequence (Fig. 7C), demonstrating a 100% alignment (red font). The cloned vector is henceforth referred to as pMX-EGFRvIII-CAR and was used to produce retroviral particles for T cell transduction. Another pMX vector encoding GFP only was used as a control vehicle (pMX-Mock).
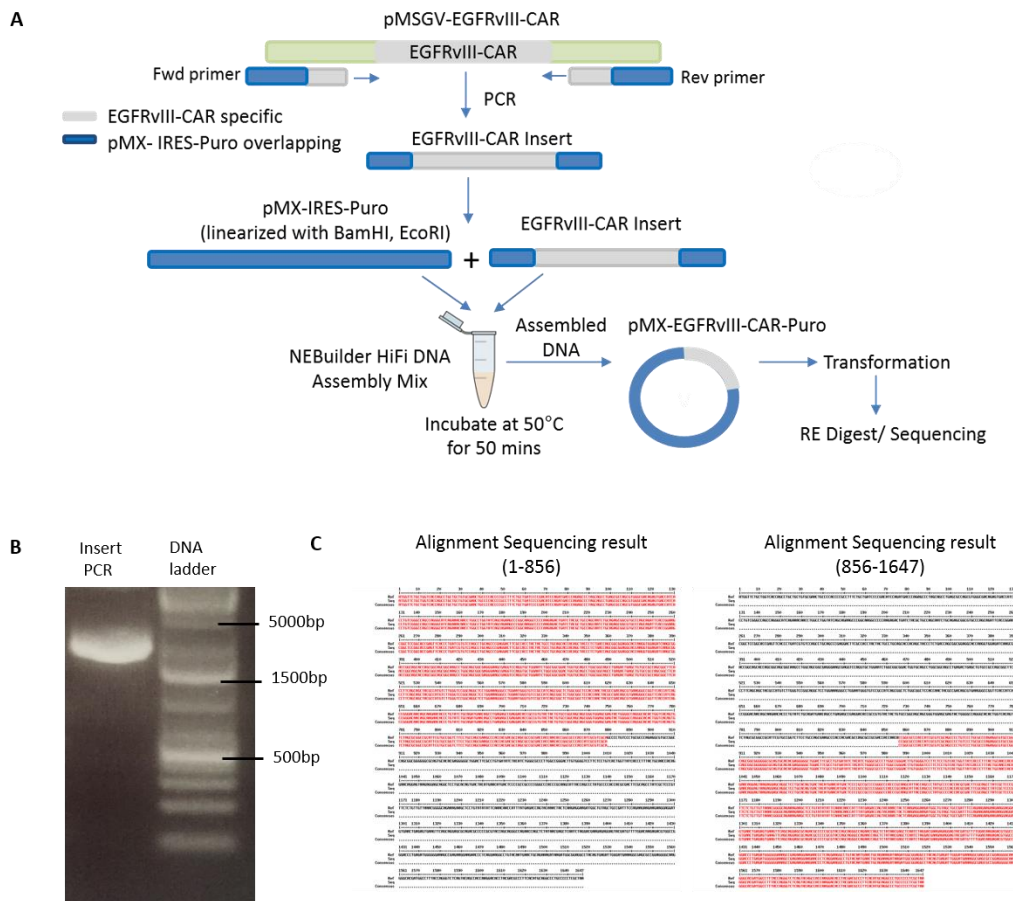
Figure 7: Cloning of the pMX-EGFRvIII-CAR vector. (A) Cloning procedure: EGFRvIII-CAR fragment was amplified using specific primers generating appropriate overlaps homologous to both ends of linearized pMX-IRES-Puro vector. Generated Insert fragment was assembled with linearized pMX-IRES-Puro using the NEBuilder Hifi DNA Assembly Kit and assembled DNA was subsequently used for transformation. After plasmid isolation and analytic digestion DNA was sent for sequencing. (B) Amplified insert fragment (EGFRvIII-CAR). Correct size of amplified PCR product, with an expected size of 1647 bp was analyzed by gel electrophoresis. The 1kb-plus DNA ladder was used as a marker. (C) Sequence verification of EGFRvIII-CAR: After cloning of EGFRvIII-CAR Insert into pMX-IRES-Puro the sequence was verified using forward and reverse primers binding to pMX-IRES-Puro flanking both ends of EGFRvIII-CAR fragment. Sequencing results were aligned with reference sequence. Homologous sequences are highlighted in red.

3.3 Generation of CAR redirected T cells

Retroviral vectors provide a stable and long-term gene expression in transduced cells and their progeny as they stably integrate into the host´s genome. In this study, T cells were modified to express either GFP or the EGFRvIII-CAR by viral gene transfer using the retroviral vectors pMX-Mock and pMX-EGFRvIII-CAR, respectively. Phoenix-Ampho cells were transfected with retroviral vectors to generate viral particles for T cell transduction.

3.3.1 Transfection of Phoenix-Ampho cells

Phoenix-Ampho cells are a packaging cell line, stably expressing the plasmids pCOLTGalV (envelope) and pHit60 (packaging). Transfection of Phoenix cells was performed as described in 2.2.6 and retroviral supernatant was collected 48 hours post transfection. In parallel, Phoenix cells were harvested to analyze transfection efficiency by FACS analysis before retroviral supernatant was used for transduction. Phoenix cells transfected with pMX-Mock-Puro were analyzed for GFP expression and cells transfected with pMX-EGFRvIII-CAR were analyzed

for EGFRvIII-CAR expression applying the ProteinL staining procedure (see section 2.3). A representative image of FACS analysis shows successful transfection for both retroviral constructs. Fig. 8A depicts a transfection efficiency of 88% for pMX-Mock transfected cell, assessed by GFP expression. Phoenix cells transfected with pMX-EGFRvIII-CAR revealed a transfection efficiency of 74% (Fig. 8B).
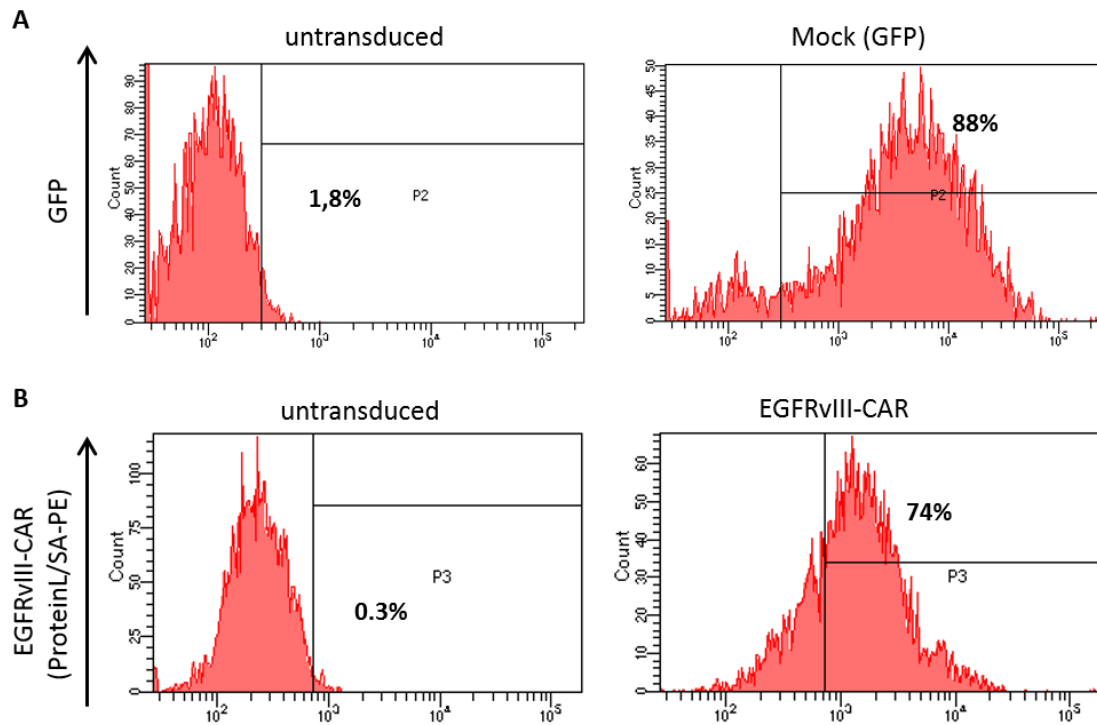

Figure 8: Transfection of Phoenix cells. Phoenix cells were transfected with retroviral vectors for generation of viral particles. Transfection efficiencies were analyzed 48 hours post transfection by FACS analysis using the BD Canto II. Representative images of flow cytometric analysis depict GFP expression of pMX-Mock transfected Phoenix cells (A) and expression of EGFRvIII-CAR following ProteinL/SA-PE staining in Phoenix cells transfected with pMX-EGFRvIII-CAR (B).

3.3.2 Phenotypic analyses of modified T cells.

For an efficient infection and integration of retroviral vectors proliferating cells are a prerequisite. Due to this limitation T cells were stimulated 2-3 days prior to transduction. To obtain T cells peripheral blood mononuclear cells (PBMCs) were isolated from buffy coats provided by the Blood Transfusion Center of the University Medical Center Mainz (UMM). PBMCs were seeded in a 24-well plate at a density of $2x10^6$ cells/well and were stimulated polyclonally by adding anti-CD3 (0.5 µg/ml), CD28 (0.5 µg/ml) and IL-2 [100 U/ml] (AIM-V +10% HS) to stimulate growth of CD3$^+$ T cells (see section 2.2.7). T cells were usually used 48-72 hours after stimulation for transduction when they appeared to be efficiently stimulated, as observed by microscopy. They were either modified to express GFP (Mock T cells) or EGFRvIII-CAR (EGFRvIII-CAR T cells) via spin infection. Transduced cells were then selected by puromycin treatment at 1.5 µg/ml according to a puromycin titration kill established beforehand to determine the lowest puromycin concentration necessary for cell death of

untransduced cells within 6 days. CD3$^+$ T cells (CD4$^+$/CD8$^+$) or CD8$^+$ T cells were isolated from the PBMC population by applying magnetic associated cell sorting (MACS) and were analyzed for GFP and EGFRvIII-CAR expression. Representative images of flow cytometric analysis show effective selection of transduced cells after puromycin treatment. The initial transduction efficiency for Mock T cells was 24%, as assessed by GFP expression of T cells (Fig.9A). Similar transduction efficiency was achieved for EGFRvIII-CAR T cells (19.8%). However, after T cells were cultured in the presence of puromycin, resulting in a positive selection of transduced cells, the portion of GFP positive T cells increased to 92.6%. Similarly, the level of EGFRvIII-CAR expressing T cells increased to 93.4% (Fig.9A). To obtain a pure T cell population, CD3 MACS isolation was performed on transduced cells. The CD3 MACS yielded a high purity of almost 100%, as demonstrated in Fig.9B after staining isolated T cells for CD3 surface expression.
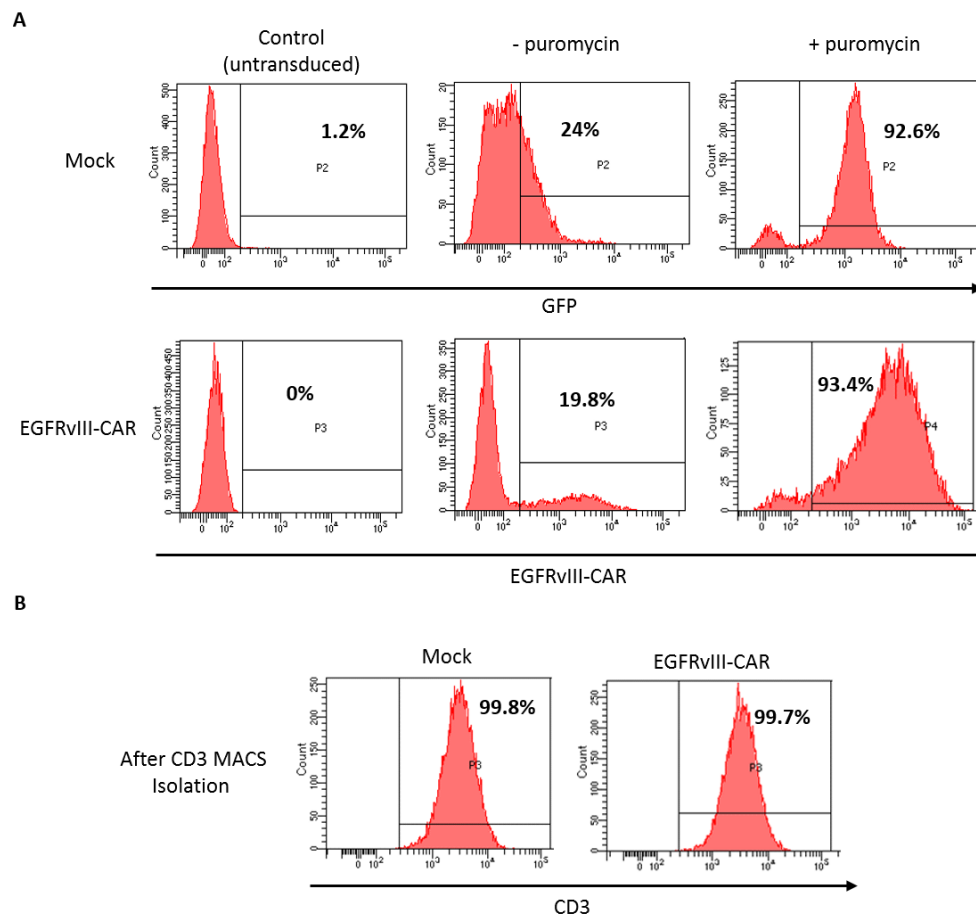
Figure 9: Transduction of PBMCs. Stimulated PBMCs were transduced with a third-generation EGFRvIII-CAR or a mock control. Expression of GFP (Mock T cells) and EGFRvIII-CAR (vIII-CAR T cells) was analyzed 48 hours post transduction before adding puromycin and 6 days after puromycin treatment (A). EGFRvIII-CAR expression was detected using biotinylated ProteinL and subsequent SA-PE staining. After puromycin treatment a CD3-MACS isolation was performed, and purity was confirmed by FACS analysis after staining of T cells with anti-CD3 antibody (B). Lymphocytes were gated using the FCS/SSC channel and 10.000 events were recorded for each sample.

3.4 EGFRvIII expression of EGFRvIII transfected tumor cell lines

To examine functional properties of generated EGFRvIII-CAR expressing T cells, target cells presenting EGFRvIII as an antigen were needed. Since no cell line or primary tumor was available that naturally expressed EGFRvIII, target cells had to be generated by transduction using the retroviral vector pMX-EGFRvIII. The following EGFRvIII transfected tumor cell lines served as target cells: the murine renal carcinoma cell line Renca-EGFRvIII, provided by J. Röder (Group of PD Dr. E. Bockamp, Inst. for Transl. Immunol., UMM Mainz), the human melanoma cell line Ma-mel EGFRvIII (provided by C. Wölfel, 3rd. Dept. of Medicine, UMM), and the human lung adenocarcinoma cell line A549-EGFRvIII (se section 2.1.11). Besides transfection of EGFRvIII, Ma-mel EGFRvIII$^+$ cells carry additional properties as they are deficient for HLA class-I surface expression due to a deletion within the β-microglobulin gene. An additional knockout of HLA class-II was introduced using TALEN technology (by C. Wölfel). Surface expression of EGFRvIII was analyzed by extracellular staining of transfected cells with the L8A4 mouse IgG and the secondary mouse IgG-PE antibody. Cell lines were stained and analyzed several times during their period of cell culture. Expression analysis confirmed surface expression of EGFRvIII on transfected tumor cells as depicted in representative FACS analysis images showing 66.8% EGFRvIII expression for Renca-TF, 89% for Ma-mel TF and 74,4% for A549 TF (Fig.10). Untransfected cell lines stained for EGFRvIII expression served as negative control. Of note, fluctuating expression levels for Ma-mel EGFRvIII and for A549 were observed when cell lines were repeatedly analyzed after several days. The lowest expression level measured for Ma-mel TF was 20% and for A549 30%, indicating a downregulation of the EGFRvIII expression during cell culture (data not shown). Transfected cell lines were analyzed for EGFRvIII expression before they were used for further functional assays to ensure that only cells with >70% surface expression were used as target cells.
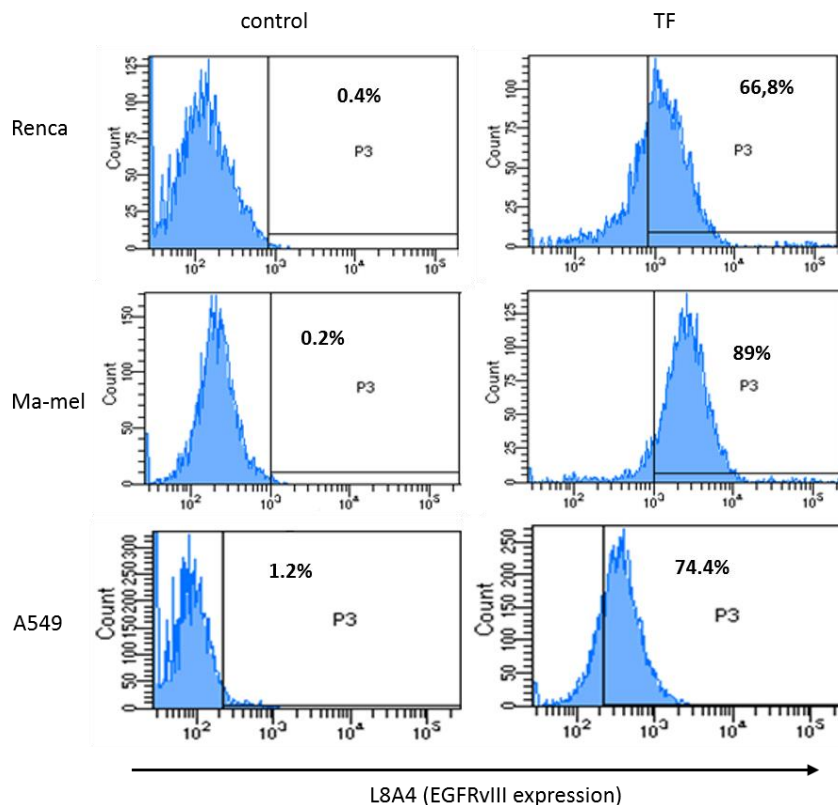
Figure 10: EGFRvIII surface expression of transfected tumor cell lines. Transfected cell lines were analyzed for EGFRvIII surface expression by flow cytometry after extracellular staining of EGFRvIII using the mouse IgG L8A4 and secondary mouse IgG-PE antibody. Cells were gated using the FSC/SSC channel and 10.000 cells were recorded within this gate. Untransfected cells served as control. Data from one representative staining experiment are shown.

3.5 Functional properties of modified T cells targeting EGFRvIII⁺ tumor cells

Functional properties of redirected T cells, positive for expression of EGFRvIII-CAR, were analyzed in several assays. To assess T cell activation and stimulation upon exposure to EGFRvIII expressing target cells, co-culture assays were performed. To quantify cytokine response of T cells upon activation ELISpot assays for detection of IFN- γ and Granzyme B were conducted. Further, to analyze lytic potential, chromium release assays were performed.

3.5.1 Co-Culture of redirected T-cells with EGFRvIII expressing target cells

Retrovirally modified CD3⁺ T cells, expressing either EGFRvIII-CAR or GFP (Mock T cells), were co-cultured with EGFRvIII expressing target cells in various effector (T cells) to target cell (tumor cells) ratios for 48 hours. Three different transfected cell lines were used as targets: the murine renal carcinoma cell line Renca EGFRvIII⁺, the human melanoma cell line Ma-mel EGFRvIII⁺ and the human adenocarcinoma cell line A549 EGFRvIII⁺. Target cells were plated in a 24-well plate and allowed to adhere before T cells were added to the culture wells the following day. T cells were seeded in effector:target ratios ranging from 4:1 to 1:1. After 48 hours live images were taken with phase contrast microscopy to observe T cell cluster formation

and confluency of target cells. We observed activation of CD3$^+$ EGFRvIII-CAR T cells when cultured with EGFRvIII expressing target cells. Fig. 11A shows the co-culture of T cells with Renca EGFRvIII$^+$ cells, demonstrating T-cell activation of EGFRvIII-CAR expressing T cells by formation of T cell clusters. In contrast, CD3$^+$ Mock T cells cultured with EGFRvIII expressing target cells do not show any cluster formation. Furthermore, adherent target cells were visible in wells when co-cultured with CD3$^+$ Mock T cells. Hardly any target cells could be detected when cultured with CD3$^+$ EGFRvIII-CAR T cells, indicating effective lysis of target cells by EGFRvIII-CAR redirected T cells. No prominent difference regarding T cell cluster formation of EGFRvIII-CAR T cells was observed for different effector:target ratios. When T cells were co-cultured with Ma-mel EGFRvIII$^+$ (Fig. 11B) similar effects were seen. While EGFRvIII-CAR T cells formed T cell clusters, Mock T cells did not appear to be efficiently activated, as no cluster formation was visible in neither effector to target ratio. Similar outcome was observed for T cells targeting A549 EGFRvIII$^+$ cells (Fig C). After 48 hours of co-culture hardly any difference was visible for EGFRvIII-CAR T cells regarding T cell activation among different effector:target ratios. Again, Mock T cells did not form T cell clusters due to insufficient activation. In these culture wells adherent target cells were clearly visible in comparison to wells containing EGFRvIII-CAR T cells. In conclusion, EGFRvIII- CAR T cells seemed to be equally activated by different tumor cells transfected with EGFRvIII.
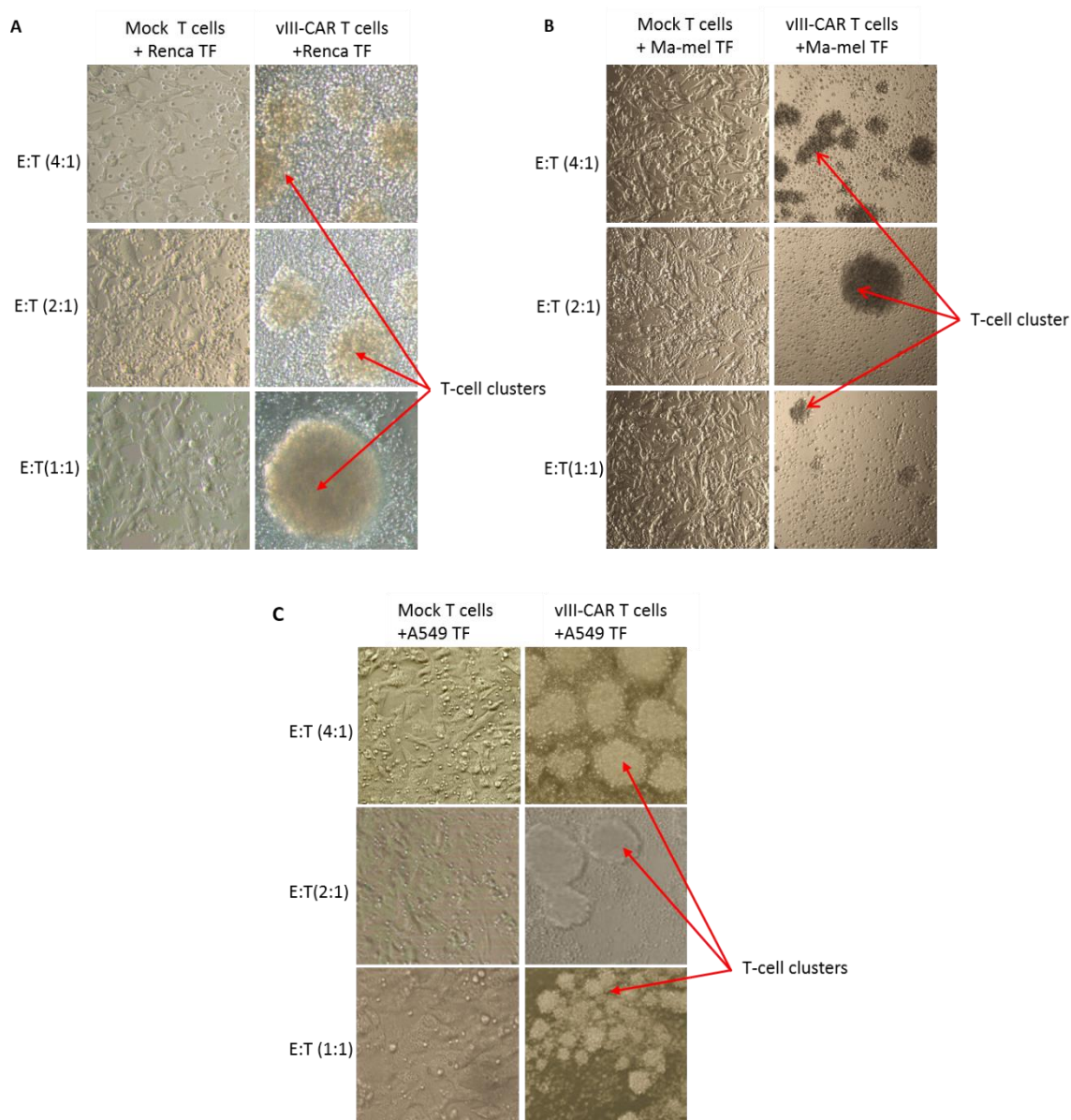
Figure 11: Co-culture of modified T cells with EGFRvIII+ tumor cells. EGFRvIII-CAR T cells (vIII-CAR T cells) were co-cultured with EGFRvIII transfected tumor cell lines. Mock T cells served as control cells. Target cells were seeded in wells of a 24-well plate and were allowed to adhere, before T cells were added in different effector:target ratios the following day. After 48 hours of co-culture representative images were taken by phase contrast microscopy, showing T cell cluster formation for vIII-CAR T cells cultured with their respective target cells. Mock and vIII-CAR T cells were cultured with Renca EGFRvIII⁺ (A), Ma-mel EGFRvIII⁺ (B) and A549 EGFRvIII+ cells (C).

3.5.2 Crystal Violet Staining Assay

A simple and fast method for an indirect quantification of cell death is staining of cells with crystal violet solution. Adherent cells detach from cell culture plates during cell death, either caused by cytotoxic compounds or lysis by effector cells. We used this method to quantify T cell induced lysis of EGFRvIII expressing target cells in a 48-hour co-culture assay. First, target cells were seeded in a 24-well plate and were allowed to adhere, before T cells were added the following day in a 2:1 ratio. T cells and tumor cells were co-cultured for 48 hours. Then, cell culture medium containing T cells growing in suspension was removed and wells were carefully washed with PBS. After fixation of cells, the remaining attached target cells were stained with

crystal violet solution (see section 2.4.1) binding to proteins and DNA. After another washing step with PBS images of the wells were taken and absorbance was measured in a 96-well plate reader. Intensity of crystal violet staining reflects the amount of remaining target cells. The more target cells were lysed by T cells the less intensity of crystal violet staining on the bottom of the wells was detected. Co-culture assays of modified T cells with Renca EGFRvIII[+], Ma-mel EGFRvIII[+] and A549 EGFRvIII[+] were conducted with a subsequent crystal violet staining procedure. Representative images of the crystal violet staining are shown in Fig.12A for modified T cells cultured with A549 EGFRvIII^{+} cells. In this example, CD3^{+} and CD8^{+} Mock or EGFRvIII-CAR T cells were co-cultured with A549 EGFRvIII^{+} (A549 TF) or A549 wt cells, serving as a negative control. A strong reduction of remaining attached target cells could be observed, when A549 EGFRvIII^{+} tumor cells are cultured with CD8^{+} or CD3^{+} EGFRvIII-CAR T cells in comparison to target cells cultured with CD3^{+} or CD8^{+} Mock T cells, indicating target cell lysis by EGFRvIII-CAR T cells. Furthermore, wt target cells that were not transfected with EGFRvIII (wt) do not show any difference in intensity of CVS, when cultured with Mock or EGFRvIII-CAR T cells, as target cells were neither lysed by Mock nor EGFRvIII-CAR T cells. The quantification of the crystal violet staining after co-culture of CD3^{+} Mock and EGFRvIII-CAR T cells targeting the different transfected tumor cell lines Renca EGFRvIII^{+} (TF), Ma-mel EGFRvIII^{+} (TF) and A549 EGFRvIII[+] (TF) is shown in Fig.12B. Each transfected cell line showed diminishing OD values when cultured with EGFRvIII-CAR T cells. OD values of transfected tumor cells cultured with CD3^{+} Mock T cells ranged from 0.4 to 0.5 and decreased to less than 0.05 when cultured with EGFRvIII-CAR T cells, indicating a specific lysis of EGFRvIII expressing tumor cells.
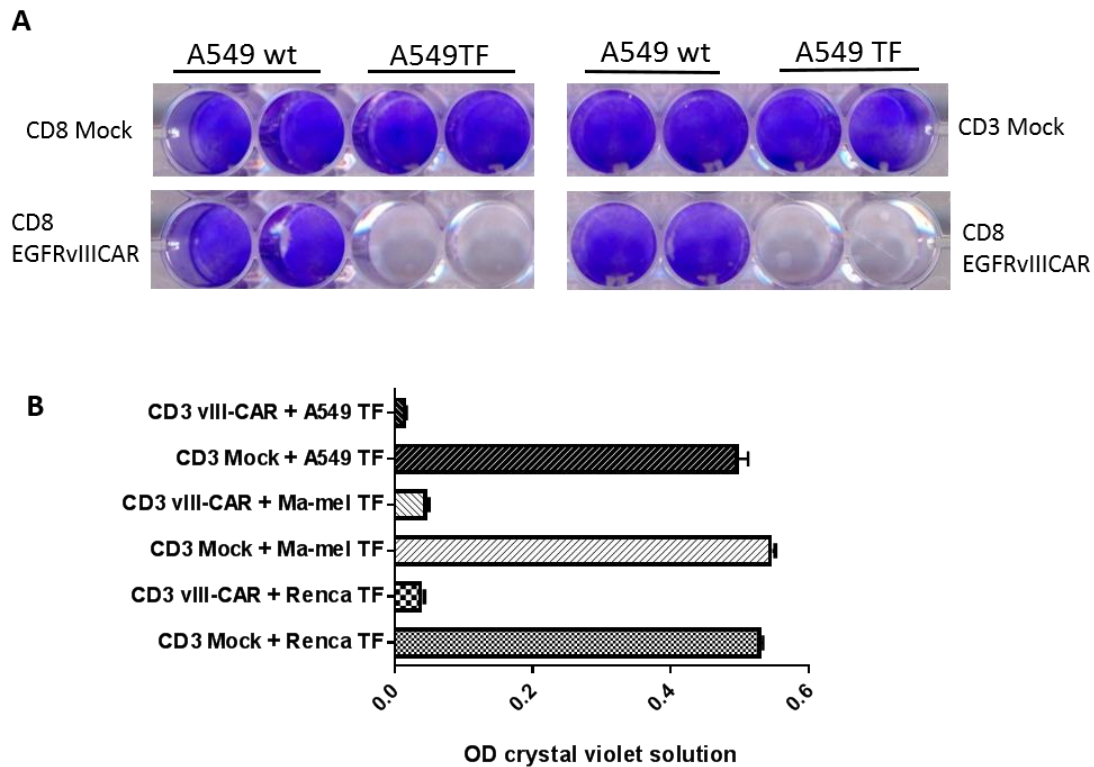
Figure 12: Crystal violet staining of Co-Culture Assay. Modified T cells were co-cultured with EGFRvIII expressing tumor cells. (A) Representative image of crystal violet staining after co-culture of modified T cells with A549 EGFRvIII and A549 wt cells. (B) Indirect quantification of T cell induced lysis of EGFRvIII⁺ tumor cell lines A549 EGFRvIII⁺ (TF), Ma-mel EGFRvIII⁺ (TF) and Renca EGFRvIII⁺ (TF). After co-culture of T cells and target cells, crystal violet staining was applied. (B) Staining with crystal violet was quantified by measuring the OD of dissolved crystal violet solution in a 96-well plate reader. Data shown are mean values ±SD, n=3.

3.5.3 IFN-γ and Granzyme B EliSpot Assay

To further evaluate functional properties of successfully generated EGFRvIII-CAR T cells their cytokine response upon antigen encounter was analyzed. Thus, IFN-γ and Granzyme B EliSpot assays were performed with modified T cells targeting Renca-EGFRvIII⁺, Ma-mel EGFRvIII⁺ or A549 EGFRvIII⁺ tumor cells. Mock and EGFRvIII-CAR T cells were generated as described in chapter 2.2.8, and assays were performed after confirming successful transduction of T cells with an EGFRvIII-CAR expression of >70% analyzed 5 days after polyclonal stimulation with OKT3. CD8⁺ T cells were selected from the CD3⁺ T cell population by MACS isolation using CD8 microbeads. T cells and target cells were seeded in a 2:1 ratio and were co-cultured for 18 hours. CD8⁺ Mock T cells served as control cells. Fig.13 shows representative images of the IFN- γ ELISpot assay for each tumor cell line and the respective quantification on the right using a CTL reader. The results illustrated a specific stimulation of EGFRvIII-CAR modified T cells upon stimulation by EGFRvIII expressing tumor cells. When T cells where cultured with Renca EGFRvIII⁺ only few IFN-γ spots were visible for Mock T cells, whereas up to 200 spots were counted for EGFRvIII-CAR T cells. The same observation was made for Mock T cells targeting Ma-mel EGFRvIII⁺. In contrast, EGFRvIII-CAR T cells showed a significant response towards Ma-mel EGFRvIII⁺ cells indicating that only EGFRvIII-CAR modified T

57

cells were stimulated upon EGFRvIII encounter. Similar results were obtained for T cells cultured with A549 EGFRvIII+ tumor cells. EGFRvIII CAR T cells demonstrated a prominent IFN-γ secretion (up to 360 spots), while Mock T cells did not show any response.
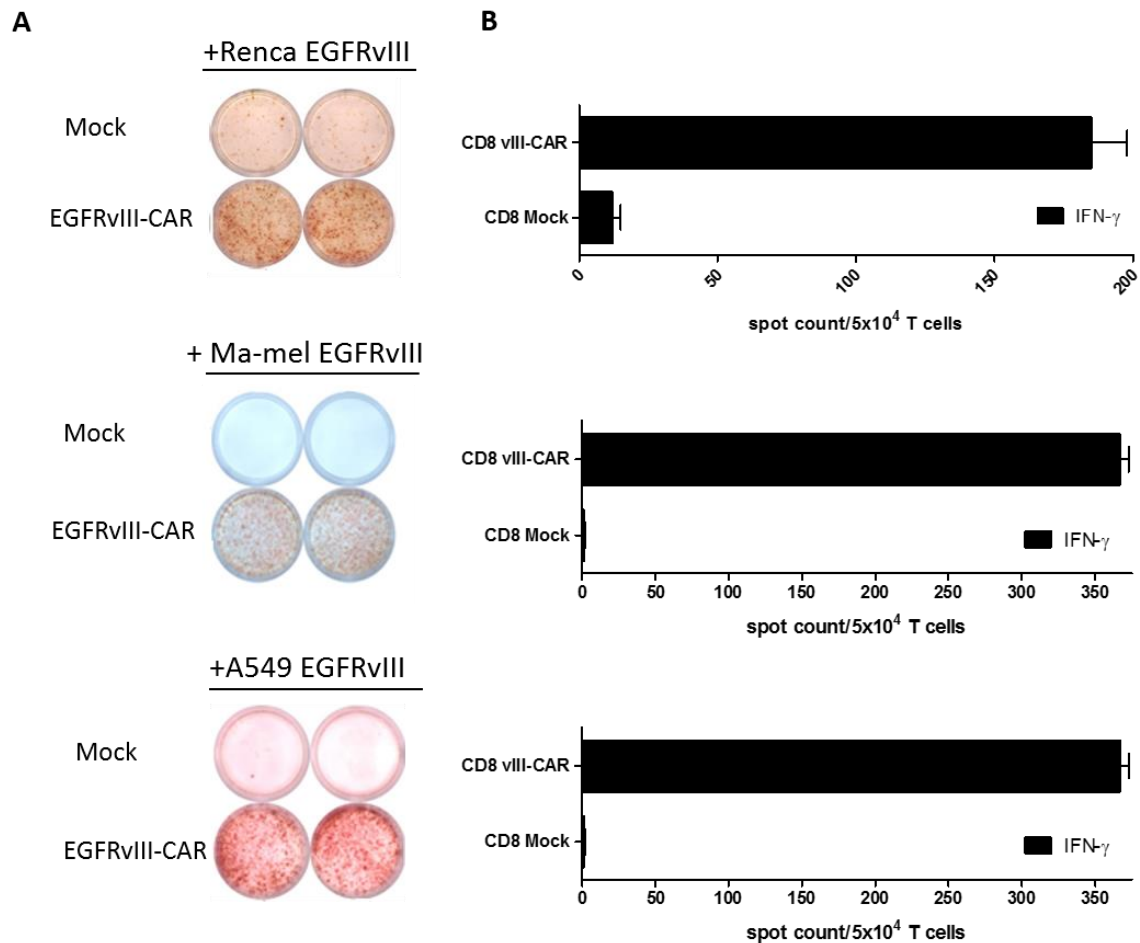

Figure 13: IFN-γ assay of modified T cells targeting EGFRvIII+ tumor cells. IFN-γ secretion of vIII-CAR T cells upon antigen encounter was measured in an 18-hour ELISpot assay using 5x104 T cells/well and 2,5x104 tumor cells/well. (A) Exemplary images of ELISPOT results are shown for one experiment. (B) Results of three independent experiments were combined and mean volumes ± SEM are indicated. IFN-γ secretion was quantified using a CTL reader.

While the IFN-γ ELISpot assay is a well-known method for measuring T cell activation, it does not directly assess cell-mediated cytotoxicity as it is not only limited to cytolytic T cells. In contrast, Granzyme B, a member of the Granzyme family serine proteases is restricted to cytotoxic T cells and natural killer cells and is involved in triggering apoptosis. Hence, a Granzyme B ELISpot assay was performed to further evaluate the cytotoxic potential of EGFRvIII-CAR modified T cells targeting Renca EGFRvIII+, Ma-mel EGFRvIII+ and A549 EGFRvIII+. Effector and target cells were again seeded in a 2:1 ratio and cultured for 18 hours. Fig.14A shows representative images of the ELISpot assay for each tumor cell line and the respective quantification by spot counting in Fig.14B using a CTL Reader. Results of the Granzyme B EliSpot indicated specific stimulation and lysis potential of EGFRvIII-CAR

modified T cells targeting the EGFRvIII expressing tumor cells. Mock T cells cultured with Renca EGFRvIII[+] (Fig.14) secreted a neglectable amount of Granzyme B, whereas around 220 spots were counted for EGFRvIII-CAR redirected T cells. Similar results were obtained for T cells targeting Ma-mel EGFRvIII[+], with no detectable spots for Mock T cells and more than 250 spots for EGFRvIII-CAR T cells. Same outcome was observed when T cells were cultured with A549 EGFRvIII[+] showing hardly any spots for Mock T cells and about 250 spots for EGFRvIII-CAR T cells.
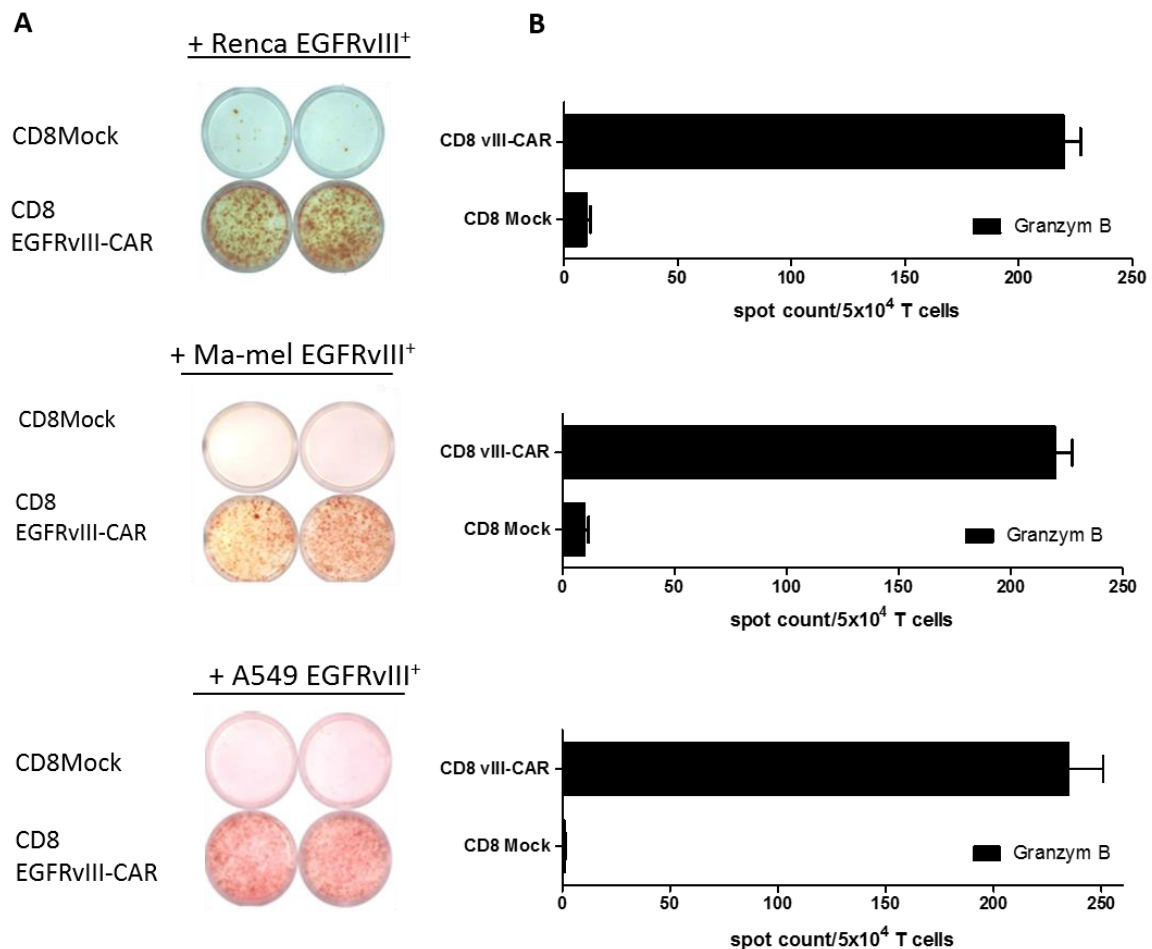
Figure 14: Granzyme B assay of modified T cells targeting EGFRvIII+ tumor cells. Granzyme B secretion of EGFRvIII-CAR T cells upon antigen encounter was measured in an 18-hour ELISpot assay using 5×10^4 T cells/well and $2,5 \times 10^4$ tumor cells/well. Mock T cells served as controls. (A) Exemplary images of ELISpot results are shown for one experiment. (B) Data of three independent experiments were combined and mean values ± SEM are indicated. Granzyme B secretion was quantified using a CTL reader.

3.5.4 Chromium Release Assay

Redirected T cells were analyzed for their lysis potential using the [51]chromium release assay, which is a commonly used method for precise and accurate quantification of cytotoxicity. Mock and EGFRvIII-CAR T cells were generated by retroviral gene transfer (see section 2.2.7) and analyzed for surface expression of EGFRvIII-CAR by FACS. Five days after polyclonal stimulation T cells were then tested for their lytic activity. First, the human EGFRvIII

expressing tumor cells Ma-mel EGFRvIII[+] and A549 EGFRvIII[+] were labelled with [51]chromium and subsequently co-cultured with EGFRvIII-CAR T cells for 5 hours. Mock T cells were used as control cells. Upon lysis of target cells by cytotoxic T cells, chromium is released and is quantified in a gamma counter.

The cytolytic activity of modified CD8^{+} T cells targeting Ma-mel EGFRvIII^{+} was analyzed. As an additional specificity control, not only CD8^{+} Mock T cells, but also CD19-CAR redirected T cells were used. When seeded at a 60:1 ratio, CD8^{+} EGFRvIII-CAR T cells showed the highest lysis activity with up to 70%, constantly dropping with lower effector:target ratios. For CD8^{+} CD19-CAR T cells and CD8^{+} Mock T cells only low cytotoxicity was observed with less than 10% for the highest effector:target ratio and less for decreasing numbers of effector T cells, implying a specific lysis by EGFRvIII-CAR T cells (Fig.15A). CD3^{+} and CD8^{+} Mock and EGFRvIII-CAR T cells were further examined for their lysis potential targeting A549 EGFRvIII^{+} cells (Fig.15B). With a 60:1 effector:target ratio CD8^{+} EGFRvIII-CAR T cells lysed target cells up to 58% and exerted lower cytotoxicity with decreasing effector:target ratios. CD3^{+} EGFRvIII-CAR T cells showed a slightly lower cytolytic activity. CD3^{+} Mock and CD8^{+} Mock T cells showed low cytolytic activity (CD8^{+} Mock: 10%; CD3^{+} Mock: 8%), which further decreased with decreasing effector:target ratios.
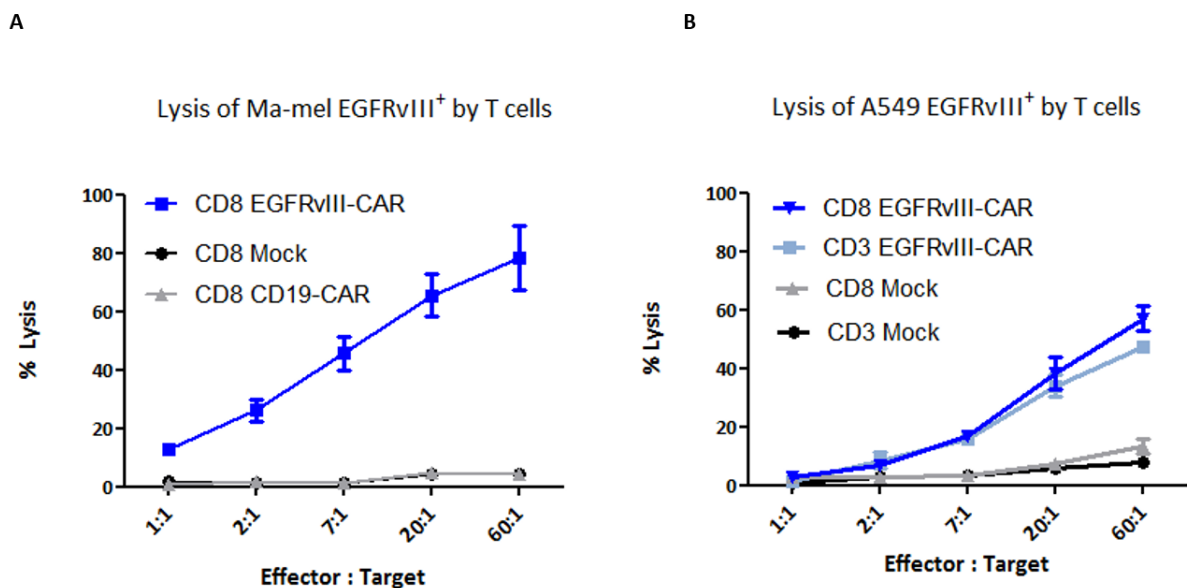
Figure 15: Chromium release assay of modified T cells targeting EGFRvIII+ tumor cells. Tumor cells were labelled with [51]Chromium and co-incubated with redirected T cells at indicated ratios for 5 hours. Released chromium was quantified in a gamma counter and lysis activity was calculated in relation to minimum and maximum release controls. (A) Chromium Release Assay of CD8^{+} EGFRvIII-CAR T cells targeting Ma-mel EGFRvIII^{+} tumor cells. CD8^{+} Mock and EGFRvIII-CAR T cells served as control cells. (B) Chromium release assay of CD3^{+} or CD8^{+} EGFRvIII-CAR T cells targeting A549 EGFRvIII^{+} tumor cells. Mock T cells served as controls. Results of two independent experiments are shown with mean values ±SEM.

3.6 Characterization of EGFRvIII-CAR redirected T cell response *in vivo*

After assessing functional properties and lysis potential of EGFRvIII-CAR modified T cells *in vitro*, we aimed to evaluate the therapeutic potential of EGFRvIII-CAR T cells *in vivo* using a xenograft model in NOD/scid IL2Rcγ null (NSG) mice. These mice are highly immunodeficient due to a lack of mature T cells, B cells and functional NK cells, and are further deficient of cytokine signaling (see section 2.6).

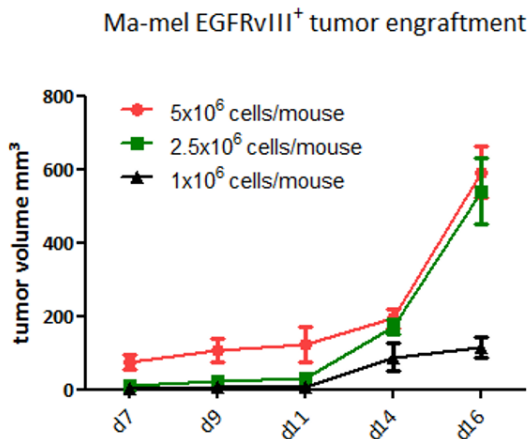**3.6.1 Engraftment kinetics of EGFRvIII expressing tumor cells in NSG mice**

First, the engraftment of the human tumor cell lines Ma-mel EGFRvIII$^+$ and A549 EGFRvIII$^+$ had to be confirmed in NSG mice. Since we wanted to determine a time point to start T cell therapy in tumor bearing mice, we examined kinetics of tumor engraftment. For this purpose, different tumor cell doses were tested for both cell lines (Ma-mel EGFRvIII$^+$: 1×10^6, 2.5×10^6 and 5×10^6 tumor cells/mouse; A549 EGFRvIII$^+$: 1×10^6 and 2×10^6 cells/mouse), which were subcutaneously injected into the right flank of NSG mice. As soon as visible, tumor size was monitored by calipering, measuring width x length x height almost every 2nd day and pace of tumor growth was observed over a period of 16 days. Tumor volume of mice injected with Ma-mel EGFRvIII$^+$ could be measured starting from day 7. From day 7 to 9 tumor pace of tumor growth was relatively slow. A rapid increase in tumor volume was observed after day 11 for the group containing 2.5×10^6 and 5×10^6 tumor cells, reaching a volume of about 600 mm^3 at day 16 (Fig.16A). In comparison, tumor size of the group with 1×10^6 tumor cells increased slowly after day 11 reaching only around 100 mm^3 on day 16. For an early stage therapy challenge, the appropriate time to start T cell therapy appeared to be before day 11, as the tumor size was modest but still palpable, allowing an intratumoral injection of T-cells. For A549 EGFRvIII$^+$ cells a rapid increase of tumor volume was observed after day 9 for the group receiving 2×10^6 tumor cells, reaching a tumor size of more than 400 mm^3 at day 16. Tumor size of the group with 1×10^6 cells also increased after day 9, but only reached a volume of about 200 mm^3 at day 16 (Fig.16B). For the A549-EGFRvIII$^+$ tumor cells the appropriate time point to start T cell therapy would be between day 7 and day 9. The human lung carcinoma cell line A549 EGFRvIII$^+$ was chosen for assessing functional properties of modified T cells *in vivo* with a cell dose of 2×10^6 cells/mouse.
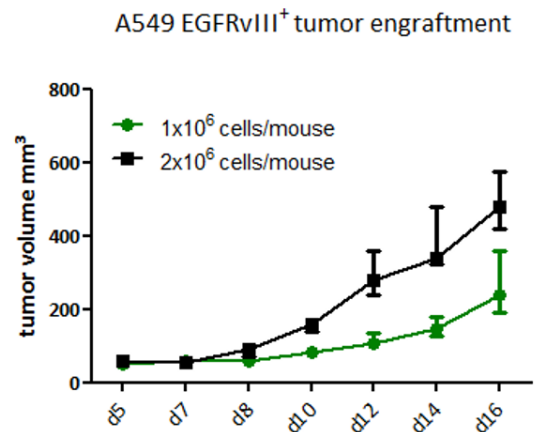
Figure 16: Kinetics of EGFRvIII+ tumor cell engraftment in NSG mice. (A) Ma-mel EGFRvIII^{+} tumor cells were injected subcutaneously into the right flank of NSG mice. Each group consisted of 5 mice and received different tumor cell doses (5×10^6 cells, 2.5×10^6 cell and 1×10^6 cells/mouse). As soon as tumors were palpable volumes were measured using a caliper. Tumor growth was observed over a period of 16 days. (B) Engraftment of A549 EGFRvIII^{+} tumor cells. Kinetics of two different tumor cell doses was analyzed (1×10^6, 2×10^6).

3.6.2 Adoptive Transfer of EGFRvIII-CAR redirected T cells in A549 EGFRvIII[+] induced tumor bearing mice

Lysis potential of EGFRvIII-CAR redirected T cells was examined in a xenograft mouse model using the non-small cell lung cancer cell line A549 EGFRvIII[+]. First, mice were subcutaneously injected with 2×10^6 A549 EGFRvIII^{+} tumor cells. When the average tumor volume reached about 100 mm[3] mice were randomized into three cohorts, each consisting of four mice and received T cell therapy. At this timepoint, 7 days after tumor engraftment, the tumor size was already palpable, allowing an intratumoral injection of T cells. The control group was left untreated, the Mock group and EGFRvIII-CAR group received 4×10^6 CD3^{+} Mock T cells and EGFRvIII-CAR T cells, respectively (Fig.17). Furthermore, a phenotypical analysis of T cells was performed to characterize composition of T cell subsets and differentiation state. Tumor volumes were then measured every second day until mice were sacrificed for endpoint analysis on day 14, which included measuring tumor volume, analyzing surface marker expression of tumor cells and analysis of T cell persistence within the tumor, spleen and peripheral blood. Furthermore, we examined if myeloid derived suppressor cells (MDSC) infiltrated tumor mass.
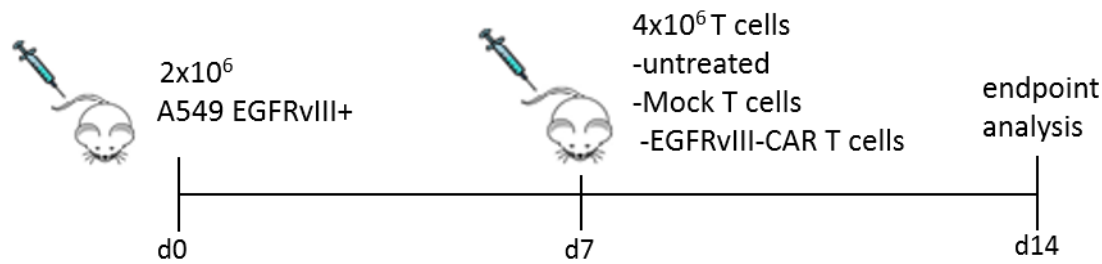
Figure 17: Experimental setup for Adoptive T cell therapy of A549 EGFRvIII+ engrafted NSG mice. NSG mice were injected subcutaneously with $2x10^6$ A549 EGFRvIII$^+$ tumor cells into the right flank. Seven days after tumor cell engraftment $4x10^6$ Mock T cells or vIII-CAR T cells were administered by intratumoral injection. The control group did not receive any T cells. Seven days after T cell transfer mice were sacrificed for endpoint analysis. Each group consisted of four mice.

3.6.2.1 Characterization of T cells on day of T cell transfer

For the adoptive transfer of T cells into A549 EGFRvIII$^+$ tumor bearing NSG mice, modified T cells that were frozen on d16 were thawed and stimulated 5 days in advance to ensure proper growth and reactivity conditions. One day before adoptive transfer they were tested for their functionality by performing a co-culture and crystal violet staining experiment (data not shown). EGFRvIII-CAR redirected T cells were further analyzed regarding their phenotype and were stained for markers of differentiation (CD45RA, CD45RO), homing (CCR7, CD62L) and for cell surface marker expression of CD4 and CD8. The T cell population of transduced T cells comprised a higher portion of CD3$^+$CD8$^+$ T cells in comparison to CD3$^+$CD4$^+$ T cells. EGFRvIIII-CAR redirected T cells comprised 73.8% CD3$^+$CD8$^+$ cytotoxic T cells and only 33% of CD3$^+$CD4$^+$ T cells. Similar CD4$^+$/CD8$^+$ ratios were found for Mock T cells (76% CD3$^+$CD8$^+$/33.9% CD3$^+$CD4$^+$ T cells, Fig. 18A). Furthermore, FACS results revealed that 38% of EGFRvIII CAR T cells exhibited central memory phenotype (CCR7$^+$CD45RO$^+$), whereas 6.3% exerted stem cell memory like phenotype (CD45RA$^+$CD62L$^+$). In comparison, 24.6% of Mock T cells reflected a central memory phenotype and 9.8% of Mock T cells were CD45RA$^+$CD62L$^+$. A high level of CD45RO$^+$CCR7$^-$ T cells was found within the T cell population, reflecting an effector memory phenotype (Fig. 18B).
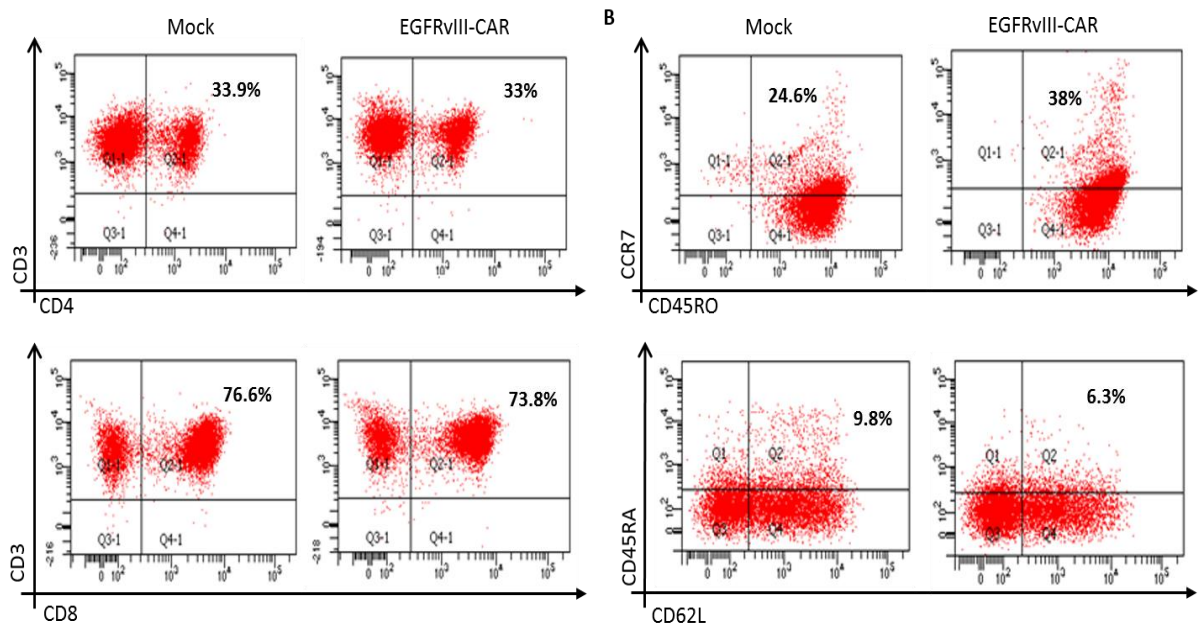
63

Figure 18: Phenotypic analysis of T cells on day of T cell transfer. Mock and EGFRvIII-CAR T cells were phenotypically analyzed by extracellular staining for FACS analysis on day of T cell transfer in tumor bearing NSG mice. Representative images of FACS analysis are shown. (A) T cells were stained for CD4^{+} and CD8^{+} expression for characterization of T cell composition. (B) T cells are characterized for surface expression pattern regarding homing and differentiation using CD45RA/CD62L and CD45RO/CCR7 antibodies.

3.6.2.2 Influence of Adoptive T cell transfer on tumor growth

As soon as palpable, tumor volume of each mouse was measured every second day. Intratumoral T cell transfer was administered on day 7 after tumor engraftment and mice were sacrificed for endpoint analysis 7 days after T cell transfer. Final tumor volumes of each mouse from different groups were assessed measuring the width, height and length using a caliper. The median final tumor volume for the untreated control group was about 200 mm^3. Surprisingly the Mock T cell treated group had a reduced final tumor volume of 128 mm^3 and no further prominent reduction was observed for the EGFRvIII-CAR treated group, where a tumor volume of 118 mm^3 was measured (Fig.19A). Mock and T cell treatment caused a slight reduction of tumor volume, which might be explained due to an alloreactive response. In this *in vivo* experiment no specific EGFRvIII-CAR anti-tumor response could be observed targeting the A549 EGFRvIII$^+$ tumor in NSG mice. Fig.19B illustrates combined results of three experiments for the course of tumor growth starting from day 5 to endpoint analysis on day 14. On day 9, two days after T cell transfer, mean tumor volumes of all cohorts are about 65 mm^3, afterwards mean tumor volume of the untreated cohort increases and reaches a final volume of about 196 mm^3, whereas the Mock and EGFRvIII-CAR treated cohorts reach a reduced final volume of 159 mm^3 and 155 mm^3, respectively.
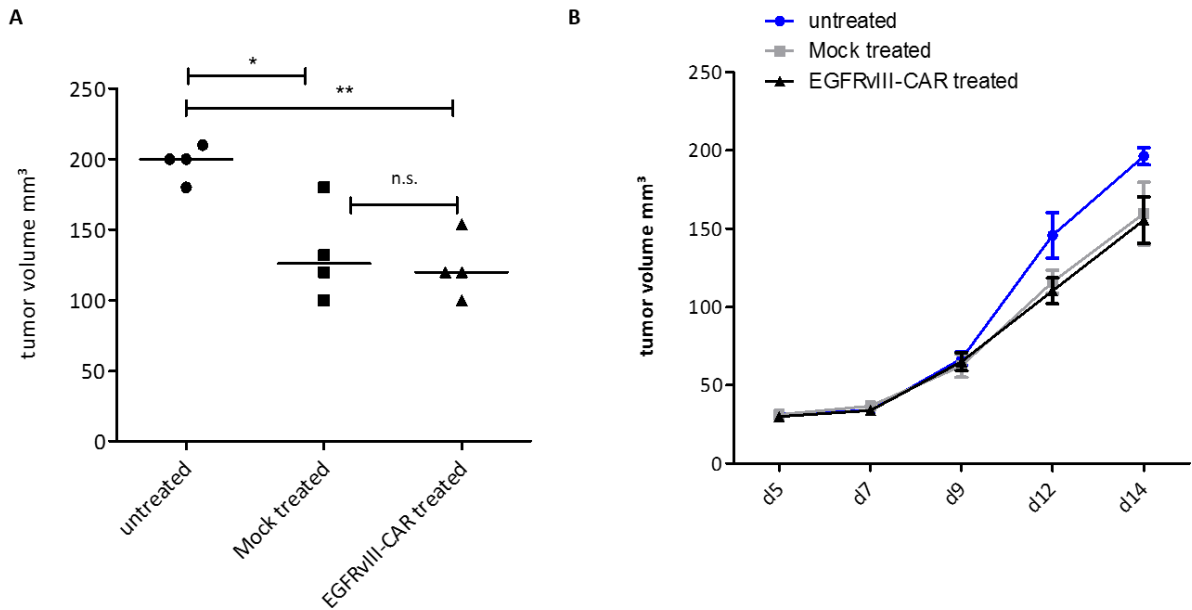
Figure 19: Tumor growth of A549 EGFRvIII+ bearing mice after T cell transfer. T cells were administered into A549 EGFRvIII⁺ engrafted mice by intratumoral injection, seven days after tumor engraftment. Mice were treated with either Mock T cells, EGFRvIII-CAR T cells or left untreated. Tumor volumes were measured starting from day 5 using a caliper. Each cohort consisted of four mice. (A) Final tumor volumes were measured on day 14 after sacrificing mice for endpoint analysis. Representative results, with median volumes are shown for one experiment out of three. $P < 0.05$, unpaired Student´s t-test. (B) Course of tumor growth during T cell treatment until endpoint analysis on d14. Combined data of three experiments are shown with mean values ± SEM.

3.6.2.3 Phenotypical analysis of engrafted tumor cells

After measuring the final tumor volumes, tumor mass was excised, gently disrupted and digested in Prep medium containing collagenase. After several washing steps tumor cells were stained for EGFRvIII using the L8A4 and mouse IgG-PE antibody to assess the current expression level of EGFRvIII on tumor cells. FACS analysis showed a low expression level of EGFRvIII on tumor cells as illustrated in Fig.20A. Tumors of the control group, that were left untreated (no T cell transfer) were 8.6% positive for EGFRvIII expression, tumors treated with Mock T cells revealed an expression level of 7.2% and the EGFRVIII-CAR treated tumor were 11.2% positive for EGFRvIII expression. The low expression of EGFRvIII on tumor cells might explain why EGFRvIII-CAR T cells could not exhibit a specific anti-tumor response. Since Mock and EGFRvIII-CAR T cell treatment led to a slightly reduced tumor volume in comparison to untreated mice, we assumed this might be a result of alloreactivity. Thus, we analyzed the HLA class-I and II surface expression of isolated tumor cells (Fig.20B), using HLA-ABC (HLA class-I) and HLA DR/DQ (HLA-class II) antibodies. As illustrated in Fig. 25B, 17.5% of tumor cell were positive for HLA-class I surface expression and 26.5% were positive for HLA-class II expression, indicating possible antitumoral reactivity caused by alloreactivity since the T cells used were allogeneic to the tumor.

65
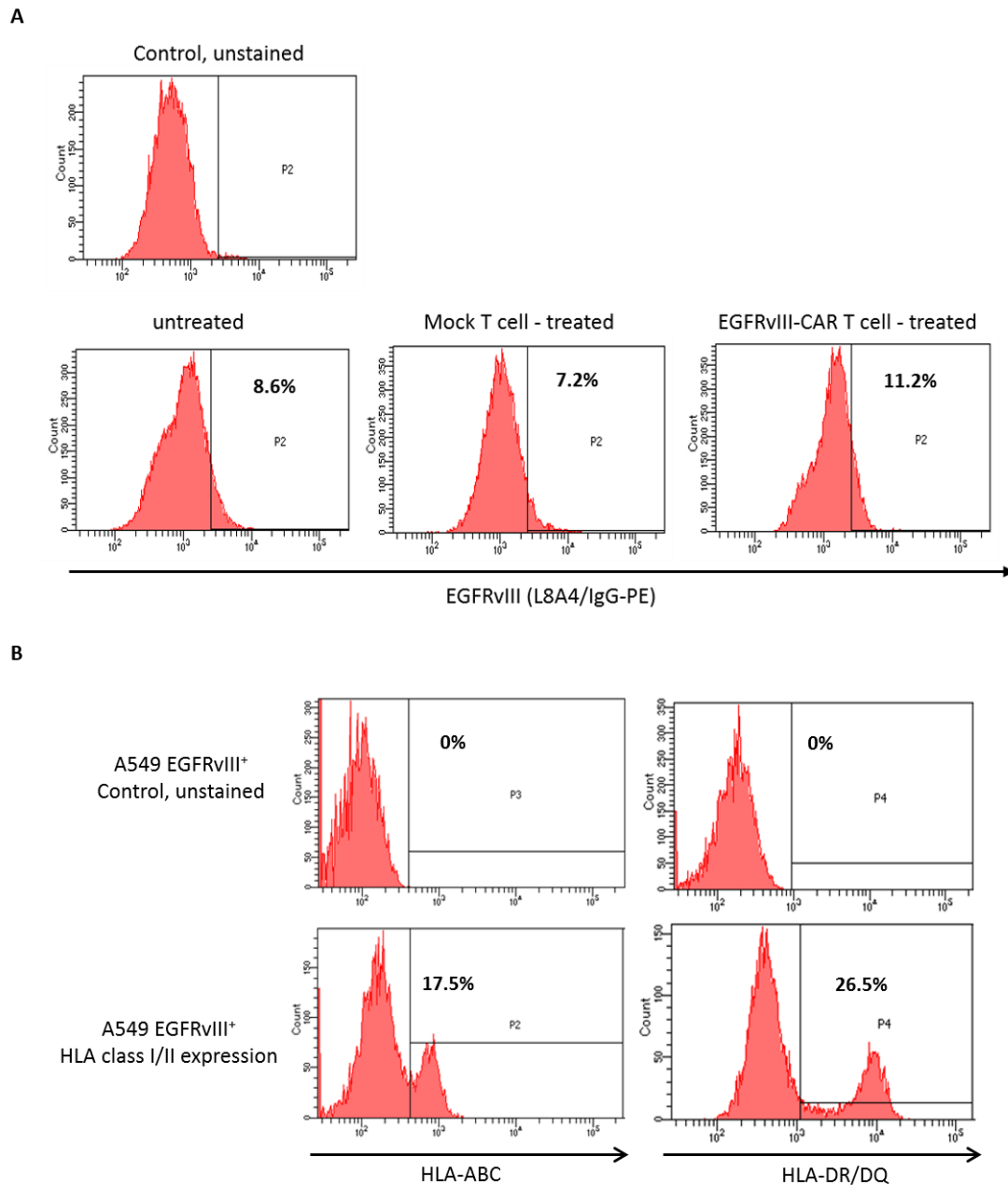
Figure 20: Phenotypical analysis of isolated A549 EGFRvIII+ tumor cells from NSG mice. Tumor mass was excised from tumor bearing mice and processed to single cell suspension for further staining of cell surface markers. (A) Tumor cells were stained for EGFRvIII surface expression using the L8A4 and mouse IgG-PE antibody. Unstained tumor samples served as controls. (B) Tumor cells were stained for surface expression of HLA-class I and II molecules using HLA-ABC and HLA-DR/DQ antibodies. Representative images of flow cytometry from one experiment are shown.

3.6.2.4 T cell persistence in NSG mice

After mice were sacrificed, tumor, spleen, bone marrow and peripheral blood were analyzed for the presence of T cells by FACS analysis. Thus, each specimen was processed to single cell suspension and stained for surface expression of CD3/CD4 and CD3/CD8 to examine if T cells were able to persist within the tumor or even able to home to secondary lymphoid organs. Only a very low level of T cells was detected within the tumor mass as shown exemplary in Fig.21.

About 0.8% of CD3$^+$CD8$^+$ and about 0.4% of CD3$^+$CD4$^+$ EGFRvIII-CAR T cells was found in the tumor. Levels of Mock T cells were less than 0.5% for CD4$^+$ or CD8$^+$ T cells. No T cell presence could be detected within spleen, bone marrow or peripheral blood (data not shown). In conclusion, these results indicate an insufficient persistence and homing of T cells, administered intratumorally into A549 EGFRvIII$^+$ bearing NSG mice.
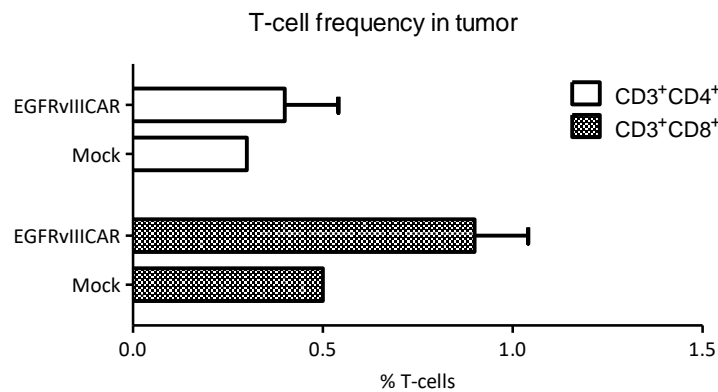

Figure 21: T cell persistence in A549 EGFRvIII+ bearing NSG mice. Seven days after adoptive transfer of T cells in tumor bearing mice, tumor mass was examined for presence of T cells. Mice were either treated with Mock or EGFRvIII-CAR T cells by intratumoral injection or left untreated. Single cell suspension of tumor cells was stained for surface expression of CD3/CD4 and CD3/CD8 for FACS analysis. Representative results with mean values ± SEM from one experiment out of three is shown.

3.6.2.5 Presence of myeloid derived suppressor cells

Due to the insufficient antitumoral responses observed *in vivo* that were also in clear contrast to the *in vitro* data we performed a first analysis on the tumor microenvironment in our model Thus, after preparing single cell suspensions of excised tumors, tumor cells were examined for the presence of myeloid derived suppressor cells. Myeloid derived suppressor cells (MDSC) are a heterogenous group of immune cells originating from the myeloid lineage, known to be a major component of the immune suppressive tumor microenvironment. Two main subtypes of MDSC have been reported for tumor-bearing mice, the granulocytic (G-MDSC), exerting a CD11b$^+$Gr-1^{high}, CD11b$^+$Ly6G$^+$ and Ly6C^{low} phenotype and monocytic (M-MDSC) defined by a CD11b$^+$Gr-1^{mid}Ly6G$^-$ and Ly6C^{high} phenotype. Therefore, we used antibodies targeting these markers to investigate infiltration of MDSC to the tumor site by FACS analysis. As illustrated in Fig.22 MDSC could be detected in tumor specimen excised from all cohorts. However, there was no prominent difference in MDSC frequency within the different groups. About 4% of G-MDSC with a CD11b$^+$Gr-1$^+$ phenotype and about 7% with a CD11b$^+$Ly6G$^+$ phenotype was found in the analyzed tumor specimen from all cohorts. A much lower number of M-MDSC defined by a CD11b$^+$LY6C$^+$ phenotype could be detected. Only less than 1% were present in tumor samples of the untreated and EGFRvIII-CAR treated group and 1.3% in the Mock treated group.
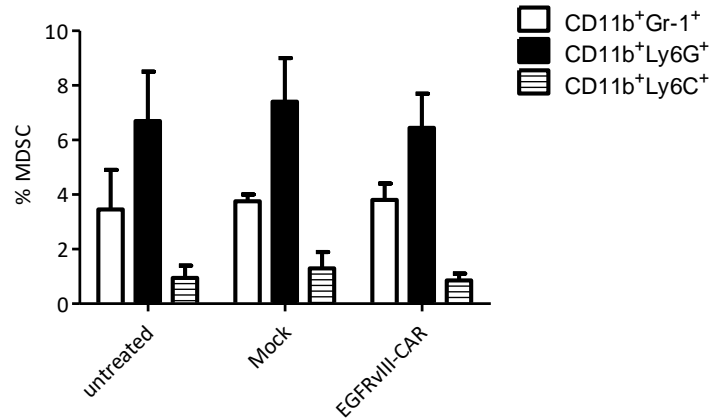
Figure 22: Presence of myeloid derived suppressor cells (MDSCs) in tumor mass of A549 EGFRvIII$^+$ bearing mice. Mice were either treated with Mock or EGFRvIII-CAR T cells by intratumoral injection or left untreated. Seven days after adoptive T cell transfer, tumor mass was examined for presence of MDSCs by staining for surface marker expression of CD11b, Gr-1, Ly6C and Ly6C for FACS analysis. Representative results with mean values ± SEM are shown for one experiment.

3.7 Generation of CAR modified T$_{SCM}$

There is growing interest in engineering less differentiated tumor specific T cells (T$_{SCM}$, T$_{CM}$) for application in adoptive cellular therapy, as they have proven enhanced capacity of self-renewal, engraftment and superior anti-tumor responses targeting B cell malignancies. After examining functional properties of regular EGFRvIII-CAR T cells we aimed to generate less differentiated EGFRvIII-CAR T cells, which will be referred to as naïve EGFRvIII-CAR T cells. As mentioned before, we observed fluctuations in the expression level of EGFRvIII on transfected tumor cell lines. Due to this issue, we chose to first establish the protocols for naïve CD19-CAR T cells since a B cell leukemia target cell line was available that stably expresses CD19. Initial experiments to establish the protocol of generating less differentiated T cells were conducted by A. Berger in the group of PD Dr. U. Hartwig.

3.7.1 Generation of naïve CD19-CAR T cells

As mentioned above the generation of naïve CD19-CAR T cells was performed based on a protocol established showing that several cytokines such as IL-7, -15 and 21 and the addition of TWS119 or Akt Inhibitor VIII promote the survival and generation of less differentiated stem cell like memory cells (T$_{SCM}$) (unpublished data). First, CD45RA$^+$ cells were isolated from bulk PBMCs and were stained for expression of naïve T cell markers (CD45RA, CD45RO, CD62L and CCR7). Three days prior to transduction T cells were stimulated polyclonally as described before and were additionally cultivated with the cytokine mix and either TWS119 or Akt Inhibitor VIII as illustrated in Fig.23A. After isolation of CD3$^+$ T cells and puromycin treatment for a positive selection of transduced T cells, naïve CAR T cells were analyzed via FACS analysis for CD19-CAR expression. For TWS119 treated naïve T cells a transduction of only

7.7% was achieved, whereas Akt treated and only cytokine treated cells showed a transduction efficiency of 15% and 18%, respectively, indicating a negative effect of TWS119 treatment on transduction efficiency (Fig.23B). However, after 7 days of puromycin treatment, each naïve T cell population was >90% positive for CD19-CAR expression.
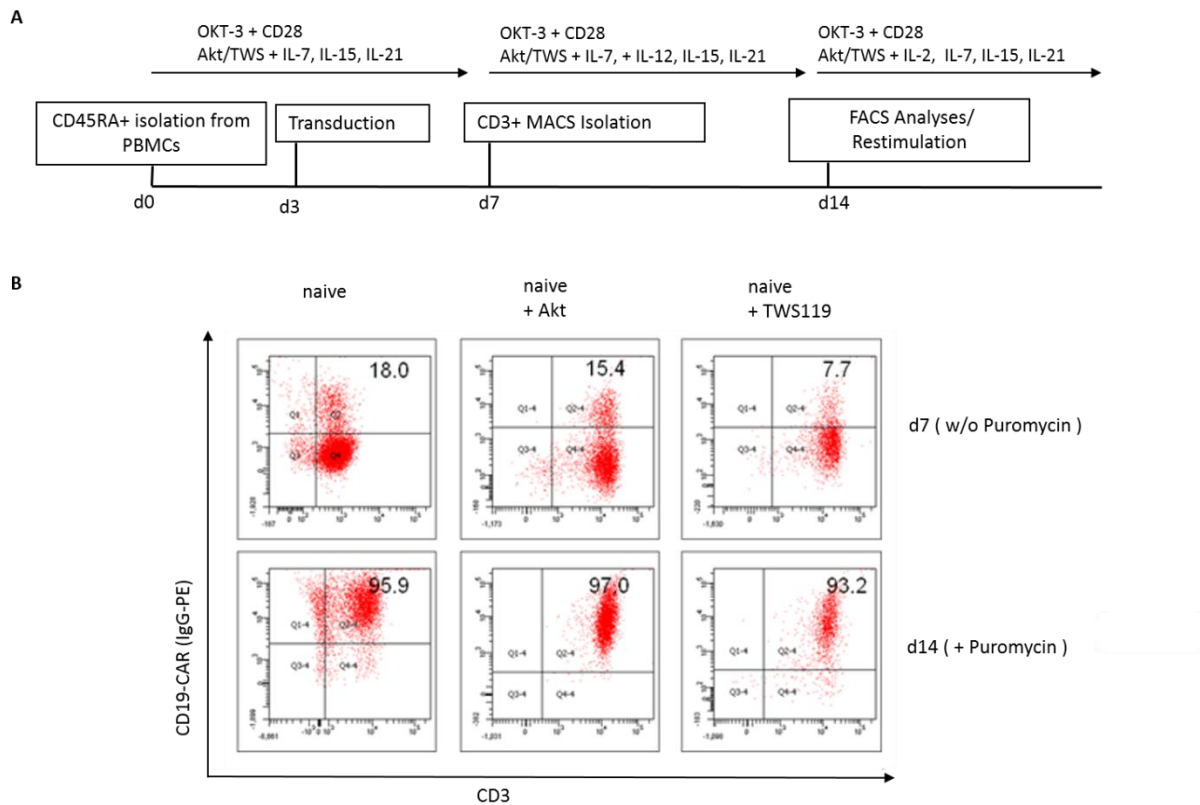
Figure 23: Generation of naïve CD19-CAR T cells. (A) Flow chart for generation of naïve CD19-CAR T cells. CD45RA^{+} naïve cells are preselected from PBMCs using CD45RA Microbeads. Naïve cells are cultured in T cell medium supplemented with either TWS119 or Akt Inhibitor VIII and a cytokine mix as indicated. Transduction of T cells is performed three days post polyclonal stimulation. On day 7, CD3^{+} T cells are isolated using CD3 Microbeads and on d14 T cells are analyzed for naïve T cell markers by flow cytometry. (B) Transduction efficiency of naïve T cells is analyzed before and after puromycin treatment by flow cytometry. Images of one representative experiment are shown.

Furthermore, the phenotypical characteristics of TWS119 and Akt Inhibitor VIII treated naïve T cells were compared to untreated regular CD19-CAR T cells, referred to as total CD19-CAR T cells by FACS analysis. Akt Inhibitor VIII and TWS119 treatment contributed to similar high expression levels of CD45RA (+Akt: 69.1 %; +TWS: 69.8 %) and CD62L / CCR7 (+Akt: 83.3 %; +TWS: 83.7 %) on day 14 for naïve CD19-CAR T cells (Fig.24), reflecting a T_{SCM} like phenotype. In contrast, untreated total CD19-CAR T cells exerted much lower expression levels of CD45RA^{+} (9.5%) and CD62L^{+}/ CCR7^{+} (total CD19-CAR: 33.3%). Notably, total CD19-CAR T cells demonstrated the highest level of CD45RO^{+} cells 58%, reflecting a T_{CM} like phenotype. Naïve derived CD19-CAR T cells without Akt treatment revealed lower expression

level of CD45RA$^+$ (26%) and a slightly decreased CD62L$^+$/CCR7$^+$ expression (72%) in comparison to Akt treated naïve CD19-CAR T cells. Overall, comparing the surface expression data of these different T cell populations, strongly suggests, that Akt and TWS119 promote a T$_{SCM}$ like phenotype.
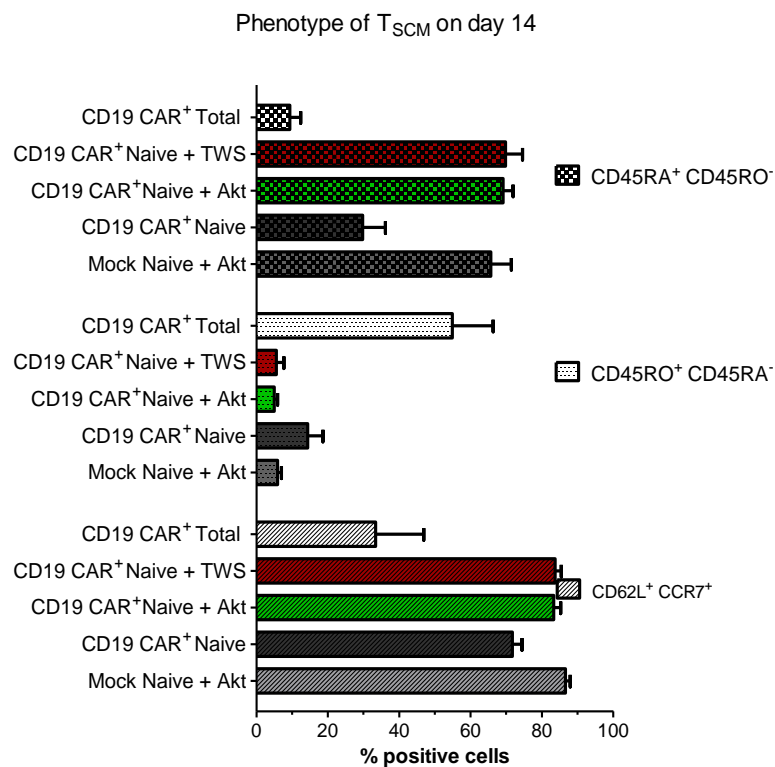
Figure 24: Overview of surface expression patterns of diverse CD19-CAR T cell subsets. Preselected naïve T cells were cultured in the presence of a cytokine mix and were treated with either Akt VIII Inhibitor or TWS119 to promote T$_{SCM}$/T$_{CM}$ formation. Total T cell were cultured in standard T cell medium without cytokine mix. Transduced naïve T cells and total T cells were analyzed for surface expression of naïve and memory markers (CD45RA/CD45RO) and homing markers (CCR7/CD62L) on day 14. Data from three independent experiments were combined. (mean values ± s.e.m. are indicated).

3.7.2 Cytokine response of naïve CD19-CAR T cells *in vitro*

After having confirmed, that TWS119 and Akt inhibitor VIII both promote T$_{SCM}$ formation, we generated naïve CD-19 CAR T cells to assess their functional properties. As described in the literature and observed in our studies, TWS119 restricts cell proliferation more than Akt treatment. Therefore, we chose Akt over TWS119 to generate naïve CAR T cell for further experiments. First, we analyzed IFN- γ secretion upon antigen encounter in an ELISpot assay. Successfully transduced naïve CD19-CAR T cells exerting a T$_{SCM}$ phenotype (CCR7$^+$CD62L$^+$CD45RA$^+$) were co-cultured with CD19$^+$ pre-B ALL cells (NALM16) for 18 hours 5 days after polyclonal stimulation. Additional T cell populations such as naïve derived CD19-CAR T cells and total CD19-CAR T cells without Akt treatment and naïve Mock T cells served as controls. Akt treated naïve CD19-CAR T cells demonstrated equally high levels of

70

IFN- γ secretion upon antigen-specific stimulation when compared to total CD19-CAR T cells (naïve CD19-CAR + Akt: 200; total CD19-CAR: 187.5). Interestingly, both naïve derived CD19-CAR T cells treated with or without Akt inhibitor VIII showed similar amounts of IFN-γ secretions (naïve CD19-CAR: 201; naïve CD19-CAR + Akt: 200), suggesting that Akt inhibitor VIII treatment did not affect the amount of IFN- γ release in naïve derived T cells (Fig.25).

Figure 25: IFN- γ ELISpot assay of naïve and total CD19-CAR T cells. Naïve CD19-CAR T cells with a memory stem cell phenotype were generated over a period of 17 days using a cytokine mix (IL-2, -7, -15, -21) and Akt VIII Inhibitor. An 18-hour ELISpot assay was conducted to assess stimulation activity of T cells upon antigen encounter. Thus, T cells and CD19+ NALM16 B-ALL cells were seeded in a 1:1 ratio. Naïve Mock T cells were used as control.

3.7.3 Lysis potential of naïve CD19-CAR T cells in vitro

Next, the lysis potential of Akt treated naïve CD19-CAR T cells was examined in comparison to total CD19-CAR T cells and naïve derived CD19-CAR T cells without Akt treatment, performing a ^{51}chromium release assay. CD19+ Pre-B ALL cells (NALM16) were labelled with chromium and co-cultured with modified T cells for 5 hours. Upon target cell lysis chromium is released and can be quantified in a gamma counter. The highest cytolytic activity was observed for naïve derived CD19-CAR T cells without Akt treatment and for Akt treated naïve CD19-CAR T cells (naïve CD19-CAR w/o Akt: 61.4%; naïve CD19-CAR +Akt: 58.2%) at a 60:1 effector:target ratio, decreasing to about 20% with decreasing effector:target ratios. In contrast, total CD19-CAR T cells exerted lower cytotoxicity with 30% at the highest effector:target ratio (Fig.26). Results of the chromium release assay indicate that Akt inhibitor VIII did not support the cytolytic activity of naïve CD19 CAR specific T cells *in vitro*, but T cells with a T$_{SCM}$ and T$_{CM}$ phenotype seemed to have a superior anti-tumor response in comparison to terminally more differentiated total CD19-CAR T cell.

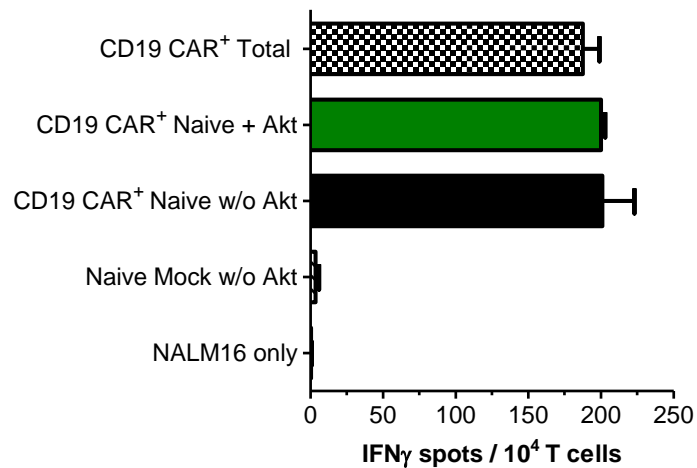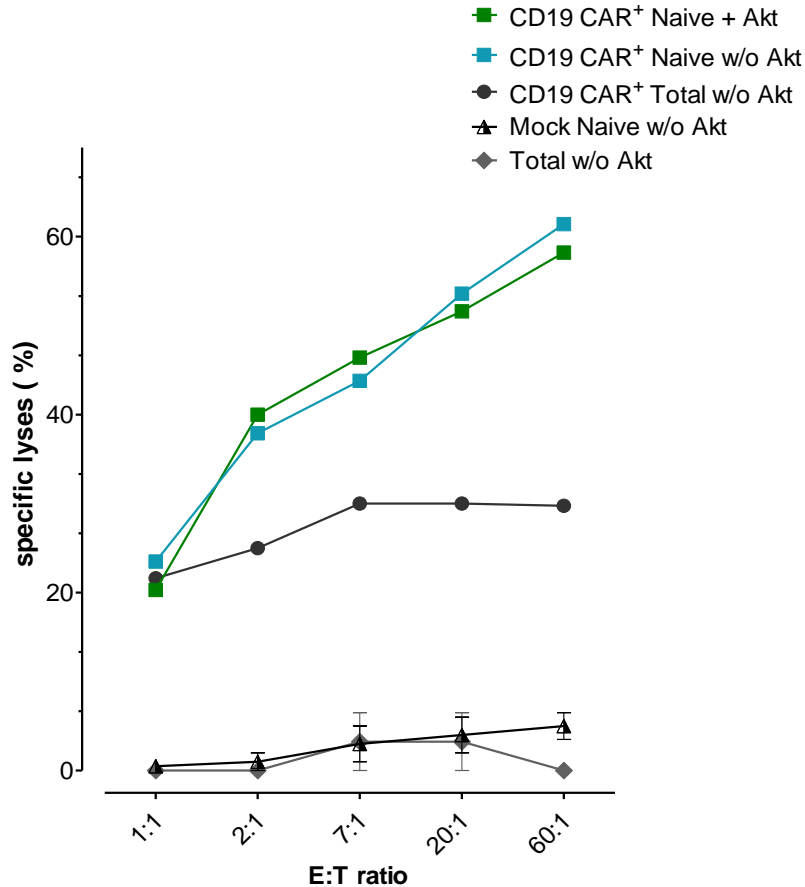**Figure 26: Cytolytic activity of Akt VIII treated naïve CD19-CAR T cells and total CD19-CAR T cells.** Naïve CD19-CAR T cells with a memory stem cell phenotype were generated over a period of 17 days using a cytokine mix (IL-2, -7, -15, -21) and Akt VIII Inhibitor. Five days after polyclonal stimulation, the cytolytic activity of T cells was determined by performing a 5-hour ^{51}Cr release assay using CD19$^+$ pre-B ALL cells (NALM16) as targets. Target cells were labelled with chromium and seeded with T cells at indicated ratios. (n = 1, mean values ± s.e.m are indicated).

3.7.4 Functional properties of naïve CD19-CAR T cells *in vivo*

After establishing the protocol for the generation of naïve CD19-CAR T cells and confirming their functional properties *in vitro*, we examined their therapeutic potential *in vivo* using a NSG mouse model. As the synergistic effect of CD4$^+$ and CD8$^+$ T cells has already been demonstrated *in vivo* (Sommermeyer, 2016), we conducted the *in vivo* experiments with T cell subsets containing CD4$^+$ (appx. 20%) and CD8$^+$ T cells (>70%). The experimental flow chart is illustrated in Fig.27. NSG mice were engrafted with 1x10^6 CD19$^+$ Pre-B ALL cells (NALM16) 8 days prior to T cell transfer. Two mice were sacrificed before administering T cells to confirm engraftment of NALM16 cells using flow cytometry analysis. Approximately 10% of CD19$^+$ NALM16 cells were detected in the murine bone marrow and 1x10^6 T cells of various T cell subsets, including total-CD19 CAR, naïve CD19-CAR and naïve derived CD19-CAR T cells without Akt treatment were injected into NSG mice. The groups receiving either no T cells or naïve Mock T cells served as controls.

Mice were examined macroscopically every 2nd day for any sign of illness during the experiment. 8 days after T cell transfer mice were sacrificed for endpoint analysis, examining the presence of CD19$^+$ NALM16 cells and CD4$^+$ or CD8$^+$ T cells in the bone marrow.
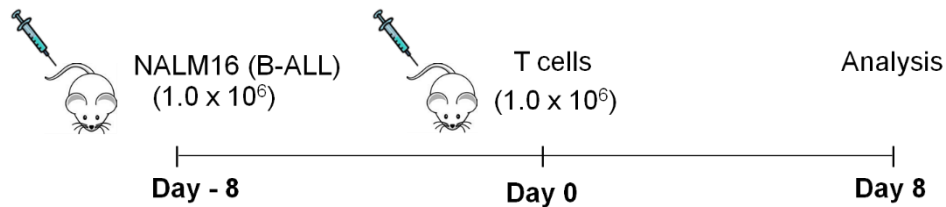

Figure 27: Flow chart for Adoptive transfer of CD19-CAR redirected T cells into NSG mice. NSG mice were i.v. injected with 1.0 x 10^6 CD19$^+$ pre-B ALL cells (NALM16). 8 days later, 1 x 10^6 T cells of diverse T cell subsets, such as naïve CD19-CAR T cells, which were generated using various cytokines (IL-2, -7, -12, -15, -21) and Akt inhibitor VIII over a period of 14 days, were transferred into mice three days after the last T cell restimulation. After additional eight days, murine bone marrow was analyzed for the presence of CD19$^+$ pre-B ALL cells as well as for human CD8$^+$ and CD4$^+$ T cells.

The quantification of CD19$^+$ NALM16 cells found in the bone marrow revealed an enhanced antitumor response for naïve CD19-CAR T cells w/o Akt and for Akt treated CD19-CAR T cells when compared to total CD19 CAR T cells (Fig.28A). For control groups, that either received no T cells or naïve Mock T cells, a relatively high number of CD19$^+$ NALM16 cells could be detected (NALM16 only: 40%, naïve Mock: 34%). Both naïve CD19 CAR T cell subsets differed only slightly in their average antitumor response, with Akt treated naïve cells reducing the amount of residual leukemia cells to 9.4% and the naïve T cells without Akt conferring a reduction of leukemic cells to 17.4%. The results implied a superior antitumor efficacy for Akt inhibitor treated naïve CD19-CAR T cells (T$_{SCM}$/T$_{CM}$ phenotype) in comparison to terminally more differentiated effector T cells (T$_{EM}$/T$_{EF}$). We further evaluated the potential of T cell persistence analyzing the presence of CD4$^+$ and CD8$^+$ T cells in the bone marrow (Fig.28B). Comparable frequencies of human CD8$^+$ T cells were found in the bone marrow for all T cell subsets (<0.5%). In contrast, naïve CD19-CAR T cells with and without Akt treatment showed a slightly better persistence of CD4$^+$ T cells in the bone marrow. However, the overall frequency found for CD4$^+$ T cells was quite low (< 1%).
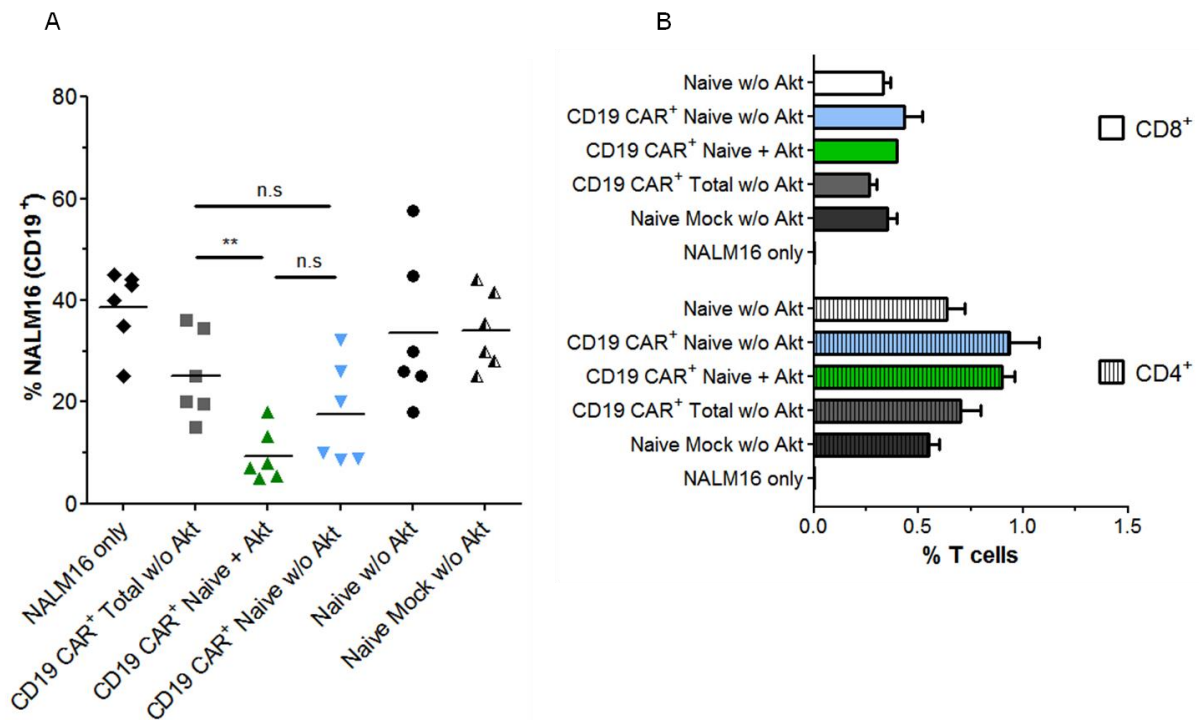
Figure 28: Anti-tumor response and T cell persistence of Akt VIII inhibitor treated naïve CD19-CAR T cells. NSG mice were i.v. injected with 1.0 x 10^6 CD19$^+$ pre-B ALL cells (NALM16) and 1 x 10^6 T cells of diverse T cell subsets (see Fig.14), such as naïve CD19-CAR T cells, generated in the presence of a cytokine cocktail (IL-2, -7, -12, -15, -21) and Akt Inhibitor VIII over a period of 17 days. 16 days after NALM16 engraftment (eight days after T cell injection), murine bone marrow was analyzed for the presence of CD19$^+$ pre-B ALL cells (**A**) as well as for human CD8$^+$ and CD4$^+$ T cells (**B**) by flow cytometry. For each T cell subtype, a group of six mice was used (n=1). The control group did not receive any T cells. Data are mean values ± s.e.m; **, p < 0.01, paired Student's t-test.

3.8 Generation of naïve EGFRvIII-CAR T cells

After establishing the generation protocol for naïve CD19-CAR modified T cells and assessing their functional properties regarding cytokine secretion and lysis potential, we aimed to generate naïve EGFRvIII-CAR T cells. Thus, naïve cells were preselected from PBMCs using CD45RA microbeads and were cultured in the presence of the cytokine mix and Akt VIII inhibitor (Fig.23A). T cells were transduced with the EGFRvIII-CAR three days after the initial stimulation. In parallel, total T cells expressing EGFRvIII-CAR were generated and cultured in standard T cell medium (AIMV+ IL-2). After puromycin treatment for positive selection of transduced cells and isolation of CD3$^+$ T cells, phenotypical analysis regarding surface expression of naïve and memory markers (CD45RA/CD45RO) and homing markers (CCR7/CD62L) was conducted by flow cytometry. Total and naïve T cells were also analyzed before transduction on day 3. Representative images of flow cytometry are shown in Fig.29, illustrating 78.8 % of CD45RA$^+$CD62L$^+$ T cells for Akt treated naïve EGFRvIII-CAR T cells on day 3, reflecting a stem cell memory phenotype. In contrast, only 16.8% of CD45RA$^+$CD62L$^+$ T cells were found in the total EGFRvIII-CAR T cell population. On day 18, hardly any change regarding TSCM population was observed within the total EGFRvIII-

CAR T cell population, whereas the level of CD45RA$^+$CD62L$^+$ T cells within the naïve EGFRvIII-CAR T cell population decreased to 49% (Fig.29A). A decrease in level of T$_{SCM}$ cells is expected as more T cell differentiate towards a T$_{CM}$ and T$_{EM}$/T$_{EF}$ state with time in culture. On day 3, about 8% of naïve EGFRvIII-CAR T cells and 31% of total EGFRvIII-CAR T cells were CD45RO$^+$CCR7$^+$, reflecting a central memory phenotype. On day 18 the amount of central memory T cell increased up to 50.2% within the naïve EGFRvIII-CAR T cell population as the level of stem cell memory cells decreased due to differentiation. In comparison, only 10.2% of total EGFRvIII-CAR T reflected a central memory phenotype as T cells differentiate towards effector memory (T$_{EM}$) and effector T cell (T$_{EF}$) phenotype indicated by high levels of CD45RO$^+$CCR7$^-$ T cells (Fig.29B). In conclusion, Akt treatment of naïve derived EGFRvIII-CAR T cells promoted a less differentiated phenotype, as on day 18 the levels of central memory (50.2% for naïve EGFRvIII-CAR T cells, 10.2% for total EGFRvIII-CAR T cells) and stem cell memory T cells (49% for naïve EGFRvIII-CAR T cells, 15% for total EGFRvIII-CAR T cells) were higher than in total EGFRvIII-CAR T cells.
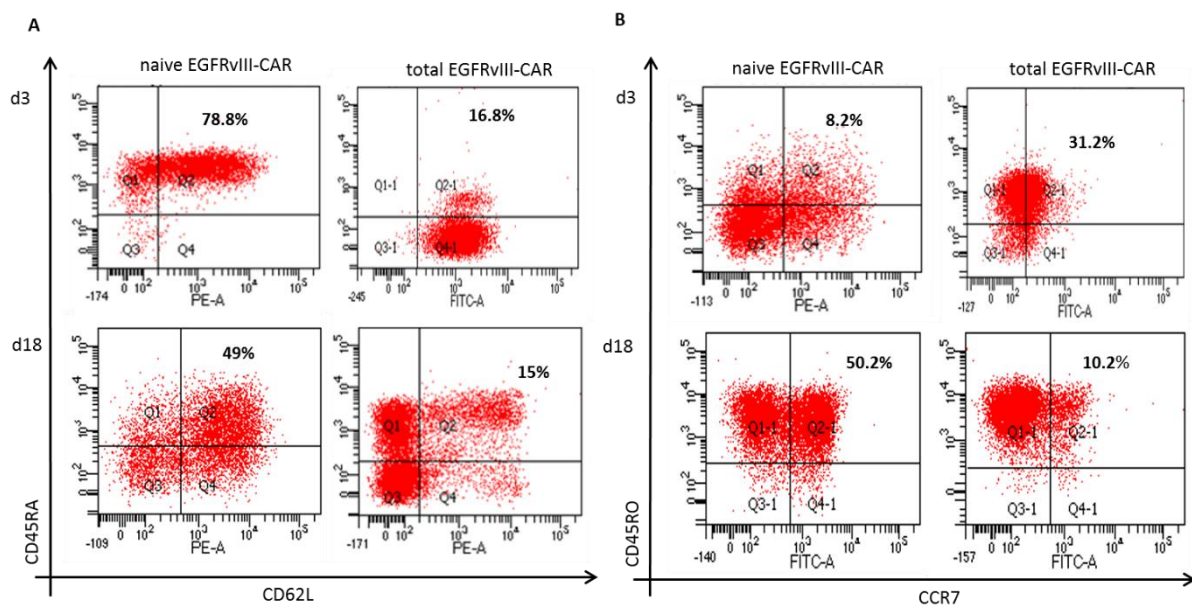
Figure 29: Phenotypical analysis of Akt VIII Inhibitor treated naïve EGFRvIII-CAR T cells. (A) Naïve Akt treated EGFRvIII-CAR T cells and total EGFRvIII-CAR T cells without Akt treatment were analyzed for levels of stem cell memory (T$_{SCM}$, CD45RA$^+$CD62L$^+$) on day 3 and 18 (B) Naïve Akt treated EGFRvIII-CAR T cells and total EGFRvIII-CAR T cells without Akt treatment were analyzed for levels of central memory T cells (T$_{CM}$, CD45RO$^+$CCR7$^+$). Representative images of flow cytometry are shown.

3.8.1 Cytokine secretion of Akt VIII treated naïve EGFRvIII-CAR T cells *in vitro*

To evaluate stimulation activity of naïve EGFRvIII-CAR T cells in comparison to total EGFRvIII-CAR T cells, we analyzed the IFN-γ secretion upon antigen encounter in an ELISpot assay. Naïve EGFRvIII-CAR T cells were generated in the same manner as naïve CD19-CAR

T cells (see Fig.23A). On day seven, CD8^{+} T cells were isolated from naïve EGFRvIII-CAR T cell population using anti-CD8 microbeads. Five days after restimulation, transduced total and naïve EGFRvIII-CAR T cells were seeded in a 2:1 ratio with A549 EGFRvIII^{+} target cells and co-incubated in an 18-hour ELISpot Assay. Before T cells were seeded on the ELISpot plate, they were washed twice with PBS to remove residual cytokine levels from the culture medium. Mock T cells served as control cells. A representative image of the IFN-γ ELISpot Assay illustrates a specific cytokine response for EGFRvIII-CAR redirected T cells (Fig.30A). No IFN-γ spots were detected for total CD3^{+} or CD8^{+} Mock T cells, neither for naïve CD8^{+} Mock T cells. Total CD3^{+} and CD8^{+} EGFRvIII-CAR T cells exerted a similar cytokine response with about 180 spots (Fig.30B) as counted using a CTL reader. Naïve CD8^{+} EGFRvIII-CAR T cells showed a slightly stronger cytokine response.
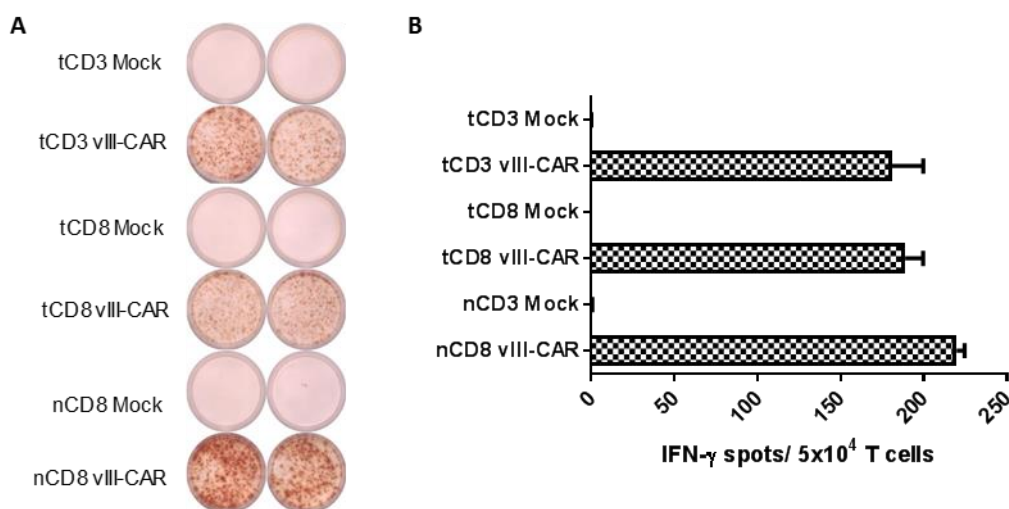
Figure 30: IFN-γ ELISpot assay of Akt treated naïve EGFRvIII-CAR T cells. (A) Representative image of an IFN-γ ELISpot Assay. Modified CD8^{+} naïve EGFRvIII-CAR T cells (nCD8 Mock/vIII-CAR, Akt treated) and CD3^{+} or CD8^{+} total EGFRvIII-CAR T cells (tCD3 Mock/vIII-CAR or tCD8 Mock/vIII-CAR, untreated) were analyzed for their stimulation upon antigen encounter using the A549 EGFRvIII^{+} tumor cells. T cells and target cells were seeded in a 2:1 ratio using 5x10^{4} T cells/well and 2.5 x10^{4} tumor cells/well and were co-incubated for 18 hours. Naïve CD8^{+} Mock T cells were used as controls. (B) Cytokine secretion is quantified by SPOT counting using a CTL reader. Data shown are mean volumes ± SEM, n=3.

Furthermore, a Granzyme B ELISpot assay was performed to assess the cytolytic potential, as Granzyme B is a serin protease, involved in apoptosis and is restricted to cytotoxic cells. Again, transduced total and naïve EGFRvIII-CAR T cells were seeded in a 2:1 ratio with A549 EGFRvIII^{+} tumor cells in an 18-hour Granzyme B ELISpot assay. Results demonstrated a specific cytokine secretion of EGFRvIII-CAR T cells upon antigen encounter. No Granzyme B spots were detected for total CD3^{+} Mock T cells and only few spots were visible for total and naïve CD8^{+} Mock T cells (Fig.31). About 230 spots were counted for total CD3^{+} EGFRvIII-CAR T cells, whereas a slightly increased cytokine release was observed for total and naïve

CD8^{+} EGFRvIII-CAR T cells (up to 300). Results of the IFN-γ and Granzyme B Assay demonstrate a specific cytokine response upon antigen encounter for total and naïve EGFRvIII-CAR T cells. Furthermore, Akt treated naïve EGFRvIII-CAR T cells showed no prominent difference in IFN-γ secretion but only a slightly enhanced level of Granzyme B secretion. Thus, Akt VIII inhibitor treatment of naïve EGFRvIII-CAR T cells had no prominent effect on cytokine response towards EGFRvIII^{+} tumor cells.
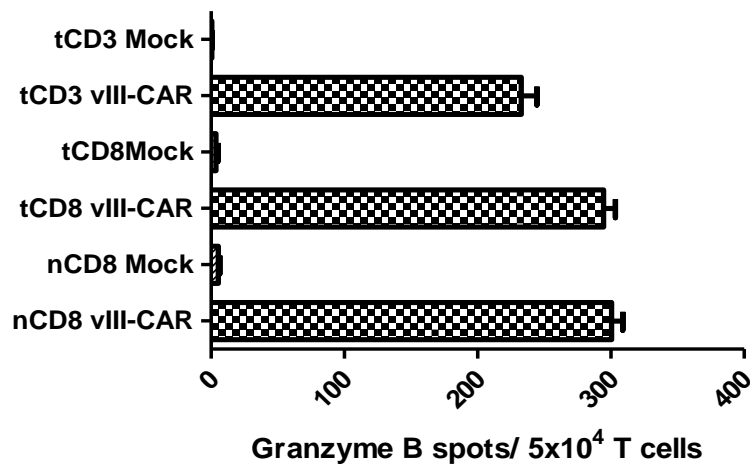
Figure 31: Granzyme B ELISpot assay of Akt inhibitor VIII treated naïve EGFRvIII-CAR T cells. Modified CD8^{+} naïve EGFRvIII-CAR T cells (nCD8 Mock/vIII-CAR, Akt treated) and CD3^{+} or CD8^{+} total EGFRvIII-CAR T cells (tCD3 Mock/vIII-CAR or tCD8 Mock/vIII-CAR, untreated) were analyzed for their stimulation upon antigen encounter using the A549 EGFRvIII^{+} tumor cells. T cells and target cells were seeded in a 2:1 ratio using $5x10^4$ T cells/well and $2.5 x10^4$ tumor cells/well and co-incubated for 18 hours. Naïve CD8^{+} Mock T cells were used as controls. Data from two independent experiments were combined and cytokine secretion is quantified by SPOT counting using a CTL reader. Data shown are mean volumes ± SEM, n=3.

3.8.2 Transmigration Assay

CD62L and CCR7 are known to play a pivotal role in T cell migration and are co-expressed on less differentiated T cells (T_{SCM}/T_{CM}), distinguishing their phenotype from more differentiated T cells (T_{EM}/T_{EF}). As analyzed in 3.7, the CCR7^{+}/CD62L^{+} fraction of naïve EGFRvIII-CAR T cells comprised 50.2% of CD45RO^{+}CCR7^{+} T cells in comparison to 10.2 % in total EGFRvIII-CAR T cells. Thus, we evaluated the migration ability of both T cell subsets using a 24 - transwell plate with 5 µm pore size inserts. The bottom chamber was filled with 600 µl T cell medium with or without the chemokine CCL21, a ligand of CCR7, at the indicated concentration (Fig. 32A). 100 µl of T cell suspension, adjusted to $5x10^6$ cells/ml was loaded into the upper chamber, which contains a cell permeable membrane, allowing T cells to migrate to the bottom chamber. After 5 hours the upper chambers were removed and the number of T cells that had migrated to the bottom chamber was counted under the microscope. Fig. 32B shows a higher number of migrated T cells for the naïve EGFRvIII-CAR T cell population.

1.4×10^5 naïve EGFRvIII-CAR T cells were counted in the bottom chambers filled with medium containing CCL21, whereas only 0.74×10^5 T cells of total EGFRvIII-CAR T cells were counted. Less total (3.6×10^4 T cells) and naïve EGFRvIII-CAR T cells (5.7×10^4) migrated to the chambers filled with T cell medium only. Hence, an enhanced migration ability of the naïve EGFRvIII-CAR T cells in comparison to total EGFRvIII-CAR T cells towards CCL21 could be demonstrated. Overall, functional properties of naïve EGFRvIII-CAR cells could be proved in regards of antigen specific stimulation, lytic potential and improved migration capacity. However, owing to time limitations, comparative studies of naïve EGFRvIII-CAR T cells *in vivo* were yet not performed.
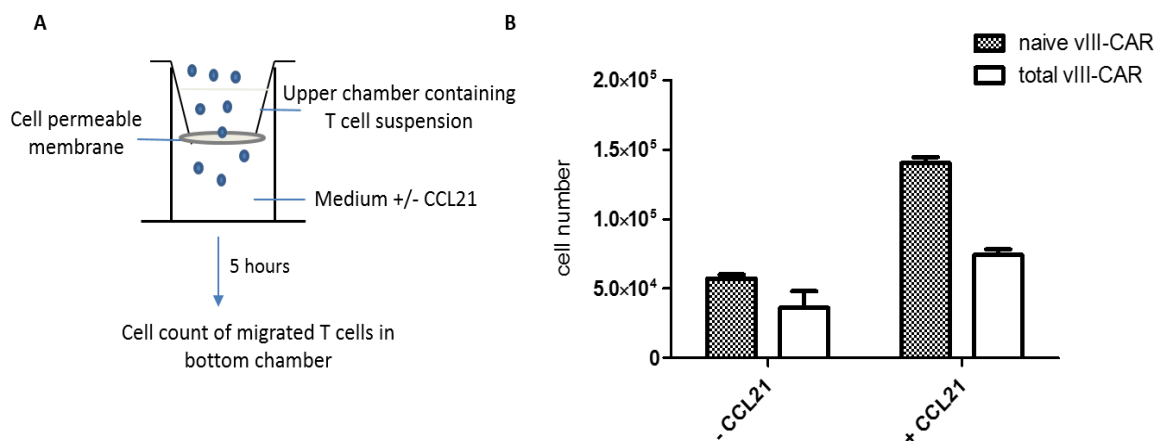
Figure 32: Transmigration assay. Naïve and total EGFRvIII-CAR expressing T cells were generated under the impact of Akt VIII inhibitor and a cytokine mix (see Fig.11A). The migration ability of both T cell subsets was evaluated using a 24 well, 5 µm size pore transwell plate, that contains a removable insert with a cell permeable membrane. 1×10^5 T cells were placed in the top chamber insert (A) in 100 µl medium. The bottom chamber was filled with 600 µl T cell medium (+/- 1 µg CCL21). The transwell plate was incubated at 37°C and 5% CO_2 for 5 hours. Afterwards, the top chamber inserts were removed and cells that had migrated to the bottom were counted. Results shown are representative from one experiment out of two.

4 Discussion

4.1 Necessity of novel targets for lung cancer treatment

In the past two decades remarkable progress in lung cancer treatment has been achieved, shifting from the empiric use of chemotherapy towards personalized patient management. Improved understanding of the tumor biology and awareness of its heterogenic mutation profile led to development of targeted therapies and immunotherapy. Tyrosine kinase inhibitors targeting EGFR or ALK showed promising results with prolonged survival, however these initial responses are mostly restricted owing to acquired resistance based on selection of resistant sub-clones [114, 115]. Introduction of immune checkpoint blockers (ICB) targeting PD-L1/PD-1 or CTLA-4 resulted in survival benefits in selected patients, yet the initial responses observed were not durable and were further accompanied by acquired resistance [37]. Several mechanisms have been described as a cause for the acquired resistance to ICB treatment, including defects in IFN-γ signaling or major histocompatibility complex presentation [116] and increased levels of indoleamine 2,3-dioxygenase (IDO1), that catabolizes tryptophan required for optimal T cell function [117, 118]. However, despite major breakthroughs in lung cancer management, overall cure and survival rates remain disappointing, with the 5-year survival rate being less than 18% [35]. Consequently, improving current treatment modalities is not only challenged by finding new druggable targets for targeted therapy but also exploring driver mutations and tumor neoantigens for immunotherapy with the intention to expand survival benefits for a broader population of patients. In this regard the tumor neoantigen EGFRvIII represents an attractive therapeutic target as it is exclusively expressed on malignant cells and has been reported to be expressed in several tumors [27], including NSCLS, where it has yet been insufficiently examined.

4.2 Rationale for EGFRvIII-CAR therapy for NSCLC

Considering the high number of lung cancer incidences, high mortality rates, poor prognosis, and limitations of currently applied targeted therapies, alternative therapy modalities are indeed desirable. As such, CAR therapy using EGFRvIII-CAR redirected T cells to target EGFRvIII$^+$ tumor cells could provide an alternative approach, especially for patients who failed standard treatments. Adoptive cellular therapy using chimeric antigen receptors (CARs) has shown great promise for the treatment of hematological malignancies, as could be witnessed for acute lymphocytic leukemia, where complete response rates were achieved in approximately 90% of refractory and recurrent ALL [87]. In contrast to conventional or genetically engineered TCRs for adoptive therapy, CARs provide an HLA-independent recognition of the antigen presented

on the surface of the target cell, and thus are applicable for a broader patient population. Furthermore, CARs can override pitfalls occurring due to tumor escape mechanisms, such as downregulation of HLA molecules to dampen antigen presentation. There are numerous ongoing clinical trials investigating different tumor associated antigens for therapy of solid tumors, including mesothelin (MSLN), HER2, EGFR/EGFRvIII, CEA and others, some of which showed promising results [119]. However, several factors hinder the success of CAR treatment for solid tumors, some of which include insufficient trafficking, an unhostile tumor microenvironment and insufficient safety control. Furthermore, off-tumor target expression can result in toxicity with varying severity depending on the affected organ tissue [120, 121]. Therefore, another major drawback is the lack of an appropriate target, that is solely expressed on malignant cells or has limited expression on healthy tissue. Considering the properties of EGFRvIII, being an antigen with a neoepitope exclusively expressed on malignant cells, conferring to tumorigenicity and being accessible on the cell surface, it appears to be an ideal target for adoptive therapy. EGFRvIII-CAR therapy has so far only been explored for glioblastoma in preclinical animal models showing therapeutic potential while clinical trials with glioblastoma patients are still ongoing [122]. Expression data of EGFRvIII expression for other tumors besides glioblastoma, including lung cancer are found to be controversial [27], however EGFRvIII expression in NSCLC has been described in several studies [29, 123–125]. We believe that more extensive research on EGFRvIII is required to harness the most potential of EGFRvIII as a clinical target for solid tumors. Consequently, despite EGFRvIII being not the most dominant mutation in NSCLC, even a low percentage of EGFRvIII expression is eligible for treatment in selected patients considering the high incidence of lung cancer worldwide. Thus, we evaluated the anti-tumor response of a third generation EGFRvIII-CAR targeting EGFRvIII$^+$ tumor cells *in vitro* and studied its potential *in vivo* using an NSG xenograft mouse model with the intention to provide valuable information as a proof of concept study for immunotherapy in lung cancer.

4.3 Generation of EGFRvIII-CAR redirected T cells by retroviral gene transfer

CAR-T cell therapy involves redirection of patient or donor T lymphocytes to specifically target and destroy malignant cells with the aim to provide durable anti tumoral response while avoiding severe adverse events. The first step to meet these goals is the safe, efficient and stable transfer of a synthetic gene encoding the chimeric antigen receptor. In our studies we used a third generation EGFRvIII-CAR (provided by the Rosenberg laboratory), comprising CD3ζ and two additional co-stimulatory molecules, CD28 and 4-1BB [113], for T cell signaling to redirect T cell specificity via retroviral gene transfer. Gene transfer technology offers multiple

sophisticated methods being used in the clinical setting, including viral gene transfer methods using α-virus, gamma-retrovirus and lentivirus and non-viral methods such as transposons and mRNA electroporation. Lentiviral and gamma-retroviral vectors are the most commonly used vectors applied for gene therapy. Their major advantage is their ability to stably integrate into the host genome. Lentiviruses can integrate their genome into both, dividing and resting cells, whereas successful transduction by retroviruses depends on target cell mitosis. Safety standards for clinical application require the viral vectors to be replication incompetent with a low genotoxicity and low immunogenicity. Gamma retroviruses such as the Moloney murine leukemia virus were among the first to be used as packaging systems for gene therapy [126]. The gene of interest replaces the gamma retrovirus coding sequence and essential viral components required for packaging, including gag, pol, and env, coding for capsid proteins, replication enzymes and envelope glycoproteins, respectively, are provided on separate helper plasmids devoid of packaging signals to lower the risk of recombination, thereby further increasing safety issues [127, 128]. The env gene defines the preference of transducing a certain cell type. Since selection of an amphotropic envelope glycoprotein from gibbon-ape leukemia virus (GALV) over the murine MLV results in a more efficient transduction of human hematopoietic cells, we selected the GALV envelope for transduction of T cells. The EGFRvIII-CAR sequence was cloned into the retroviral vector pMX-IRES-Puro, that is based on the Moloney murine leukemia virus (MMLV) and is equipped with long terminal repeats LTRs flanking the gene of the interest to facilitate host genome integration. The resulting pMX-EGFRvIII-CAR transfer vector was applied for transfection of the packaging cell line Phoenix-Ampho, stably transfected with the helper plasmids gag, pol and env (pCOLT GALV) to produce viral particles. Transfected Phoenix-Ampho cells were harvested for FACS analysis to examine GFP expression or EGFRvIII-CAR expression of pMX-MOCK or pMX-EGFRvIII-CAR transfected cells, respectively, showing positive results with transfection efficiencies ranging from 70% to 90% (see chapter 3.3.1). When viral particles fuse with the target cell membrane, the virion core is released into the cytosol and requires a disrupted nuclear membrane to enter the nucleus and thus depends on target cell mitosis [127, 129]. Due to this limitation T cells had to be stimulated with OKT-3, CD28 and IL-2 two to three days prior to transduction with the pMX-EGFRvIII-CAR to ensure efficient proliferation of T cells. Transduction of T cells with the pMX-EGFRvIII-CAR or the control vehicle pMX-Mock encoding for GFP yielded an average of approximately 20% of transduced cells, as confirmed by FACS analysis. Several factors confer to improved transduction including transfection efficiencies of Phoenix-Ampho cells, quality of PBMCs used for transduction and efficient

stimulation and proliferation of T cells. Nonetheless, since the retroviral vector pMX provides puromycin resistance, which allows for a positive selection of transduced cells, the T cell population comprised approximately >90% of transduced cells after puromycin treatment (6 d) as assessed by FACS analysis of EGFRvIII-CAR or Mock T cells (see chapter 3.3.2).

4.4 Generation of EGRvIII⁺ transfected cell lines

After generating EGFRvIII-CAR redirected T cells, their functional properties in response to antigen encounter had to be examined. Since no cell line was available that naturally expressed EGFRvIII, transfected cell lines expressing EGFRvIII were generated by retroviral transduction. This in fact is a common approach when it comes to research on EGFRvIII. It has been described that cell lines lose EGFR amplification and mutation when commonly grown in vitro and thus, most research data on EGFRvIII is based on transfected cell lines [27]. However, Del Vecchio and colleagues reported the cell line DK-MG, which is established from a glioblastoma multiform, to express EGFRvIII endogenously. The cell line is further characterized as a heterogenous line with populations positive and negative for EGFRvIII expression. [130]. Stech and colleagues utilized this cell line to establish clones with the highest EGFRvIII expression levels, referred to as DK-MG^high. Interestingly, they could show that neither EGFRvIII mRNA levels nor amplicon number changed in DK-MG^high cells over prolonged culturing of cells, while observing loss of EGFRvIII amplicons in their own attempts at establishing stable EGFRvIII⁺ glioblastoma cell lines from primary tumor cells [131]. Some research groups described a three-dimensional culture of cell lines derived from EGFRvIII⁺ tumors as neurospheres , that have been propagated *in vivo* to maintain reproducible EGFRvIII expression [132, 133]. For our initial experiments we used the murine renal carcinoma cell line Renca EGFRvIII⁺. This cell line was kindly provided by the Group of PD Dr. E. Bockamp (Inst. for Transl. Immunol., UMM Mainz). FACS analysis displayed an EGFRvIII surface expression level of 66.8% (chapter 3.4). The human melanoma cell line Ma-mel EGFRvIII⁺, deficient of HLA class I and class II surface expression following genome editing, was used as a representative cell line for solid tumors and was transfected with the pMX-EGFRvIII vector bearing neomycin resistance (kindly provided by C. Wölfel, IIIrd. Dept of Medicine, UMM). We further transfected the adenocarcinoma cell line A549 with the retroviral pMX-EGFRvIII vector providing puromycin resistance to generate the A549 EGFRvIII⁺ cell line. Target cell lines were treated with the appropriate antibiotics and were analyzed for surface expression of EGFRvIII by FACS analysis. Both human tumor cell lines were efficiently transduced, showing average surface expression levels of EGFRvIII ranging from approximately 75-90% (chapter 3.4). However, we observed fluctuating levels of surface expression for EGFRvIII⁺ in both cell

lines during cell culture. EGFRvIII expression levels dropped to nearly 20% in Ma-mel EGFRvIII$^+$ cells and to approximately 30% in A549 EGFRvIII$^+$ cells over time which was surprising, since both cell lines were permanently cultured in their respective selection medium using either neomycin or puromycin. This could possibly be caused by degradation or internalization of the receptor. Thus, to ensure optimal conditions for functional assays, we repeatedly stained cells for surface expression of EGFRvIII, and if necessary, used a new aliquot of frozen target cells, to ensure that only cells with an expression level of > 75% were applied for functional assays.

4.5 Functional properties of EGFRvIII-CAR redirected T cells *in vitro*

T cells that have been transduced to express EGFRvIII-CAR underwent a puromycin selection treatment for 6 days to increase the number of successfully transduced cells. T cells were analyzed by FACS for surface expression of the EGFRvIII-CAR, CD4 and CD8 and markers defining their differentiation stage. Functional properties of successfully transduced and selected T cells were then analyzed in several assays for (CAR)-antigen specific stimulation, cytokine secretion and lysis potential upon antigen encounter. Mock T cells, that were transduced with the pMX-Mock vector, containing GFP only, were used as control cells.

4.5.1 Stimulation of EGFRvIII-CAR redirected cells upon antigen encounter *in vitro*

Mock and EGFRvIII-CAR T cells were examined for their antigen specific stimulation response in a 48-hour co-culture assay using different tumor cells expressing EGFRvIII. Effector cells (T cells) and target cells (tumor cells) were co-cultured in ratios ranging from 4:1 and 1:1. Using phase contrast microscopy we could visually assess T cell stimulation and observed T cell cluster formation only for EGFRvIII-CAR redirected T cells cultured with the murine Renca EGFRvIII$^+$, the human Ma-mel EGFRvIII$^+$, and A549 EGFRvIII$^+$ tumor cells. In contrast, Mock T cells cultured with EGFRvIII$^+$ target cells did not form any clusters, indicating a specific activation of the EGFRvIII-CAR T cells by their antigen expressed on tumor cells (3.5.1). Another characteristic of activated T cell is the production of cytokines such as IFN-γ among others. IFN-γ is a dimerized soluble cytokine that plays an important role in anti-pathogen, immune-regulatory, and anti-tumor properties [134]. IFN-γ is mainly produced by activated natural killer cells (NK cells), natural killer T cells (NKT cells) and by antigen-specific Th$_1$ CD4$^+$ and CD8$^+$ effector T cells. High levels of IFN-γ production are associated with an efficient immune response. To determine the frequency of IFN-γ producing T cells we conducted an EliSpot assay (3.5.3), which is a well-established method for the detection and enumeration of cytokine secreting cell on a single-cell level. Mock and EGFRvIII-CAR T cells

were co-cultured with EGFRvIII expressing tumor cells in a 2:1 ratio using an ELISpot plate precoated with a capture antibody specific for INF-γ. Quantification of the ELISpot assay confirmed the observations made in the co-culture assay described above. EGFRvIII-CAR T cells demonstrated a specific IFN-γ secretion when cultured with the different EGFRvIII^{+} tumor cells Renca (190 spots/well), Ma-mel (220 spots/well) and A549 (370 spots/well), whereas Mock T cells did not show any cytokine response when co-cultured with the human Ma-mel EGFRvIII[+] and A549 EGFRvIII[+] and only a few spots were visible for Mock T cells cultured with the murine Renca EGFRvIII[+]. Since the Ma-mel EGFRvIII[+] are characterized by a deficiency of HLA class I and class II molecules it was not surprising, that no allospecific cytokine response was triggered by Mock T cells. We would have expected to detect a minor cytokine response of Mock T cells cultured with the human A549 EGFRvIII, that might cause an alloreactive response as they are not deficient of HLA class I and II surface expression. Surprisingly, hardly any spots were detected, and this might be explained by insufficient HLA-class I/II antigen presentation or the co-culture period of 18 hours, which was probably too short to cause a primary alloreactive response. However, a minor unspecific response of Mock T cells targeting the murine Renca EGFRvIII[+] was observed resulting in about 15 IFN- γ spots per well. This might reflect xenoreactivity although it is unclear whether in this case target cells of murine origin cause more immunity than allogeneic targets. Despite this minor background there was a clear difference of spots counted for Mock T cells (15 spots/well) and EGFRvIII-CAR T cells targeting Renca EGFRvIII[+] (190 spots/well), confirming the specific immune response of EGFRvIII-CAR T cells upon antigen encounter (chapter 3.5.3).

4.5.2 Lysis potential of EGFRvIII-CAR redirected cells *in vitro*

Lysis activity of T cells targeting EGFRvIII^{+} tumor cells was quantified using different assays. For an indirect quantification of target cell lysis, we applied the crystal violet staining assay after a 48-hour co-culture of Mock and EGFRvIII-CAR T cells with the EGFRvIII[+] Renca, Ma-mel and A549 tumor cells. When adherent cells undergo cell death e.g. caused by T cell lysis, they detach from culture wells. Crystal violet solution (CVS) binds to the DNA and proteins of the cell, consequently, the intensity of crystal violet solution correlates with the amount of remaining adherent target cells. The less target cells are lysed the more is the intensity of CVS. Images of the CVS (chapter 3.5.2) showed clear differences among the wells, where either Mock or EGFRvIII-CAR T cells were cultured with EGFRvIII^{+} tumor cells. When Mock T cells were cultured with the respective target cells a relatively confluent cell layer of target cells was visible resulting in a violet colored well bottom. In contrast, when tumor cells were cultured with EGFRvIII-CAR T cells hardly any crystal violet staining was visible since almost all target

cells were lysed by EGFRvIII-CAR T cells. The Granzyme B assay, which was applied to further quantify frequency of cytokine secreting cells elicited similar data, confirming the results obtained by CVS staining. Granzyme B is a serine protease, that in contrary to IFN-γ is restricted to cytotoxic lymphocytes and NK cells. Together with perforin and other toxic mediators Granzyme B triggers target cell death by apoptosis in a caspase dependent and independent manner. Results of the Granzyme B ELISpot assay proved an antigen-specific lysis of EGFRvIII$^+$ tumor cells, with prominent Granzyme B secretion detected for EGFRvIII-CAR T cells targeting Renca-EGFRvIII$^+$ (220 spots/well), Ma-mel EGFRvIII$^+$ (240 spots/well) and A549 EGFRvIII$^+$ (240 spots/well) and a neglectable number of spots (<10 spots/well) counted in the wells cultured with Mock T cells (chapter 3.5.3). Measuring T cell cytotoxicity can also be quantitatively determined by the chromium 51 (^{51}Cr) release assay. When target cells, that have been labeled with ^{51}Cr are cultured with cytotoxic T cells, chromium is released by cytolysis and can be measured using a gamma counter. In line with results of the CVS assay and Granzyme B assay, ^{51}Cr release assay demonstrated an antigen specific response of EGFRvIII-CAR T cells towards EGFRvIII$^+$ Ma-mel and A549 cells. At the highest effector:target ratio (60:1) CD8$^+$ EGFRvIII-CAR T cells exhibited a lytic activity of up to 70% targeting Ma-Mel EGFRvIII$^+$ and up to 58% targeting the A549 EGFRvIII$^+$. CD3$^+$ EGFRvIII-CAR T cells exhibited slightly lower cytolytic activity as the T cell population was not only composed of effector CD8$^+$ T cells but also contained CD4$^+$ T cells. Mock T cells elicited a low cytolytic activity of up to 10% at the highest effector:target ratios targeting Ma-mel EGFRvIII$^+$ and A549 EGFRvIII$^+$ accounting for unspecific alloreactive response. Moreover, the antigen-specific response of EGFRvIII-CAR T cells towards EGFRvIII$^+$ tumor cells was further supported by examining CD19-CAR T cell lytic activity targeting the Ma-mel EGFRvIII$^+$, which was neglectable with only less than 10% at the highest effector:target ratio (chapter 3.5.4).

4.6 Adoptive transfer of EGFRvIII-CAR T cells *in vivo*

After having confirmed the lysis potential of EGFRvIII-CAR T cells *in vitro,* we sought to evaluate the therapeutic potential of EGFRvIII-CAR T cells in a xenograft NSG mouse model. NOD-scid IL2rγ^{null} (NSG) are characterized by a severe combined immune deficiency mutation (SCID) and a knockout of the interleukin-2 gamma chain receptor. Consequently, these mice are deficient of NK cells, mature B and T cells, and are further incapable of cytokine signaling through the common gamma chain. First, mice were engrafted with A549 EGFRvIII$^+$ tumor cells by subcutaneous injection based on results of engraftment kinetics established beforehand (chapter 3.6.1). When the tumor reached a volume of approximately 40 mm^3 on day 7, T cells

(4x10^6) were injected intratumorally. A549 EGFRvIII$^+$ bearing mice either received Mock T cells, EGFRvIII-CAR T cells or were left untreated. Under optimal conditions, an adoptive transfer of CAR T cells involves proficient T cell persistence, proliferation and specific cytolytic activity towards EGFRvIII$^+$ tumor cells, resulting in tumor regression or at least tumor halt when treated with tumor specific CAR-T cells. It has already been demonstrated that there is a synergistic effect of CD4$^+$ and CD8 $^+$ cells and that transfer of both T cell subsets yields better antitumor response [135]. Hence, we generated CD3$^+$ EGFRvIII-CAR T cells containing CD4$^+$ and CD8$^+$ T cells and studied T cell composition by FACS analysis on day of T cell transfer. There was a higher proportion of CD8$^+$ T cells within the CD3$^+$ EGFRvIII-CAR T cell population, with 33% being CD3$^+$CD4$^+$ and 73.8% being CD3$^+$CD8$^+$. Comparable ratios were found for the Mock T cell population (CD3$^+$CD4$^+$ 33.9%, CD3$^+$CD8$^+$ 76.6%). Furthermore, most of the T cells were CD45RO$^+$CCR7$^-$, reflecting a more differentiated effector memory phenotype, while 38% reflected a central memory phenotype (CD45RO$^+$CCR7$^+$) and only 6.3% displayed a less differentiated stem cell memory phenotype (CD45RA$^+$CD2L$^+$). Similar results were obtained for Mock T cells as described in chapter 3.6.2.1. Seven days after T cell transfer mice were sacrificed, and final mean tumor volumes were assessed, showing no notable difference among the Mock T cell and EGFRvIII-CAR T cell treated cohorts. However, there was a significant difference when comparing the untreated control group with the Mock and EGFRvIII-CAR T cell treated group, indicating nonspecific antitumoral responses by Mock T cells. This observation can likely be explained by HLA class I and class II surface expression on tumor cells causing an alloreactive response of T cells. We analyzed tumor cells for surface expression of HLA class I and class II molecules by FACS analysis revealing expression levels of 17.5% for HLA class I and 26.5% for HLA class II molecules. We further examined surface expression of EGFRvIII, which was only 8.6% in the untreated cohort, 7.2% in the Mock and 11.2% in the EGFRvIII-CAR treated group (chapter 3.6.2.3). This low expression level of EGFRvIII on tumor cells engrafted in mice is likely to be the main reason for a small but insufficient tumor-specific anti-EGFRvIII driven immune response of EGFRvIII-CAR T cells observed in our *in vivo* experiments, and supports our data on inconsistent and variable EGFRvIII expression on the tumor cell lines Ma-mel EGFRvIII$^+$ and A549 EGFRvIII$^+$ *in vitro*. Loss of EGFR and EGFRvIII amplification and mutation for traditional cell lines cultured *in vitro* has been reported, however, the mechanisms are poorly understood [136]. Another factor for the inefficient antitumor-response could be T cell exhaustion and insufficient T cell proliferation. When tumor mass, bone barrow and spleen were analyzed for T cell presence hardly any T cells were to be detected within the tumor. Only 0.8% of CD3$^+$CD8$^+$ EGFRvIII-

CAR T cells and 0.5% of Mock T cells were found in the tumor and none in bone marrow or spleen, pointing to a poor persistence of T cells and their incapability of migrating to secondary lymphoid organs (chapter 3.6.2.4). It is conceivable that the majority of T cells administered have been differentiated into effector T cells, described to have an inferior T cells persistence and proliferation capacity. However, since NSG mice lack a functional immunological micromilieu and an appropriate cytokine support for human lymphocytes, adoptively transferred T cell cannot properly home in secondary immunological tissues and are deficient of adequate cytokines such as in particular the homeostatic cytokines IL-7 and IL-15 as no additional cytokines were administered *in vivo*. Furthermore, the presence of myeloid derived suppressor cells (MDMC) could be an additional dampening factor for T cell function. MDMCs are a heterogenous group comprising myeloid cell progenitors and precursors of granulocytes, macrophages and dendritic cells that accumulate during chronic inflammation and tumor progression [137–140]. We detected a low level of murine myeloid derived suppressor cells (MDMCs) within the tumor mass as analyzed by FACS (chapter 3.6.2.5). Two main MDSC subtypes designated as granulocytic (G-MDSC) and monocytic (M-MDSC) have been reported for tumor-bearing mice. G-MDSC are defined by a $CD11b^+Gr-1^{high}$, $CD11b^+Ly6G^+$ and $Ly6C^{low}$ phenotype, whereas M-MDSC exert a $CD11b^+Gr-1^{mid}Ly6G^-$ and $Ly6C^{high}$ phenotype [141, 142]. Notably, no prominent difference was observed within the different groups. For tumor specimen derived from the EGFRvIII-CAR T cell treated group we found about 3.8% of G-MDMC reflecting a $CD11b^+Gr-1^{high}$ and approximately 6.4 % reflecting a $CD11b^+Ly6G$ phenotype. Similar levels were found for the untreated and Mock T cell treated groups while hardly any M-MDSC ($CD11b^+Gr-1^{mid}Ly6G^-$ and $Ly6C^{high)}$ were detected in the different groups (<1%). M-MDSC and G-MDSC are described to exert immunosuppressive activities and inhibit T cell function using different mechanisms, which are however not exclusively used [143, 137]. Modes of action include for example secretion of arginase (ARG-1) causing deprivation of arginine, which is essential for T cell proliferation and anti-tumor reactivity [144], production of nitric oxide (NO) and reactive oxygen species (ROS) that can result in nitration of T cell receptors (TCR) and chemokines needed for sufficient T cell migration [137, 139, 145]. Other mechanisms describe upregulation of PD-L1, enhanced secretion of IL-10 and transforming growth factor (TGF)-β1 causing further inhibition of immune effector functions [146–148] and reduction of the TCR-ζ chain expression, affecting the TCR-mediated antigen recognition [149, 150]. However, it is unclear and remains to be studied in detail whether and to which extent the presence of murine MDSC affects human T cells. Further exploration is necessary to clarify the role of MDMCs in the xenograft mouse model.

4.7 Generation of less differentiated EGFRvIII-CAR T cells

According to their differentiation stage, T lymphocytes are divided into naïve T cells and four main activated subtypes, including stem cell memory (T_{SCM}) being the most less differentiated subset of antigen-experienced cells, central memory (T_{CM}), effector memory (T_{EM}), and terminally differentiated effector cells (T_{EFF}) [151]. The subsets differ in their phenotypic characteristics, proliferative capacity, immune reconstitution and long-term survival [152, 153]. It has been shown that less differentiated subsets (T_{SCM} and T_{CM}) exhibit superior expansion, persistence and antitumor activity *in vivo* [154–157]. Gattinoni and colleagues were the first to describe T_{SCM} cells in 2011 as a rare memory subset accounting for only 2-4% of the total $CD4^+$ and $CD8^+$ T cell population [11, 157]. T_{SCM} cells are characterized by their ability to differentiate into central memory and effector memory subsets and display an enhanced self-renewal capacity and longevity compared to the other memory subsets [11, 107]. In line with the developmental hierarchy, the least differentiated T_{SCM} cells elicit more potent antitumor responses than T_{CM} cells, which in turn, are therapeutically superior to further differentiated T_{EM} and T_{EFF} cells [11, 107, 158], making them an attractive subset to be deployed in adoptive therapy. However, considering the low frequency of less differentiated T cells in the periphery, expansion of these subsets is required and maintenance of the T_{SCM} like phenotype during *in vitro* expansion remains a challenge.

Based on various published data for the generation of less differentiated T_{SCM} and T_{CM} cells, relying on the isolation of naïve like T cells from PBMCs [109, 108], we aimed to generate less differentiated EGFRvIII-CAR redirected T cells (naïve EGFRvIII-CAR T cells) using the Akt Inhibitor VIII and a specific cytokine mix. IL-7 and IL-15 have been reported to support generation of tumor-redirected or suicide-gene modified T_{SCM} cells, whereby IL-7 is essential for the development of these cells and IL-15 primarily sustains their expansion [109, 159]. Gattinoni et al. demonstrated, that by mimicking the Wnt-signaling pathway, T cell differentiation could be retained while engineering tumor-specific T cells [11]. These TCR redirected T cells reflected a T_{SCM} like $CCR7^+CD62L^+$ phenotype with superior anti-tumor efficacy. Another clinical-grade protocol described the usage of IL-7, IL-21 and the Wnt agonist TWS119 during activation of naïve T cells to promote the generation of tumor reactive T_{SCM} cells [108]. In comparison to IL-15, that also confers to maintenance of memory T cells, IL-21 is reported to be more effective in suppressing T cell differentiation towards effector T cells [160] due to its ability to activate STAT3 (signal transducer and activator of transcription 3) signaling [161]. Furthermore, by stabilizing β-catenin, it elicits a synergistic effect with IL-21 for enhanced expression of TCF7 and LEF1, both transcription factors associated with naïve T

cells and known to be downregulated during progressive differentiation [108, 11]. CAR redirected T_{SCM} cells that are generated according to these protocols display characteristics of their naturally occurring counterparts in terms of phenotype, functionality and transcription profile. Despite causing restriction to T cell proliferation, T_{SCM} cells can be redirected and expanded for clinical application [108]. Van der Waart further evaluated the inhibition of PI3K/Akt/m-TOR signaling, that plays an important role in T cell metabolism and differentiation [110]. Several studies point to the impact of sustained Akt and mTOR on driving T cells towards terminal differentiation, indicating that Akt inhibition favored formation of superior tumor reactive T cells reflecting stem cell memory properties [112].

According to the protocol for the generation of CD19-CAR redirected T_{SCM} cells using either TWS119 or Akt Inhibitor VIII and a cytokine mix, we generated less differentiated EGFRvIII-CAR T cells. We followed a protocol established in our group for the generation of CD19-CAR T_{SCM}/T_{CM} cells using either TWS119 or Akt Inhibitor VIII in combination with various cytokines (conducted by Aileen Berger, chapter 3.7.1). Both inhibitors, TWS119 and Akt Inhibitor VIII resulted in firm inhibition of cell growth during the generation of CD19-CAR T_{SCM}/T_{CM} cells. However, in our studies Akt treatment had less impact on proliferative capacity as compared to TWS119, and thus we deployed the Akt Inhibitor VIII for the generation of EGFRvIII-CAR T cells. First, naïve CD45RA$^+$ cells were isolated from PBMCs using CD45RA microbeads and cultured in the presence of Akt Inhibitor VIII, IL-7, IL-15 and IL-21 owing to their T_{SCM} favoring properties as described above. After one week of cell culture and defined isolation of CD3$^+$ or CD8$^+$ T cell subsets, IL-12 was added to the culture medium, which is described to support T cell memory formation [162]. After 14 days, T_{SCM} culture medium was supplemented with IL-2, that not only confers to expansion of effector T cells but has been described to support proliferation of memory T cells when added in lower concentrations [163].

4.8 Phenotypical and functional characteristics of naïve EGFRvIII-CAR redirected T cells

EGFRvIII-CAR T cells generated under abovementioned culture conditions were analyzed for their phenotypic characteristics using FACS to assess surface marker expression defining T cell memory and effector subsets. T cells were stained for surface expression of the naïve and memory markers (CD45RA/CD45RO) and homing markers (CCR7/CD62L) and were compared to EGFRvIII-CAR T cells derived from unselected T cells generated under standard T cell culture conditions (total EGFRvIII-CAR T cells). Naïve EGFRvIII-CAR T cells analyzed on day 3 comprised 78.8% of a T cell population with a CD45RA$^+$CD62L$^+$ phenotype (78.8%) reflecting T_{SCM} phenotype, while only 16.8% of CD45RA$^+$CD62L$^+$ were found within the total

EGFRvIII-CAR T cell population (chapter 3.8). Furthermore, FACS results illustrated that 31% of T cells expressed the markers CD45RO and CCR7, reflecting a central memory phenotype for total EGFRvIII-CAR T cells, which decreased to approximately 10% on day 18 as more memory cells differentiated towards effector cells. By contrast, the initial central memory population for naïve EGFRvIII-CAR T cells consisted of 8% and increased to 50.2%, pointing to the differentiation of T_{SCM} cells into T_{CM} cells. On day 18, naïve EGFRvIII-CAR T cells comprised 49% of CD45RA$^+$CD62L$^+$ T_{SCM} cells, while no notable difference was seen for total EGFRvIII-CAR T cells. In conclusion, treatment of naïve EGFRvIII-CAR T cells with the cytokine mix and Akt led to increased numbers of CD45RA$^+$CD62L$^+$ T cells and CD45RO$^+$CCR7$^+$ T cells in comparison to untreated total EGFRvIII-CAR T cells. Hence, these findings confirm the properties of the applied cytokines and Akt Inhibitor VIII to restrain T cell differentiation. Enhanced levels of CD45RA$^+$CD62L$^+$ T cells can be achieved by further optimizing protocols for the preselection of naïve subsets from PBMCs. Since we selected T cells by CD45RA surface expression only, which is also expressed on effector T cells, the initial T cell subset already contains a small portion of more differentiated T cells, which in turn can speed up the differentiation of naive T cells into effector T cells [164]. An alternative option to improve purity of preselected naïve T cells is considering CD62L as an additional selection criterion since effector cells do only express CD45RA but not CD62L. Sebastino and colleagues published a protocol for the generation of clinical-grade CD19-CAR T_{SCM} cells, that were generated using clinical-grade or research-grade Fab streptamers for enrichment of CD8$^+$CD62L$^+$CD45RA$^+$ cells by a serial positive bead isolation [108]. We next examined functional properties of naïve EGFRvIII-CAR T cells regarding IFN-γ secretion, Granzyme B secretion and migration capacity in comparison to total EGFRvIII-CAR T cells. T_{SCM} cells have been described to be capable of secreting cytokines including TNF-α, IFN-γ and IL-2 [11]. Results of the IFN-γ ELISpot assay proved functional stimulation and activation of Akt treated naïve EGFRvIII-CAR T cells as seen by effective IFN-γ secretion upon co-culture with EGFRvIII$^+$ tumor cells. Moreover, cytokine secretion was specific to EGFRvIII$^+$ cells as naïve Akt treated Mock T cells did not show any IFN-γ spots. About 180 spots were counted for total CD8$^+$ EGFRvIII-CAR T cells and a slightly increased number (240) was counted for CD8$^+$ naïve EGFRvIII-CAR T cells (chapter 3.8.1). These results are consistent with findings of van der Waart reporting slightly enhanced IFN-γ production of MiHA-specific CD8$^+$ T cells treated with Akt when compared to control cells [112], while Sebatino and colleagues observed similar levels of IFN-γ secretion for total CD19-CAR T cells and CD19-CAR T_{SCM} cells [108]. To further analyze the cytolytic potential of Akt treated naïve EGFRvIII-CAR T cells we

conducted a Granzyme B assay, revealing similar results to the IFN-γ ELISpot assay, including an antigen specific response of EGFRvIII-CAR redirected T cells, with hardly any Granzyme B spots detectable for Mock T cells. Naïve CD8$^+$ EGFRvIII-CAR T cells yielded comparable levels of Granzyme B secretion as total EGFRvIII-CAR T cells with up to 300 spots counted for each group (chapter 3.8.1). Furthermore, we analyzed their capability of migration in comparison to total EGFRvIII-CAR T cells conducting a Transwell-migration assay, demonstrating an improved chemotactic capacity of naïve EGFRvIII-CAR T cells. Since less differentiated EGFRvIII-CAR T cells exhibited higher levels of the chemokine receptor CCR7, increased number of cells were found to migrate through the cell permeable membrane towards their ligand CCL21 (chapter 3.8.2).

4.5 Summary and outlook

Challenges imposed by solid cancers have dampened effectiveness of CAR T cell therapy involving many factors such as insufficient trafficking, unhostile tumor microenvironment and poor T cell persistence. One of the major hurdles, however, is the lack of an appropriate tumor antigen. EGFRvIII is one such rare ideal target, being exclusively expressed on malignant cells, that is accessible on the cell surface. EGFRvIII has been described for other cancers as well, including breast cancer, prostate cancer, head and neck cancer, ovarian cancer and lung cancer. In this preclinical study we sought to evaluate the potential of a third-generation EGFRvIII-CAR towards EGFRvIII expressing tumor cells. We succeeded in generating EGFRvIII-CAR redirected T cells by retroviral transduction and analyzed surface expression and phenotypical characteristics regarding memory and homing markers by FACS analysis. We used a transfected melanoma cell line Ma-mel EGFRvIII$^+$ as a representative for solid tumors and the adenocarcinoma cell line A549 EGFRvIII$^+$ as target cells. Conducting various *in vitro* assays, we could prove the antigen specific stimulation and activation of EGFRvIII-CAR T cells when co-cultured with EGFRvIII expressing tumor cells: Only EGFRvIII-CAR T cells but not Mock T cells formed T cell clusters in co-culture assays and displayed profound IFN-γ secretion. Lysis potential of EGFRvIII-CAR T cells was further assessed using several assays, including the crystal violet staining, Granzyme B ELISpot assay and the ^{51}Cr-release assay, all proving antigen specific lytic activity of EGFRvIII-CAR T cells. Moreover, we generated less differentiated EGFRvIII-CAR T cells using Akt Inhibitor VIII and a cytokine mix, reflecting a stem cell memory or central memory phenotype (T$_{SCM}$/T$_{CM}$) as confirmed by FACS analysis. Functional properties of T$_{SCM}$/T$_{CM}$ EGFRvIII-CAR T cells were examined in regard of stimulation and lysis potential targeting EGFRvIII expressing tumor cells using IFN-γ and Granzyme B ELISpot assay, respectively. Comparable cytokine secretion of IFN-γ and

Granzyme B were elicited by T_SCM/T_CM EGFRvIII-CAR T cells when compared to total EGFRvIII-CAR T cells. Furthermore, Akt treated naïve EGFRvIII-CAR T cells showed a more enhanced migration capacity than total EGFRvIII-CAR T cells *in vitro*. To examine the therapeutic potential *in vivo*, we used a xenograft NSG mouse model and administered EGFRvIII-CAR T cells into A549 EGFRvIII$^+$ bearing mice. Unfortunately, we could not show a tumor specific T cell response and no significant difference was observed by means of tumor growth among Mock and EGFRvIII-CAR treated mice. This outcome might be explained due to insufficient expression of the EGFRvIII on tumor cells an inefficient T cell proliferation. For further optimization of this preclinical study, the issue of EGFRvIII expression on target cells needs to be addressed. We observed a downregulation of EGFRvIII on transfected cell lines likely due to downregulation or internalization. One idea would be to construct a truncated version of the EGFRvIII without the cytoplasmic domain to circumvent the issue of internalization. Moreover, the best solution would be to establish a cell line derived from tumor samples expressing EGFRvIII. It has been demonstrated that *in vitro* culture of tumor cells as neurospheres in a specialized media can maintain EGFRvIII expression [132, 133, 165]. To improve T cell persistence *in vivo* less differentiated EGFRvIII-CAR redirected should be generated for adoptive transfer in tumor bearing NSG mice. Due to their superior proliferative capacity, longevity, and capability to differentiate into all possible T cell subsets, T_SCM cells have proven to elicit a more profound antitumor response [31, 166] . Several studies further describe the correlation of tumor response with the level of T cell engraftment and expansion capacity early after transfer [90, 167, 168]. One strategy to overcome limitations imposed by the immunosuppressive tumor environment in solid tumors and T cell exhaustion, likely caused by permanent exposure to antigen, is to design armored CAR-T cells. These CARs, also designated 4th generation CARs, combine the CAR functional activity with additional secretion of supportive molecules. For example, armored CARs equipped with anit-PDL-1 Abs molecules have shown to elicit an enhanced anti-tumor response [169] and CARs have been designed to secrete cytokines such as IL-12 and IL-15 [170] for improved persistence and activity. Combining EGFRvIII-CAR functionality with anti-inhibitory features or molecules supporting T cell persistence and further selecting the ideal T cell subset for adoptive transfer could be one approach to unleash the full potential of antitumor response by EGFRvIII-CARs.

References

1. Chaplin, D.D. Overview of the Immune Response. *The Journal of allergy and clinical immunology* **2010**, *125*, S3-23, doi:10.1016/j.jaci.2009.12.980.

2. Lieber, M.R.; Chang, C.P.; Gallo, M.; Gauss, G.; Gerstein, R.; Islas, A. The mechanism of V(D)J recombination: site-specificity, reaction fidelity and immunologic diversity. *Seminars in immunology* **1994**, *6*, 143–153, doi:10.1006/smim.1994.1020.

3. Nitta, T.; Murata, S.; Ueno, T.; Tanaka, K.; Takahama, Y. Chapter 3 Thymic Microenvironments for T-Cell Repertoire Formation. In *Advances in Immunology,* 1. Aufl.; Alt, F.W., Ed.; Elsevier textbooks: s.l., 2008; pp 59–94.

4. Fink, P.J.; Hendricks, D.W. Post-thymic maturation: young T cells assert their individuality. *Nature reviews. Immunology* **2011**, *11*, 544–549, doi:10.1038/nri3028.

5. Salmond, R.J.; Filby, A.; Qureshi, I.; Caserta, S.; Zamoyska, R. T-cell receptor proximal signaling via the Src-family kinases, Lck and Fyn, influences T-cell activation, differentiation, and tolerance. *Immunological reviews* **2009**, *228*, 9–22, doi:10.1111/j.1600-065X.2008.00745.x.

6. Nurieva, R.I.; Liu, X.; Dong, C. Yin-Yang of costimulation: crucial controls of immune tolerance and function. *Immunological reviews* **2009**, *229*, 88–100, doi:10.1111/j.1600-065X.2009.00769.x.

7. Seddon, B.; Zamoyska, R. TCR signals mediated by Src family kinases are essential for the survival of naive T cells. *Journal of Immunology (Baltimore, Md. : 1950)* **2002**, *169*, 2997–3005.

8. Lieberman, J. The ABCs of granule-mediated cytotoxicity: new weapons in the arsenal. *Nature reviews. Immunology* **2003**, *3*, 361–370, doi:10.1038/nri1083.

9. Nagata, S. Fas-mediated apoptosis. *Advances in experimental medicine and biology* **1996**, *406*, 119–124.

10. Andersen, M.H.; Schrama, D.; Thor Straten, P.; Becker, J.C. Cytotoxic T cells. *The Journal of investigative dermatology* **2006**, *126*, 32–41, doi:10.1038/sj.jid.5700001.

11. Gattinoni, L.; Lugli, E.; Ji, Y.; Pos, Z.; Paulos, C.M.; Quigley, M.F.; Almeida, J.R.; Gostick, E.; Yu, Z.; Carpenito, C.*; et al.* A human memory T cell subset with stem cell-like properties. *Nature medicine* **2011**, *17*, 1290–1297, doi:10.1038/nm.2446.

12. Irving, M.; Vuillefroy de Silly, R.; Scholten, K.; Dilek, N.; Coukos, G. Engineering Chimeric Antigen Receptor T-Cells for Racing in Solid Tumors: Don't Forget the Fuel. *Frontiers in immunology* **2017**, *8*, 267, doi:10.3389/fimmu.2017.00267.

13. Carraway, K.L.; Cantley, L.C. A neu acquaintance for erbB3 and erbB4: a role for receptor heterodimerization in growth signaling. *Cell* **1994**, *78*, 5–8.

14. van der Geer, P.; Hunter, T.; Lindberg, R.A. Receptor protein-tyrosine kinases and their signal transduction pathways. *Annual review of cell biology* **1994**, *10*, 251–337, doi:10.1146/annurev.cb.10.110194.001343.

15. Roskoski, R. The ErbB/HER family of protein-tyrosine kinases and cancer. *Pharmacological research* **2014**, *79*, 34–74, doi:10.1016/j.phrs.2013.11.002.

16. Mayer, B.J. The discovery of modular binding domains: building blocks of cell signalling. *Nature reviews. Molecular cell biology* **2015**, *16*, 691–698, doi:10.1038/nrm4068.

17. Thorpe, L.M.; Yuzugullu, H.; Zhao, J.J. PI3K in cancer: divergent roles of isoforms, modes of activation and therapeutic targeting. *Nature reviews. Cancer* **2015**, *15*, 7–24, doi:10.1038/nrc3860.

18. Scaltriti, M.; Baselga, J. The epidermal growth factor receptor pathway: a model for targeted therapy. *Clinical cancer research : an official journal of the American Association for Cancer Research* **2006**, *12*, 5268–5272, doi:10.1158/1078-0432.CCR-05-1554.

19. Nicholson, K.M.; Anderson, N.G. The protein kinase B/Akt signalling pathway in human malignancy. *Cellular signalling* **2002**, *14*, 381–395.

20. Harris, R.C.; Chung, E.; Coffey, R.J. EGF receptor ligands. *Experimental cell research* **2003**, *284*, 2–13.

21. Hynes, N.E.; Lane, H.A. ERBB receptors and cancer: the complexity of targeted inhibitors. *Nature reviews. Cancer* **2005**, *5*, 341–354, doi:10.1038/nrc1609.

22. Yewale, C.; Baradia, D.; Vhora, I.; Patil, S.; Misra, A. Epidermal growth factor receptor targeting in cancer: a review of trends and strategies. *Biomaterials* **2013**, *34*, 8690–8707, doi:10.1016/j.biomaterials.2013.07.100.

23. Thompson, D.M.; Gill, G.N. The EGF receptor: structure, regulation and potential role in malignancy. *Cancer surveys* **1985**, *4*, 767–788.

24. Yamazaki, H.; Ohba, Y.; Tamaoki, N.; Shibuya, M. A deletion mutation within the ligand binding domain is responsible for activation of epidermal growth factor receptor gene in human brain tumors. *Japanese journal of cancer research : Gann* **1990**, *81*, 773–779.

25. Grandal, M.V.; Zandi, R.; Pedersen, M.W.; Willumsen, B.M.; van Deurs, B.; Poulsen, H.S. EGFRvIII escapes down-regulation due to impaired internalization and sorting to lysosomes. *Carcinogenesis* **2007**, *28*, 1408–1417, doi:10.1093/carcin/bgm058.

26. Gan, H.K.; Kaye, A.H.; Luwor, R.B. The EGFRvIII variant in glioblastoma multiforme. *Journal of clinical neuroscience : official journal of the Neurosurgical Society of Australasia* **2009**, *16*, 748–754, doi:10.1016/j.jocn.2008.12.005.

27. Gan, H.K.; Cvrljevic, A.N.; Johns, T.G. The epidermal growth factor receptor variant III (EGFRvIII): where wild things are altered. *The FEBS journal* **2013**, *280*, 5350–5370, doi:10.1111/febs.12393.

28. Al-Nedawi, K.; Meehan, B.; Micallef, J.; Lhotak, V.; May, L.; Guha, A.; Rak, J. Intercellular transfer of the oncogenic receptor EGFRvIII by microvesicles derived from tumour cells. *Nature cell biology* **2008**, *10*, 619–624, doi:10.1038/ncb1725.

29. Garcia de Palazzo, I.E.; Adams, G.P.; Sundareshan, P.; Wong, A.J.; Testa, J.R.; Bigner, D.D.; Weiner, L.M. Expression of mutated epidermal growth factor receptor by non-small cell lung carcinomas. *Cancer research* **1993**, *53*, 3217–3220.

30. Moscatello, D.K.; Holgado-Madruga, M.; Godwin, A.K.; Ramirez, G.; Gunn, G.; Zoltick, P.W.; Biegel, J.A.; Hayes, R.L.; Wong, A.J. Frequent expression of a mutant

epidermal growth factor receptor in multiple human tumors. *Cancer research* **1995**, *55*, 5536–5539.

31. Wikstrand, C.J.; Hale, L.P.; Batra, S.K.; Hill, M.L.; Humphrey, P.A.; Kurpad, S.N.; McLendon, R.E.; Moscatello, D.; Pegram, C.N.; Reist, C.J. Monoclonal antibodies against EGFRvIII are tumor specific and react with breast and lung carcinomas and malignant gliomas. *Cancer research* **1995**, *55*, 3140–3148.

32. Ekstrand, A.J.; Sugawa, N.; James, C.D.; Collins, V.P. Amplified and rearranged epidermal growth factor receptor genes in human glioblastomas reveal deletions of sequences encoding portions of the N- and/or C-terminal tails. *Proceedings of the National Academy of Sciences of the United States of America* **1992**, *89*, 4309–4313.

33. Wong, A.J.; Ruppert, J.M.; Bigner, S.H.; Grzeschik, C.H.; Humphrey, P.A.; Bigner, D.S.; Vogelstein, B. Structural alterations of the epidermal growth factor receptor gene in human gliomas. *Proceedings of the National Academy of Sciences of the United States of America* **1992**, *89*, 2965–2969.

34. Shinojima, N.; Tada, K.; Shiraishi, S.; Kamiryo, T.; Kochi, M.; Nakamura, H.; Makino, K.; Saya, H.; Hirano, H.; Kuratsu, J.-I.*; et al.* Prognostic value of epidermal growth factor receptor in patients with glioblastoma multiforme. *Cancer research* **2003**, *63*, 6962–6970.

35. Zappa, C.; Mousa, S.A. Non-small cell lung cancer: current treatment and future advances. *Translational lung cancer research* **2016**, *5*, 288–300, doi:10.21037/tlcr.2016.06.07.

36. Riely, G.J.; Marks, J.; Pao, W. KRAS mutations in non-small cell lung cancer. *Proceedings of the American Thoracic Society* **2009**, *6*, 201–205, doi:10.1513/pats.200809-107LC.

37. Herbst, R.S.; Morgensztern, D.; Boshoff, C. The biology and management of non-small cell lung cancer. *Nature* **2018**, *553*, 446–454, doi:10.1038/nature25183.

38. Batra, S.K.; Castelino-Prabhu, S.; Wikstrand, C.J.; Zhu, X.; Humphrey, P.A.; Friedman, H.S.; Bigner, D.D. Epidermal growth factor ligand-independent, unregulated, cell-transforming potential of a naturally occurring human mutant EGFRvIII gene. *Cell growth & differentiation : the molecular biology journal of the American Association for Cancer Research* **1995**, *6*, 1251–1259.

39. Lee, J.C.; Vivanco, I.; Beroukhim, R.; Huang, J.H.Y.; Feng, W.L.; DeBiasi, R.M.; Yoshimoto, K.; King, J.C.; Nghiemphu, P.; Yuza, Y.*; et al.* Epidermal growth factor receptor activation in glioblastoma through novel missense mutations in the extracellular domain. *PLoS medicine* **2006**, *3*, e485, doi:10.1371/journal.pmed.0030485.

40. Howington, J.A.; Blum, M.G.; Chang, A.C.; Balekian, A.A.; Murthy, S.C. Treatment of stage I and II non-small cell lung cancer: Diagnosis and management of lung cancer, 3rd ed: American College of Chest Physicians evidence-based clinical practice guidelines. *Chest* **2013**, *143*, e278S-e313S, doi:10.1378/chest.12-2359.

41. Brunelli, A. Preoperative functional workup for patients with advanced lung cancer. *Journal of thoracic disease* **2016**, *8*, S840-S848, doi:10.21037/jtd.2016.03.73.

42. Masters, G.A.; Temin, S.; Azzoli, C.G.; Giaccone, G.; Baker, S.; Brahmer, J.R.; Ellis, P.M.; Gajra, A.; Rackear, N.; Schiller, J.H.*; et al.* Systemic Therapy for Stage IV Non-

Small-Cell Lung Cancer: American Society of Clinical Oncology Clinical Practice Guideline Update. *Journal of clinical oncology : official journal of the American Society of Clinical Oncology* **2015**, *33*, 3488–3515, doi:10.1200/JCO.2015.62.1342.

43. Hanna, N.; Johnson, D.; Temin, S.; Masters, G. Systemic Therapy for Stage IV Non-Small-Cell Lung Cancer: American Society of Clinical Oncology Clinical Practice Guideline Update Summary. *Journal of oncology practice* **2017**, *13*, 832–837, doi:10.1200/JOP.2017.026716.

44. Ramalingam, S.; Belani, C. Systemic chemotherapy for advanced non-small cell lung cancer: recent advances and future directions. *The oncologist* **2008**, *13 Suppl 1*, 5–13, doi:10.1634/theoncologist.13-S1-5.

45. Schiller, J.H.; Harrington, D.; Belani, C.P.; Langer, C.; Sandler, A.; Krook, J.; Zhu, J.; Johnson, D.H. Comparison of four chemotherapy regimens for advanced non-small-cell lung cancer. *The New England journal of medicine* **2002**, *346*, 92–98, doi:10.1056/NEJMoa011954.

46. Mok, T.S.; Wu, Y.-L.; Thongprasert, S.; Yang, C.-H.; Chu, D.-T.; Saijo, N.; Sunpaweravong, P.; Han, B.; Margono, B.; Ichinose, Y.*; et al.* Gefitinib or carboplatin-paclitaxel in pulmonary adenocarcinoma. *The New England journal of medicine* **2009**, *361*, 947–957, doi:10.1056/NEJMoa0810699.

47. Lynch, T.J.; Bell, D.W.; Sordella, R.; Gurubhagavatula, S.; Okimoto, R.A.; Brannigan, B.W.; Harris, P.L.; Haserlat, S.M.; Supko, J.G.; Haluska, F.G.*; et al.* Activating mutations in the epidermal growth factor receptor underlying responsiveness of non-small-cell lung cancer to gefitinib. *The New England journal of medicine* **2004**, *350*, 2129–2139, doi:10.1056/NEJMoa040938.

48. Paez, J.G.; Jänne, P.A.; Lee, J.C.; Tracy, S.; Greulich, H.; Gabriel, S.; Herman, P.; Kaye, F.J.; Lindeman, N.; Boggon, T.J.*; et al.* EGFR mutations in lung cancer: correlation with clinical response to gefitinib therapy. *Science (New York, N.Y.)* **2004**, *304*, 1497–1500, doi:10.1126/science.1099314.

49. Russo, A.; Franchina, T.; Ricciardi, G.R.R.; Picone, A.; Ferraro, G.; Zanghì, M.; Toscano, G.; Giordano, A.; Adamo, V. A decade of EGFR inhibition in EGFR-mutated non small cell lung cancer (NSCLC): Old successes and future perspectives. *Oncotarget* **2015**, *6*, 26814–26825, doi:10.18632/oncotarget.4254.

50. Kobayashi, S.; Boggon, T.J.; Dayaram, T.; Jänne, P.A.; Kocher, O.; Meyerson, M.; Johnson, B.E.; Eck, M.J.; Tenen, D.G.; Halmos, B. EGFR mutation and resistance of non-small-cell lung cancer to gefitinib. *The New England journal of medicine* **2005**, *352*, 786–792, doi:10.1056/NEJMoa044238.

51. Sequist, L.V.; Waltman, B.A.; Dias-Santagata, D.; Digumarthy, S.; Turke, A.B.; Fidias, P.; Bergethon, K.; Shaw, A.T.; Gettinger, S.; Cosper, A.K.*; et al.* Genotypic and histological evolution of lung cancers acquiring resistance to EGFR inhibitors. *Science translational medicine* **2011**, *3*, 75ra26, doi:10.1126/scitranslmed.3002003.

52. Peters, S.; Zimmermann, S.; Adjei, A.A. Oral epidermal growth factor receptor tyrosine kinase inhibitors for the treatment of non-small cell lung cancer: comparative pharmacokinetics and drug-drug interactions. *Cancer treatment reviews* **2014**, *40*, 917–926, doi:10.1016/j.ctrv.2014.06.010.

53. Jänne, P.A.; Yang, J.C.-H.; Kim, D.-W.; Planchard, D.; Ohe, Y.; Ramalingam, S.S.; Ahn, M.-J.; Kim, S.-W.; Su, W.-C.; Horn, L.*; et al.* AZD9291 in EGFR inhibitor-resistant non-small-cell lung cancer. *The New England journal of medicine* **2015**, *372*, 1689–1699, doi:10.1056/NEJMoa1411817.

54. Mok, T.S.; Wu, Y.-L.; Ahn, M.-J.; Garassino, M.C.; Kim, H.R.; Ramalingam, S.S.; Shepherd, F.A.; He, Y.; Akamatsu, H.; Theelen, W.S.M.E.*; et al.* Osimertinib or Platinum-Pemetrexed in EGFR T790M-Positive Lung Cancer. *The New England journal of medicine* **2017**, *376*, 629–640, doi:10.1056/NEJMoa1612674.

55. Soria, J.-C.; Ohe, Y.; Vansteenkiste, J.; Reungwetwattana, T.; Chewaskulyong, B.; Lee, K.H.; Dechaphunkul, A.; Imamura, F.; Nogami, N.; Kurata, T.*; et al.* Osimertinib in Untreated EGFR-Mutated Advanced Non-Small-Cell Lung Cancer. *The New England journal of medicine* **2018**, *378*, 113–125, doi:10.1056/NEJMoa1713137.

56. Wu, Y.-L.; Liang, J.; Zhang, W.; Tanaka, Y.; Sugiyama, H. Immunotherapies: the blockade of inhibitory signals. *International journal of biological sciences* **2012**, *8*, 1420–1430, doi:10.7150/ijbs.5273.

57. Dong, H.; Strome, S.E.; Salomao, D.R.; Tamura, H.; Hirano, F.; Flies, D.B.; Roche, P.C.; Lu, J.; Zhu, G.; Tamada, K.*; et al.* Tumor-associated B7-H1 promotes T-cell apoptosis: a potential mechanism of immune evasion. *Nature medicine* **2002**, *8*, 793–800, doi:10.1038/nm730.

58. Iwai, Y.; Ishida, M.; Tanaka, Y.; Okazaki, T.; Honjo, T.; Minato, N. Involvement of PD-L1 on tumor cells in the escape from host immune system and tumor immunotherapy by PD-L1 blockade. *Proceedings of the National Academy of Sciences of the United States of America* **2002**, *99*, 12293–12297, doi:10.1073/pnas.192461099.

59. Garon, E.B.; Rizvi, N.A.; Hui, R.; Leighl, N.; Balmanoukian, A.S.; Eder, J.P.; Patnaik, A.; Aggarwal, C.; Gubens, M.; Horn, L.*; et al.* Pembrolizumab for the treatment of non-small-cell lung cancer. *The New England journal of medicine* **2015**, *372*, 2018–2028, doi:10.1056/NEJMoa1501824.

60. Topalian, S.L.; Hodi, F.S.; Brahmer, J.R.; Gettinger, S.N.; Smith, D.C.; McDermott, D.F.; Powderly, J.D.; Carvajal, R.D.; Sosman, J.A.; Atkins, M.B.*; et al.* Safety, activity, and immune correlates of anti-PD-1 antibody in cancer. *The New England journal of medicine* **2012**, *366*, 2443–2454, doi:10.1056/NEJMoa1200690.

61. Herbst, R.S.; Soria, J.-C.; Kowanetz, M.; Fine, G.D.; Hamid, O.; Gordon, M.S.; Sosman, J.A.; McDermott, D.F.; Powderly, J.D.; Gettinger, S.N.*; et al.* Predictive correlates of response to the anti-PD-L1 antibody MPDL3280A in cancer patients. *Nature* **2014**, *515*, 563–567, doi:10.1038/nature14011.

62. Brahmer, J.; Reckamp, K.L.; Baas, P.; Crinò, L.; Eberhardt, W.E.E.; Poddubskaya, E.; Antonia, S.; Pluzanski, A.; Vokes, E.E.; Holgado, E.*; et al.* Nivolumab versus Docetaxel in Advanced Squamous-Cell Non-Small-Cell Lung Cancer. *The New England journal of medicine* **2015**, *373*, 123–135, doi:10.1056/NEJMoa1504627.

63. Borghaei, H.; Paz-Ares, L.; Horn, L.; Spigel, D.R.; Steins, M.; Ready, N.E.; Chow, L.Q.; Vokes, E.E.; Felip, E.; Holgado, E.*; et al.* Nivolumab versus Docetaxel in Advanced Nonsquamous Non-Small-Cell Lung Cancer. *The New England journal of medicine* **2015**, *373*, 1627–1639, doi:10.1056/NEJMoa1507643.

64. Langer, C.J.; Gadgeel, S.M.; Borghaei, H.; Papadimitrakopoulou, V.A.; Patnaik, A.; Powell, S.F.; Gentzler, R.D.; Martins, R.G.; Stevenson, J.P.; Jalal, S.I.*; et al.* Carboplatin and pemetrexed with or without pembrolizumab for advanced, non-squamous non-small-cell lung cancer: a randomised, phase 2 cohort of the open-label KEYNOTE-021 study. *The Lancet Oncology* **2016**, *17*, 1497–1508, doi:10.1016/S1470-2045(16)30498-3.

65. 1909-karzinomforschung.

66. Dunn, G.P.; Old, L.J.; Schreiber, R.D. The three Es of cancer immunoediting. *Annual review of immunology* **2004**, *22*, 329–360, doi:10.1146/annurev.immunol.22.012703.104803.

67. Swann, J.B.; Smyth, M.J. Immune surveillance of tumors. *The Journal of clinical investigation* **2007**, *117*, 1137–1146, doi:10.1172/JCI31405.

68. Hanahan, D.; Weinberg, R.A. Hallmarks of cancer: the next generation. *Cell* **2011**, *144*, 646–674, doi:10.1016/j.cell.2011.02.013.

69. Choi, A.H.; O'Leary, M.P.; Fong, Y.; Chen, N.G. From Benchtop to Bedside: A Review of Oncolytic Virotherapy. *Biomedicines* **2016**, *4, doi:*10.3390/biomedicines4030018.

70. Gardner, T.A.; Elzey, B.D.; Hahn, N.M. Sipuleucel-T (Provenge) autologous vaccine approved for treatment of men with asymptomatic or minimally symptomatic castrate-resistant metastatic prostate cancer. *Human vaccines & immunotherapeutics* **2012**, *8*, 534–539, doi:10.4161/hv.19795.

71. Marsh, R.A.; Lane, A.; Mehta, P.A.; Neumeier, L.; Jodele, S.; Davies, S.M.; Filipovich, A.H. Alemtuzumab levels impact acute GVHD, mixed chimerism, and lymphocyte recovery following alemtuzumab, fludarabine, and melphalan RIC HCT. *Blood* **2016**, *127*, 503–512, doi:10.1182/blood-2015-07-659672.

72. Schmidt, K.; Kleinschnitz, K.; Rakocevic, G.; Dalakas, M.C.; Schmidt, J. Molecular treatment effects of alemtuzumab in skeletal muscles of patients with IBM. *BMC neurology* **2016**, *16*, 48, doi:10.1186/s12883-016-0568-5.

73. Rosati, G.; Aprile, G.; Cardellino, G.G.; Avallone, A. A review and assessment of currently available data of the EGFR antibodies in elderly patients with metastatic colorectal cancer. *Journal of geriatric oncology* **2016**, *7*, 134–141, doi:10.1016/j.jgo.2016.01.006.

74. Yang, J.; Li, S.; Wang, B.; Wu, Y.; Chen, Z.; Lv, M.; Lin, Y.; Yang, J. Potential biomarkers for anti-EGFR therapy in metastatic colorectal cancer. *Tumour biology : the journal of the International Society for Oncodevelopmental Biology and Medicine* **2016**, *37*, 11645–11655, doi:10.1007/s13277-016-5140-9.

75. Azoury, S.C.; Straughan, D.M.; Shukla, V. Immune Checkpoint Inhibitors for Cancer Therapy: Clinical Efficacy and Safety. *Current cancer drug targets* **2015**, *15*, 452–462.

76. Mahoney, K.M.; Freeman, G.J.; McDermott, D.F. The Next Immune-Checkpoint Inhibitors: PD-1/PD-L1 Blockade in Melanoma. *Clinical therapeutics* **2015**, *37*, 764–782, doi:10.1016/j.clinthera.2015.02.018.

77. Horowitz, M.M.; Gale, R.P.; Sondel, P.M.; Goldman, J.M.; Kersey, J.; Kolb, H.J.; Rimm, A.A.; Ringdén, O.; Rozman, C.; Speck, B. Graft-versus-leukemia reactions after bone marrow transplantation. *Blood* **1990**, *75*, 555–562.

78. Morgan, D.A.; Ruscetti, F.W.; Gallo, R. Selective in vitro growth of T lymphocytes from normal human bone marrows. *Science (New York, N.Y.)* **1976**, *193*, 1007–1008.

79. Rosenberg, S.A.; Packard, B.S.; Aebersold, P.M.; Solomon, D.; Topalian, S.L.; Toy, S.T.; Simon, P.; Lotze, M.T.; Yang, J.C.; Seipp, C.A. Use of tumor-infiltrating lymphocytes and interleukin-2 in the immunotherapy of patients with metastatic melanoma. A preliminary report. *The New England journal of medicine* **1988**, *319*, 1676–1680, doi:10.1056/NEJM198812223192527.

80. Dudley, M.E.; Wunderlich, J.R.; Robbins, P.F.; Yang, J.C.; Hwu, P.; Schwartzentruber, D.J.; Topalian, S.L.; Sherry, R.; Restifo, N.P.; Hubicki, A.M.*; et al.* Cancer Regression and Autoimmunity in Patients After Clonal Repopulation with Antitumor Lymphocytes. *Science (New York, N.Y.)* **2002**, *298*, 850–854, doi:10.1126/science.1076514.

81. Morgan, R.A.; Dudley, M.E.; Wunderlich, J.R.; Hughes, M.S.; Yang, J.C.; Sherry, R.M.; Royal, R.E.; Topalian, S.L.; Kammula, U.S.; Restifo, N.P.*; et al.* Cancer Regression in Patients After Transfer of Genetically Engineered Lymphocytes. *Science (New York, N.Y.)* **2006**, *314*, 126–129, doi:10.1126/science.1129003.

82. Kershaw, M.H.; Westwood, J.A.; Slaney, C.Y.; Darcy, P.K. Clinical application of genetically modified T cells in cancer therapy. *Clinical & translational immunology* **2014**, *3*, e16, doi:10.1038/cti.2014.7.

83. Zhou, G.; Levitsky, H. Towards curative cancer immunotherapy: overcoming posttherapy tumor escape. *Clinical & developmental immunology* **2012**, *2012*, 124187, doi:10.1155/2012/124187.

84. Catalán, E.; Charni, S.; Jaime, P.; Aguiló, J.I.; Enríquez, J.A.; Naval, J.; Pardo, J.; Villalba, M.; Anel, A. MHC-I modulation due to changes in tumor cell metabolism regulates tumor sensitivity to CTL and NK cells. *Oncoimmunology* **2015**, *4*, e985924, doi:10.4161/2162402X.2014.985924.

85. Fesnak, A.D.; June, C.H.; Levine, B.L. Engineered T cells: the promise and challenges of cancer immunotherapy. *Nature reviews. Cancer* **2016**, *16*, 566–581, doi:10.1038/nrc.2016.97.

86. Chmielewski, M.; Hombach, A.A.; Abken, H. Of CARs and TRUCKs: chimeric antigen receptor (CAR) T cells engineered with an inducible cytokine to modulate the tumor stroma. *Immunological reviews* **2014**, *257*, 83–90, doi:10.1111/imr.12125.

87. Wang, Z.; Wu, Z.; Liu, Y.; Han, W. New development in CAR-T cell therapy. *Journal of hematology & oncology* **2017**, *10*, 53, doi:10.1186/s13045-017-0423-1.

88. Kalos, M.; Levine, B.L.; Porter, D.L.; Katz, S.; Grupp, S.A.; Bagg, A.; June, C.H. T cells with chimeric antigen receptors have potent antitumor effects and can establish memory in patients with advanced leukemia. *Science translational medicine* **2011**, *3*, 95ra73, doi:10.1126/scitranslmed.3002842.

89. Grupp, S.A.; Kalos, M.; Barrett, D.; Aplenc, R.; Porter, D.L.; Rheingold, S.R.; Teachey, D.T.; Chew, A.; Hauck, B.; Wright, J.F.*; et al.* Chimeric antigen receptor-modified T cells for acute lymphoid leukemia. *The New England journal of medicine* **2013**, *368*, 1509–1518, doi:10.1056/NEJMoa1215134.

90. Brentjens, R.J.; Davila, M.L.; Riviere, I.; Park, J.; Wang, X.; Cowell, L.G.; Bartido, S.; Stefanski, J.; Taylor, C.; Olszewska, M.*; et al.* CD19-targeted T cells rapidly induce

molecular remissions in adults with chemotherapy-refractory acute lymphoblastic leukemia. *Science translational medicine* **2013**, *5*, 177ra38, doi:10.1126/scitranslmed.3005930.

91. American Society of Hematology. Safe and Effective Re-Induction Of Complete Remissions In Adults With Relapsed B-ALL Using 19-28z CAR CD19-Targeted T Cell Therapy. http://www.bloodjournal.org/content/122/21/69 (accessed on 2 August 2018).

92. Gill, S.; Maus, M.V.; Porter, D.L. Chimeric antigen receptor T cell therapy: 25years in the making. *Blood reviews* **2016**, *30*, 157–167, doi:10.1016/j.blre.2015.10.003.

93. Fousek, K.; Ahmed, N. The Evolution of T-cell Therapies for Solid Malignancies. *Clinical cancer research : an official journal of the American Association for Cancer Research* **2015**, *21*, 3384–3392, doi:10.1158/1078-0432.CCR-14-2675.

94. Sharpe, M.; Mount, N. Genetically modified T cells in cancer therapy: opportunities and challenges. *Disease models & mechanisms* **2015**, *8*, 337–350, doi:10.1242/dmm.018036.

95. Morgan, R.A.; Yang, J.C.; Kitano, M.; Dudley, M.E.; Laurencot, C.M.; Rosenberg, S.A. Case report of a serious adverse event following the administration of T cells transduced with a chimeric antigen receptor recognizing ERBB2. *Molecular therapy : the journal of the American Society of Gene Therapy* **2010**, *18*, 843–851, doi:10.1038/mt.2010.24.

96. Jungbluth, A.A.; Stockert, E.; Huang, H.J.S.; Collins, V.P.; Coplan, K.; Iversen, K.; Kolb, D.; Johns, T.J.; Am Scott; Gullick, W.J.*; et al.* A monoclonal antibody recognizing human cancers with amplification/overexpression of the human epidermal growth factor receptor. *Proceedings of the National Academy of Sciences of the United States of America* **2003**, *100*, 639–644, doi:10.1073/pnas.232686499.

97. Voldborg, B.R.; Damstrup, L.; Spang-Thomsen, M.; Poulsen, H.S. Epidermal growth factor receptor (EGFR) and EGFR mutations, function and possible role in clinical trials. *ANNALS OF ONCOLOGY* **1997**, *8*, 1197–1206.

98. Del Vecchio, C.A.; Jensen, K.C.; Nitta, R.T.; Shain, A.H.; Giacomini, C.P.; Wong, A.J. Epidermal Growth Factor Receptor Variant III Contributes to Cancer Stem Cell Phenotypes in Invasive Breast Carcinoma. *Cancer research* **2012**, *72*, 2657–2671, doi:10.1158/0008-5472.CAN-11-2656.

99. Morgan, R.A.; Johnson, L.A.; Davis, J.L.; Zheng, Z.; Woolard, K.D.; Reap, E.A.; Feldman, S.A.; Chinnasamy, N.; Kuan, C.-T.; Song, H.*; et al.* Recognition of Glioma Stem Cells by Genetically Modified T Cells Targeting EGFRvIII and Development of Adoptive Cell Therapy for Glioma. *HUMAN GENE THERAPY* **2012**, *23*, 1043–1053, doi:10.1089/hum.2012.041.

100. Johnson, L.A.; Scholler, J.; Ohkuri, T.; Kosaka, A.; Patel, P.R.; McGettigan, S.E.; Nace, A.K.; Dentchev, T.; Thekkat, P.; Loew, A.*; et al.* Rational development and characterization of humanized anti-EGFR variant III chimeric antigen receptor T cells for glioblastoma. *Science translational medicine* **2015**, *7, doi:*10.1126/scitranslmed.aaa4963.

101. Newick, K.; Moon, E.; Albelda, S.M. Chimeric antigen receptor T-cell therapy for solid tumors. *Molecular therapy oncolytics* **2016**, *3*, 16006, doi:10.1038/mto.2016.6.

102. TIVOL, E.A.; BORRIELLO, F.; SCHWEITZER, A.N.; LYNCH, W.P.; BLUESTONE, J.A.; SHARPE, A.H. LOSS OF CTLA-4 LEADS TO MASSIVE LYMPHOPROLIFERATION AND FATAL MULTIORGAN TISSUE

DESTRUCTION, REVEALING A CRITICAL NEGATIVE REGULATORY ROLE OF CTLA-4. *IMMUNITY* **1995**, *3*, 541–547.

103. Keir, M.E.; Butte, M.J.; Freeman, G.J.; Sharpel, A.H. PD-1 and its ligands in tolerance and immunity. In *Thymus organogenesis*; Rodewald, H.-R., Ed., 2008; pp 677–704.

104. Garon, E.B.; Rizvi, N.A.; Hui, R.; Leighl, N.; Balmanoukian, A.S.; Eder, J.P.; Patnaik, A.; Aggarwal, C.; Gubens, M.; Horn, L.*; et al.* Pembrolizumab for the Treatment of Non-Small-Cell Lung Cancer. *NEW ENGLAND JOURNAL OF MEDICINE* **2015**, *372*, 2018–2028, doi:10.1056/NEJMoa1501824.

105. Hodi, F.S.; O'Day, S.J.; McDermott, D.F.; Weber, R.W.; Sosman, J.A.; Haanen, J.B.; Gonzalez, R.; Robert, C.; Schadendorf, D.; Hassel, J.C.*; et al.* Improved Survival with Ipilimumab in Patients with Metastatic Melanoma. *NEW ENGLAND JOURNAL OF MEDICINE* **2010**, *363*, 711–723, doi:10.1056/NEJMoa1003466.

106. Mirzaei, H.R.; Rodriguez, A.; Shepphird, J.; Brown, C.E.; Badie, B. Chimeric Antigen Receptors T Cell Therapy in Solid Tumor: Challenges and Clinical Applications. *Frontiers in immunology* **2017**, *8*, 1850, doi:10.3389/fimmu.2017.01850.

107. Gattinoni, L.; Zhong, X.-S.; Palmer, D.C.; Ji, Y.; Hinrichs, C.S.; Yu, Z.; Wrzesinski, C.; Boni, A.; Cassard, L.; Garvin, L.M.*; et al.* Wnt signaling arrests effector T cell differentiation and generates CD8+ memory stem cells. *Nature medicine* **2009**, *15*, 808–813, doi:10.1038/nm.1982.

108. Sabatino, M.; Hu, J.; Sommariva, M.; Gautam, S.; Fellowes, V.; Hocker, J.D.; Dougherty, S.; Qin, H.; Klebanoff, C.A.; Fry, T.J.*; et al.* Generation of clinical-grade CD19-specific CAR-modified CD8+ memory stem cells for the treatment of human B-cell malignancies. *Blood* **2016**, *128*, 519–528, doi:10.1182/blood-2015-11-683847.

109. Cieri, N.; Camisa, B.; Cocchiarella, F.; Forcato, M.; Oliveira, G.; Provasi, E.; Bondanza, A.; Bordignon, C.; Peccatori, J.; Ciceri, F.*; et al.* IL-7 and IL-15 instruct the generation of human memory stem T cells from naive precursors. *Blood* **2013**, *121*, 573–584, doi:10.1182/blood-2012-05-431718.

110. Kim, E.H.; Suresh, M. Role of PI3K/Akt signaling in memory CD8 T cell differentiation. *Frontiers in immunology* **2013**, *4*, 20, doi:10.3389/fimmu.2013.00020.

111. Kim, E.H.; Sullivan, J.A.; Plisch, E.H.; Tejera, M.M.; Jatzek, A.; Choi, K.Y.; Suresh, M. Signal Integration by Akt Regulates CD8 TCell Effector and Memory Differentiation. *Journal of Immunology (Baltimore, Md. : 1950)* **2012**, *188*, 4305–4314, doi:10.4049/jimmunol.1103568.

112. van der Waart, A.B.; van de Weem, N.M.P.; Maas, F.; Kramer, C.S.M.; Kester, M.G.D.; Falkenburg, J.H.F.; Schaap, N.; Jansen, J.H.; van der Voort, R.; Gattinoni, L.*; et al.* Inhibition of Akt signaling promotes the generation of superior tumor-reactive T cells for adoptive immunotherapy. *Blood* **2014**, *124*, 3490–3500, doi:10.1182/blood-2014-05-578583.

113. Sampson, J.H.; Choi, B.D.; Sanchez-Perez, L.; Suryadevara, C.M.; Snyder, D.J.; Flores, C.T.; Schmittling, R.J.; Nair, S.K.; Reap, E.A.; Norberg, P.K.*; et al.* EGFRvIII mCAR-modified T-cell therapy cures mice with established intracerebral glioma and generates host immunity against tumor-antigen loss. *Clinical cancer research : an official journal*

of the American Association for Cancer Research **2014**, *20*, 972–984, doi:10.1158/1078-0432.CCR-13-0709.

114. Engelman, J.A.; Zejnullahu, K.; Mitsudomi, T.; Song, Y.; Hyland, C.; Park, J.O.; Lindeman, N.; Gale, C.-M.; Zhao, X.; Christensen, J.*; et al.* MET amplification leads to gefitinib resistance in lung cancer by activating ERBB3 signaling. *Science (New York, N.Y.)* **2007**, *316*, 1039–1043, doi:10.1126/science.1141478.

115. Turke, A.B.; Zejnullahu, K.; Wu, Y.-L.; Song, Y.; Dias-Santagata, D.; Lifshits, E.; Toschi, L.; Rogers, A.; Mok, T.; Sequist, L.*; et al.* Preexistence and clonal selection of MET amplification in EGFR mutant NSCLC. *Cancer cell* **2010**, *17*, 77–88, doi:10.1016/j.ccr.2009.11.022.

116. Gettinger, S.; Choi, J.; Hastings, K.; Truini, A.; Datar, I.; Sowell, R.; Wurtz, A.; Dong, W.; Cai, G.; Melnick, M.A.*; et al.* Impaired HLA Class I Antigen Processing and Presentation as a Mechanism of Acquired Resistance to Immune Checkpoint Inhibitors in Lung Cancer. *Cancer discovery* **2017**, *7*, 1420–1435, doi:10.1158/2159-8290.CD-17-0593.

117. Zaretsky, J.M.; Garcia-Diaz, A.; Shin, D.S.; Escuin-Ordinas, H.; Hugo, W.; Hu-Lieskovan, S.; Torrejon, D.Y.; Abril-Rodriguez, G.; Sandoval, S.; Barthly, L.*; et al.* Mutations Associated with Acquired Resistance to PD-1 Blockade in Melanoma. *The New England journal of medicine* **2016**, *375*, 819–829, doi:10.1056/NEJMoa1604958.

118. Holmgaard, R.B.; Zamarin, D.; Munn, D.H.; Wolchok, J.D.; Allison, J.P. Indoleamine 2,3-dioxygenase is a critical resistance mechanism in antitumor T cell immunotherapy targeting CTLA-4. *The Journal of experimental medicine* **2013**, *210*, 1389–1402, doi:10.1084/jem.20130066.

119. Li, J.; Li, W.; Huang, K.; Zhang, Y.; Kupfer, G.; Zhao, Q. Chimeric antigen receptor T cell (CAR-T) immunotherapy for solid tumors: lessons learned and strategies for moving forward. *Journal of hematology & oncology* **2018**, *11*, 22, doi:10.1186/s13045-018-0568-6.

120. Lamers, C.H.J.; Sleijfer, S.; Vulto, A.G.; Kruit, W.H.J.; Kliffen, M.; Debets, R.; Gratama, J.W.; Stoter, G.; Oosterwijk, E. Treatment of metastatic renal cell carcinoma with autologous T-lymphocytes genetically retargeted against carbonic anhydrase IX: first clinical experience. *Journal of clinical oncology : official journal of the American Society of Clinical Oncology* **2006**, *24*, e20-2, doi:10.1200/JCO.2006.05.9964.

121. Morgan, R.A.; Chinnasamy, N.; Abate-Daga, D.; Gros, A.; Robbins, P.F.; Zheng, Z.; Dudley, M.E.; Feldman, S.A.; Yang, J.C.; Sherry, R.M.*; et al.* Cancer regression and neurological toxicity following anti-MAGE-A3 TCR gene therapy. *Journal of immunotherapy (Hagerstown, Md. : 1997)* **2013**, *36*, 133–151, doi:10.1097/CJI.0b013e3182829903.

122. Johnson, L.A.; Scholler, J.; Ohkuri, T.; Kosaka, A.; Patel, P.R.; McGettigan, S.E.; Nace, A.K.; Dentchev, T.; Thekkat, P.; Loew, A.*; et al.* Rational development and characterization of humanized anti–EGFR variant III chimeric antigen receptor T cells for glioblastoma. *Science translational medicine* **2015**, *7*, 275ra22, doi:10.1126/scitranslmed.aaa4963.

123. Okamoto, I.; Kenyon, L.C.; Emlet, D.R.; Mori, T.; Sasaki, J.-i.; Hirosako, S.; Ichikawa, Y.; Kishi, H.; Godwin, A.K.; Yoshioka, M.*; et al.* Expression of constitutively activated EGFRvIII in non-small cell lung cancer. *Cancer science* **2003**, *94*, 50–56.

124. Ohtsuka, K.; Ohnishi, H.; Fujiwara, M.; Kishino, T.; Matsushima, S.; Furuyashiki, G.; Takei, H.; Koshiishi, Y.; Goya, T.; Watanabe, T. Abnormalities of epidermal growth factor receptor in lung squamous-cell carcinomas, adenosquamous carcinomas, and large-cell carcinomas: tyrosine kinase domain mutations are not rare in tumors with an adenocarcinoma component. *Cancer* **2007**, *109*, 741–750, doi:10.1002/cncr.22476.

125. Duan, J.; Wang, Z.; Bai, H.; An, T.; Zhuo, M.; Wu, M.; Wang, Y.; Yang, L.; Wang, J. Epidermal growth factor receptor variant III mutation in Chinese patients with squamous cell cancer of the lung. *Thoracic cancer* **2015**, *6*, 319–326, doi:10.1111/1759-7714.12204.

126. Baum, C.; Schambach, A.; Bohne, J.; Galla, M. Retrovirus vectors: toward the plentivirus? *Molecular therapy : the journal of the American Society of Gene Therapy* **2006**, *13*, 1050–1063, doi:10.1016/j.ymthe.2006.03.007.

127. Kay, M.A.; Glorioso, J.C.; Naldini, L. Viral vectors for gene therapy: the art of turning infectious agents into vehicles of therapeutics. *Nature medicine* **2001**, *7*, 33–40, doi:10.1038/83324.

128. Lynch, C.M.; Miller, A.D. Production of high-titer helper virus-free retroviral vectors by cocultivation of packaging cells with different host ranges. *Journal of Virology* **1991**, *65*, 3887–3890.

129. Suerth, J.D.; Schambach, A.; Baum, C. Genetic modification of lymphocytes by retrovirus-based vectors. *Current opinion in immunology* **2012**, *24*, 598–608, doi:10.1016/j.coi.2012.08.007.

130. Del Vecchio, C.A.; Giacomini, C.P.; Vogel, H.; Jensen, K.C.; Florio, T.; Merlo, A.; Pollack, J.R.; Wong, A.J. EGFRvIII gene rearrangement is an early event in glioblastoma tumorigenesis and expression defines a hierarchy modulated by epigenetic mechanisms. *Oncogene* **2013**, *32*, 2670–2681, doi:10.1038/onc.2012.280.

131. Stec, W.J.; Rosiak, K.; Siejka, P.; Peciak, J.; Popeda, M.; Banaszczyk, M.; Pawlowska, R.; Treda, C.; Hulas-Bigoszewska, K.; Piaskowski, S.*; et al.* Cell line with endogenous EGFRvIII expression is a suitable model for research and drug development purposes. *Oncotarget* **2016**, *7*, 31907–31925, doi:10.18632/oncotarget.8201.

132. Rieske, P.; Golanska, E.; Zakrzewska, M.; Piaskowski, S.; Hulas-Bigoszewska, K.; Wolańczyk, M.; Szybka, M.; Witusik-Perkowska, M.; Jaskolski, D.J.; Zakrzewski, K.*; et al.* Arrested neural and advanced mesenchymal differentiation of glioblastoma cells-comparative study with neural progenitors. *BMC cancer* **2009**, *9*, 54, doi:10.1186/1471-2407-9-54.

133. Witusik-Perkowska, M.; Rieske, P.; Hułas-Bigoszewska, K.; Zakrzewska, M.; Stawski, R.; Kulczycka-Wojdala, D.; Bieńkowski, M.; Stoczyńska-Fidelus, E.; Grešner, S.M.; Piaskowski, S.*; et al.* Glioblastoma-derived spheroid cultures as an experimental model for analysis of EGFR anomalies. *Journal of neuro-oncology* **2011**, *102*, 395–407, doi:10.1007/s11060-010-0352-0.

134. Schroder, K.; Hertzog, P.J.; Ravasi, T.; Hume, D.A. Interferon-gamma: an overview of signals, mechanisms and functions. *Journal of leukocyte biology* **2004**, *75*, 163–189, doi:10.1189/jlb.0603252.

135. Church, S.E.; Jensen, S.M.; Antony, P.A.; Restifo, N.P.; Fox, B.A. Tumor-specific CD4+ T cells maintain effector and memory tumor-specific CD8+ T cells. *European journal of immunology* **2014**, *44*, 69–79, doi:10.1002/eji.201343718.

136. Stoczynska-Fidelus, E.; Piaskowski, S.; Bienkowski, M.; Banaszczyk, M.; Hulas-Bigoszewska, K.; Winiecka-Klimek, M.; Radomiak-Zaluska, A.; Och, W.; Borowiec, M.; Zieba, J.*; et al.* The failure in the stabilization of glioblastoma-derived cell lines: spontaneous in vitro senescence as the main culprit. *PloS one* **2014**, *9*, e87136, doi:10.1371/journal.pone.0087136.

137. Gabrilovich, D.I.; Ostrand-Rosenberg, S.; Bronte, V. Coordinated regulation of myeloid cells by tumours. *Nature reviews. Immunology* **2012**, *12*, 253–268, doi:10.1038/nri3175.

138. Talmadge, J.E.; Gabrilovich, D.I. History of myeloid-derived suppressor cells. *Nature reviews. Cancer* **2013**, *13*, 739–752, doi:10.1038/nrc3581.

139. Kumar, V.; Patel, S.; Tcyganov, E.; Gabrilovich, D.I. The Nature of Myeloid-Derived Suppressor Cells in the Tumor Microenvironment. *Trends in immunology* **2016**, *37*, 208–220, doi:10.1016/j.it.2016.01.004.

140. Parker, K.H.; Beury, D.W.; Ostrand-Rosenberg, S. Myeloid-Derived Suppressor Cells: Critical Cells Driving Immune Suppression in the Tumor Microenvironment. *Advances in cancer research* **2015**, *128*, 95–139, doi:10.1016/bs.acr.2015.04.002.

141. Bronte, V.; Brandau, S.; Chen, S.-H.; Colombo, M.P.; Frey, A.B.; Greten, T.F.; Mandruzzato, S.; Murray, P.J.; Ochoa, A.; Ostrand-Rosenberg, S.*; et al.* Recommendations for myeloid-derived suppressor cell nomenclature and characterization standards. *Nature communications* **2016**, *7*, 12150, doi:10.1038/ncomms12150.

142. Lindau, D.; Gielen, P.; Kroesen, M.; Wesseling, P.; Adema, G.J. The immunosuppressive tumour network: myeloid-derived suppressor cells, regulatory T cells and natural killer T cells. *Immunology* **2013**, *138*, 105–115, doi:10.1111/imm.12036.

143. Gabrilovich, D.I.; Nagaraj, S. Myeloid-derived suppressor cells as regulators of the immune system. *Nature reviews. Immunology* **2009**, *9*, 162–174, doi:10.1038/nri2506.

144. Bronte, V.; Zanovello, P. Regulation of immune responses by L-arginine metabolism. *Nature reviews. Immunology* **2005**, *5*, 641–654, doi:10.1038/nri1668.

145. Molon, B.; Ugel, S.; Del Pozzo, F.; Soldani, C.; Zilio, S.; Avella, D.; Palma, A. de; Mauri, P.; Monegal, A.; Rescigno, M.*; et al.* Chemokine nitration prevents intratumoral infiltration of antigen-specific T cells. *The Journal of experimental medicine* **2011**, *208*, 1949–1962, doi:10.1084/jem.20101956.

146. Noman, M.Z.; Desantis, G.; Janji, B.; Hasmim, M.; Karray, S.; Dessen, P.; Bronte, V.; Chouaib, S. PD-L1 is a novel direct target of HIF-1α, and its blockade under hypoxia enhanced MDSC-mediated T cell activation. *The Journal of experimental medicine* **2014**, *211*, 781–790, doi:10.1084/jem.20131916.

147. Ostrand-Rosenberg, S. Myeloid-derived suppressor cells: more mechanisms for inhibiting antitumor immunity. *Cancer immunology, immunotherapy : CII* **2010**, *59*, 1593–1600, doi:10.1007/s00262-010-0855-8.

148. Pickup, M.; Novitskiy, S.; Moses, H.L. The roles of TGFβ in the tumour microenvironment. *Nature reviews. Cancer* **2013**, *13*, 788–799, doi:10.1038/nrc3603.

149. Meirow, Y.; Kanterman, J.; Baniyash, M. Paving the Road to Tumor Development and Spreading: Myeloid-Derived Suppressor Cells are Ruling the Fate. *Frontiers in immunology* **2015**, *6*, 523, doi:10.3389/fimmu.2015.00523.

150. Umansky, V.; Sevko, A. Melanoma-induced immunosuppression and its neutralization. *Seminars in cancer biology* **2012**, *22*, 319–326, doi:10.1016/j.semcancer.2012.02.003.

151. Sallusto, F.; Geginat, J.; Lanzavecchia, A. Central memory and effector memory T cell subsets: function, generation, and maintenance. *Annual review of immunology* **2004**, *22*, 745–763, doi:10.1146/annurev.immunol.22.012703.104702.

152. Gattinoni, L.; Klebanoff, C.A.; Restifo, N.P. Paths to stemness: building the ultimate antitumour T cell. *Nature reviews. Cancer* **2012**, *12*, 671–684, doi:10.1038/nrc3322.

153. Busch, D.H.; Fräßle, S.P.; Sommermeyer, D.; Buchholz, V.R.; Riddell, S.R. Role of memory T cell subsets for adoptive immunotherapy. *Seminars in immunology* **2016**, *28*, 28–34, doi:10.1016/j.smim.2016.02.001.

154. Crompton, J.G.; Sukumar, M.; Restifo, N.P. Uncoupling T-cell expansion from effector differentiation in cell-based immunotherapy. *Immunological reviews* **2014**, *257*, 264–276, doi:10.1111/imr.12135.

155. Gattinoni, L.; Restifo, N.P. Moving T memory stem cells to the clinic. *Blood* **2013**, *121*, 567–568, doi:10.1182/blood-2012-11-468660.

156. Gattinoni, L.; Klebanoff, C.A.; Palmer, D.C.; Wrzesinski, C.; Kerstann, K.; Yu, Z.; Finkelstein, S.E.; Theoret, M.R.; Rosenberg, S.A.; Restifo, N.P. Acquisition of full effector function in vitro paradoxically impairs the in vivo antitumor efficacy of adoptively transferred CD8+ T cells. *The Journal of clinical investigation* **2005**, *115*, 1616–1626, doi:10.1172/JCI24480.

157. Lugli, E.; Gattinoni, L.; Roberto, A.; Mavilio, D.; Price, D.A.; Restifo, N.P.; Roederer, M. Identification, isolation and in vitro expansion of human and nonhuman primate T stem cell memory cells. *Nature protocols* **2013**, *8*, 33–42, doi:10.1038/nprot.2012.143.

158. Klebanoff, C.A.; Gattinoni, L.; Palmer, D.C.; Muranski, P.; Ji, Y.; Hinrichs, C.S.; Borman, Z.A.; Kerkar, S.P.; Scott, C.D.; Finkelstein, S.E.*; et al.* Determinants of successful CD8+ T-cell adoptive immunotherapy for large established tumors in mice. *Clinical cancer research : an official journal of the American Association for Cancer Research* **2011**, *17*, 5343–5352, doi:10.1158/1078-0432.CCR-11-0503.

159. Ding, Z.-C.; Liu, C.; Cao, Y.; Habtetsion, T.; Kuczma, M.; Pi, W.; Kong, H.; Cacan, E.; Greer, S.F.; Cui, Y.*; et al.* IL-7 signaling imparts polyfunctionality and stemness potential to CD4(+) T cells. *Oncoimmunology* **2016**, *5*, e1171445, doi:10.1080/2162402X.2016.1171445.

160. Hinrichs, C.S.; Spolski, R.; Paulos, C.M.; Gattinoni, L.; Kerstann, K.W.; Palmer, D.C.; Klebanoff, C.A.; Rosenberg, S.A.; Leonard, W.J.; Restifo, N.P. IL-2 and IL-21 confer

opposing differentiation programs to CD8+ T cells for adoptive immunotherapy. *Blood* **2008**, *111*, 5326–5333, doi:10.1182/blood-2007-09-113050.

161. Cui, W.; Liu, Y.; Weinstein, J.S.; Craft, J.; Kaech, S.M. An interleukin-21-interleukin-10-STAT3 pathway is critical for functional maturation of memory CD8+ T cells. *IMMUNITY* **2011**, *35*, 792–805, doi:10.1016/j.immuni.2011.09.017.

162. Xiao, Z.; Casey, K.A.; Jameson, S.C.; Curtsinger, J.M.; Mescher, M.F. Programming for CD8 T cell memory development requires IL-12 or type I IFN. *Journal of Immunology (Baltimore, Md. : 1950)* **2009**, *182*, 2786–2794, doi:10.4049/jimmunol.0803484.

163. Kaartinen, T.; Luostarinen, A.; Maliniemi, P.; Keto, J.; Arvas, M.; Belt, H.; Koponen, J.; Loskog, A.; Mustjoki, S.; Porkka, K.*; et al.* Low interleukin-2 concentration favors generation of early memory T cells over effector phenotypes during chimeric antigen receptor T-cell expansion. *Cytotherapy* **2017**, *19*, 689–702, doi:10.1016/j.jcyt.2017.03.067.

164. Klebanoff, C.A.; Scott, C.D.; Leonardi, A.J.; Yamamoto, T.N.; Cruz, A.C.; Ouyang, C.; Ramaswamy, M.; Roychoudhuri, R.; Ji, Y.; Eil, R.L.*; et al.* Memory T cell-driven differentiation of naive cells impairs adoptive immunotherapy. *The Journal of clinical investigation* **2016**, *126*, 318–334, doi:10.1172/JCI81217.

165. Schulte, A.; Günther, H.S.; Martens, T.; Zapf, S.; Riethdorf, S.; Wülfing, C.; Stoupiec, M.; Westphal, M.; Lamszus, K. Glioblastoma stem-like cell lines with either maintenance or loss of high-level EGFR amplification, generated via modulation of ligand concentration. *Clinical cancer research : an official journal of the American Association for Cancer Research* **2012**, *18*, 1901–1913, doi:10.1158/1078-0432.CCR-11-3084.

166. Gattinoni, L.; Speiser, D.E.; Lichterfeld, M.; Bonini, C. T memory stem cells in health and disease. *Nature medicine* **2017**, *23*, 18–27, doi:10.1038/nm.4241.

167. Maude, S.L.; Frey, N.; Shaw, P.A.; Aplenc, R.; Barrett, D.M.; Bunin, N.J.; Chew, A.; Gonzalez, V.E.; Zheng, Z.; Lacey, S.F.*; et al.* Chimeric antigen receptor T cells for sustained remissions in leukemia. *The New England journal of medicine* **2014**, *371*, 1507–1517, doi:10.1056/NEJMoa1407222.

168. Porter, D.L.; Hwang, W.-T.; Frey, N.V.; Lacey, S.F.; Shaw, P.A.; Loren, A.W.; Bagg, A.; Marcucci, K.T.; Shen, A.; Gonzalez, V.*; et al.* Chimeric antigen receptor T cells persist and induce sustained remissions in relapsed refractory chronic lymphocytic leukemia. *Science translational medicine* **2015**, *7*, 303ra139, doi:10.1126/scitranslmed.aac5415.

169. Suarez, E.R.; Chang, D.K.; Sun, J.; Sui, J.; Freeman, G.J.; Signoretti, S.; Zhu, Q.; Marasco, W.A. Chimeric antigen receptor T cells secreting anti-PD-L1 antibodies more effectively regress renal cell carcinoma in a humanized mouse model. *Oncotarget* **2016**, *7*, 34341–34355, doi:10.18632/oncotarget.9114.

170. Hsu, C.; Hughes, M.S.; Zheng, Z.; Bray, R.B.; Rosenberg, S.A.; Morgan, R.A. Primary Human T Lymphocytes Engineered with a Codon-Optimized IL-15 Gene Resist Cytokine Withdrawal-Induced Apoptosis and Persist Long-Term in the Absence of Exogenous Cytokine1. *Journal of Immunology (Baltimore, Md. : 1950)* **2005**, *175*, 7226–7234.

Appendix

List of Abbreviations

°C	Degree Celsius
µg	microgram
µL	microliter
µM	MicroMolar
^{51}Cr	Chromium 51
AEC	3-amino-9-ethylcarbazole
ACT	Adoptive cell transfer
Amp	Ampicillin
APC	Avidin-peroxidase complex
bp(s)	base pair(s)
BSA	Bovine serum albumin
CAR	Chimeric antigen receptor
CD	Cluster of differentiation
CTLA-4	Cytotoxic T lymphocyte antigen-4
CVS	Crystal Violet Solution
d	day
DC	Dendritic cell
dH$_2$O	Distilled water
DLI	Donor lymphocyte infusion
DMEM	Dulbecco's Modified Eagle Medium
DMSO	Dimethyl Sulfoxide
DNA	Deoxyribonucleic acid
DPBS	Dulbecco's Phosphate buffered saline
E.coli	Escherichia coli
EDTA	Ethylenediaminetetraacetic acid
EGF	Epidermal growth factor
EGFR	Epidermal growth factor receptor
EGFRvIII	Epidermal growth factor receptor variant III
ELISpot	Enzyme-Linked Immunosorbent Spot

Env	Envelope
Et al.	Et alteres (and others)
FSC	Fetal calf serum
FITC	Fluorescein isothiocyanate
FOXO	Forkhead box O
g	Acceleration of gravity
Gag	Group specific antigen
GALV	Gibbon Ape Leukemia Virus
GFP	Green fluorescent protein
GSK-3ß	Serine-theronine kinase glycogen synthase kinase-3ß
HIV	Human immunodeficiency virus
HLA	Human leukocyte antigen
hr(s)	hour(s)
HS	Human serum
HSCT	Hematopoietic stem cell transfer
ICAM-1	Intercellular adhesion molecule - 1
IDO	Indoleamine 2,3-dioxygenase
IFN	Interferon
Ig	Immunoglobulin
IL	Interleukin
IRES	Internal ribosomal entry site
IU	International Unit
kb	Kilobase
LB-medium	Lysogeny broth medium
Lef	Lymphocyte-Enhancer-Factor
LTR	Long terminal repeat
M	Molar
mAb	Monoclonal antibody
MACS	Magnetic activated cell sorting
MHC	Major Histocompatibility Complex
min(s)	minute(s)
mL	Milliliter

MLV	Murine leukemia virus
mM	Millimolar
mTOR	Mammalian target of rapamycin
mTORC	Mammalian target of rapamycin complex
ng	Nanogram
NK cell	Natural killer cell
NKT cell	Natural killer T cell
NSCLC	Non-small cell lung cancer
P / S	Penicillin / Streptomycin
PBMCs	Peripheral blood mononuclear cell
PCR	Polymerase chain reaction
PD-1	Programmed death 1
PD-L1	Programmed death ligand 1
PE	Phycoerythrin
PFA	Paraformaldehyde
Phx	Phoenix
PI3	Phosphatidylinositol 3-kinase
PIP2	Phosphatidylinositol-4,5-bisphosphate
PIP3	Phosphatidylinositol-4,5,6-trisphosphate
Pol	Polymerase
Puro	Puromycin
rpm	Rounds per minute
RPMI medium	Roswell Park Memorial Institute Medium
RTK	Receptor tyrosine kinase
scFv	Single chain variable fragment
sec(s)	Second(s)
TAA	Tumor associated antigen
TCF	T Cell Factor
T_{CM}	Central memory T cell
TCR	T cell receptor
T_{EFF}	Effector T cell
T_{EM}	Effector memory T cell

TGF	Transforming-growth factor
TIL	Tumor infiltrating lymphocytes
T_N	Naive T cell
Tris	Tris(hydroxymethyl)-aminomethan
T_{SCM}	Stem cell like memory T cell
T_{total}	Total T cell
TWS119	4,6 disubstituted pyrrolopyrimidine
U	Unit
UV	Ultraviolet
v/v	volume per volume
VSV-G	Vesicular stomatitis virus glycoprotein G

Index of Figures

Index of Tables

Plasmid Maps

pMSGV-EGFRvIII-CAR

pMX-EGFRvIII-CAR

pMX-Mock

pMX_Mock_IRES_Puro
6561 bp

(6465) **SspI**
(6238) **DraI**
(6141) **ScaI**
(5883) **FspI**
(5542) **FseI**
(5083) **PspFI**
(5079) **BseYI**
(4883) **DrdI**
(4659) **BspQI - SapI**
(3898) **HincII**
(3896) **SalI**
(3627) **StuI**
(3412) **RsrII**
(3409) **BspEI***
(3352) **BsiWI**

SpeI (752)
PshAI (874)
Bsu36I (1126)
EcoNI (1500)
BglII (1527)
AgeI (1690)
PacI (1913)
BamHI (1917)
EcoRI (1939)
PaeR7I - PspXI - XhoI (2668)
NotI (2687)
SnaBI (2696)
PspOMI (2819)
ApaI (2823)
AvrII (2857)
HindIII (2930)
PflMI (3159)
BmgBI (3249)

Mo-MuLv 5' LTR
PstI
Mo-MuIV pol region
MCS
EGFP
MCS
IRES
PuroR
Mo-MuLV 3' LTR
AmpR

114
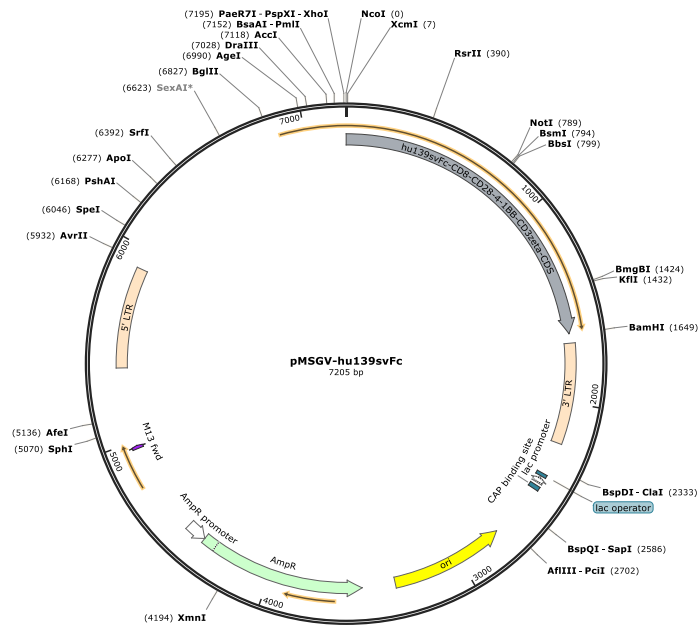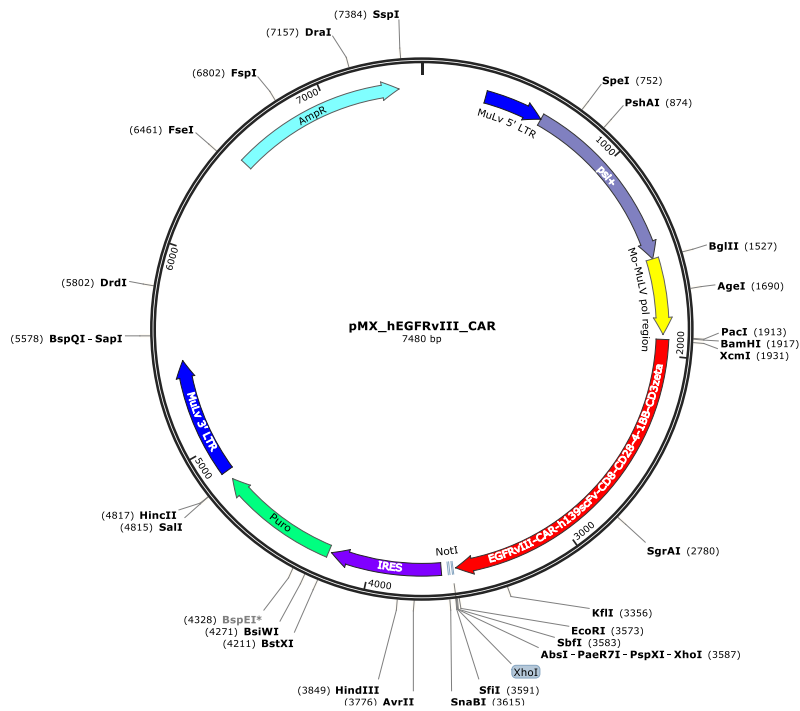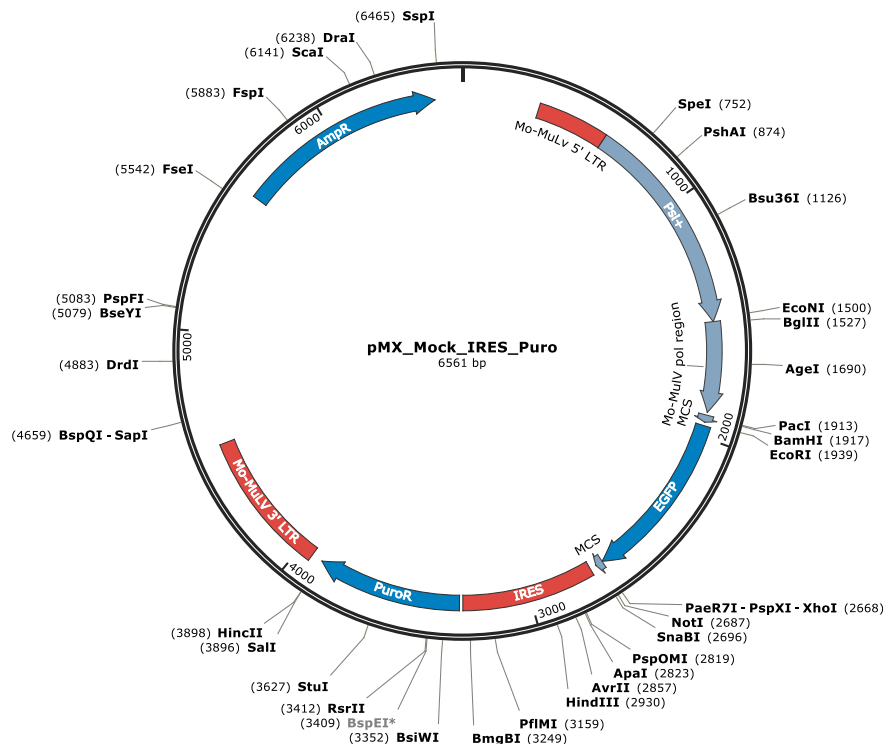
Acknowledgements

Curriculum Vitae